

2016

Development Of Reactions And Methods For Labeling Biomolecules In Cells

Enoch Agbesi Adogla
University of South Carolina

Follow this and additional works at: <https://scholarcommons.sc.edu/etd>

 Part of the [Chemistry Commons](#)

Recommended Citation

Adogla, E. A. (2016). *Development Of Reactions And Methods For Labeling Biomolecules In Cells*. (Doctoral dissertation). Retrieved from <https://scholarcommons.sc.edu/etd/3897>

This Open Access Dissertation is brought to you by Scholar Commons. It has been accepted for inclusion in Theses and Dissertations by an authorized administrator of Scholar Commons. For more information, please contact digres@mailbox.sc.edu.

DEVELOPMENT OF REACTIONS AND METHODS FOR LABELING BIOMOLECULES IN CELLS

by

Enoch Agbesi Adogla

Bachelor of Science
University of Ghana, 2002

Master of Science
New Mexico Institute of Mining and Technology, 2011

Submitted in Partial Fulfillment of the Requirements

For the Degree of Doctor of Philosophy in

Chemistry

College of Arts and Sciences

University of South Carolina

2016

Accepted by:

Qian Wang, Major Professor

Linda S. Shimizu, Committee Member

Andrew B. Greytak, Committee Member

Guiren Wang, Committee Member

Cheryl L. Addy, Vice Provost and Dean of the Graduate School

© Copyright by Enoch Agbesi Adogla, 2016
All Rights Reserved.

DEDICATION

To the love of my life, Kafui, and my two daughters, Nayram and Aseye.

ACKNOWLEDGEMENTS

I would like to extend my sincere appreciation to my advisor Dr. Qian Wang for his guidance, instruction and support. I have learned a lot under your tutelage and would always be grateful for the opportunity to be part of your team and do my graduate work under you.

My appreciation also goes to my committee members for their support, time spent in guiding me through each step of graduate school, and their invaluable advice.

I would like to thank the following former and current members of the Wang's lab. Dr. Honglin Lin, for guiding and teaching me how to design and carry out experiments. Dr. Jun Hu, Dr. Dan Menasco Dr. Xinrui Duan, Dr. Hong Guan and Dr. Matsepo Ramaboli. My appreciation also goes to Yanmei Xu, Lin Lu, Panita Maturavongsadi (Yok) and the rest of the Wang's lab group. You all help in diverse ways, and in the spirit of collaborations and camaraderie have made this journey a success.

Special thanks also goes to our collaborators, Dr. Qiao Lin and Yibo Zhu from Columbia University.

I would not have made it this far without the support of so many people, some of whom did not live to see this day. I remain forever grateful for the support and kindness I received from all of you. Thanks to my uncle, Vincent Doe for supporting me throughout college and to Uncle Richard and Aunt Gladys for your support

Lastly, I would like to thank my beautiful wife, Kafui for her love and unflinching support.

It has not been easy, but your love, faith and support have enabled us come this far. And to our two girls, Nayram and Aseye, we did it all because of you.

ABSTRACT

The complexity of cellular environments presents a challenge to efforts at studying and elucidating biomolecules in cells. Covalent ligation of biomolecules with fluorescent molecules that have a reactive functional group that can react with a complementary functional group on biomolecules is one way that has been utilized to study biomolecules. It enables visualization and tracking of ligation and transportation of molecules within the cell. However, the myriad of functional groups within the cell makes achieving selectivity difficult. To circumvent this problem, reactions that do not interfere with biology have been developed. These reactions, referred to as bioorthogonal reactions must be rapid, selective to the reactive species in the cellular environment and non-toxic to the cells. In Chapter 1 of this work, we discussed some of the key reactions developed to date and their applications in bioconjugation.

In Chapter 2, we investigated the regioselectivity of secondary amine-catalyzed inverse electron demand Diels-Alder reaction (iDA) of unsymmetrical tetrazines with aldehyde or ketones. Only one regioisomer was observed for the reactions of the unsymmetrical tetrazines with aldehydes and ketones. In addition, fluorogenic dyes were developed with tetrazine as the “triggering group”. The reaction was amenable to aqueous environment and hence was used to label aldehydes in cells.

In Chapter 3, a quartz crystal microbalance (QCM)-based sensor for detecting aldehydes was developed. By immobilizing graphene followed by 1,8-diaminonaphthalene (DAN) on a QCM chip, a sensitive and facile aldehyde and ketone sensor was developed. The binding of the aldehydes to the DAN on the QCM chip resulted in a decrease in the fundamental resonant frequency of the functionalized QCM chips. The magnitude of the frequency change is directly proportional to the mass added. The utility of the probe for labeling biomolecules was demonstrated by using as a sensor for sialic acids pretreated with sodium periodate at mild conditions. In addition, the sensor was used to detect sialic acid on a sialoprotein and on bone marrow mesenchymal stem cells.

In Chapter 4, pyrene-anchored boronic acids were designed, synthesized and subsequently used to label glycans on cells. The boronic acids bound to the diols of glycans while pyrenes allowed for fluorescence imaging and tracking of the molecule in the cell. We observed the binding of the boronic acids to the glycans allowed for transport of the pyrene-anchored boronic acids into the cytoplasm of the cell.

TABLE OF CONTENTS

DEDICATION	iii
ACKNOWLEDGEMENTS	iv
ABSTRACT	vi
LIST OF FIGURES	x
LIST OF SCHEMES	xii
CHAPTER 1 INTRODUCTION TO BIOCONJUGATION REACTIONS	1
1.1 BIOCONJUGATION AND CLICK CHEMISTRY	1
1.2 STRAINED ALKYNES	4
1.3 REACTION OF AZIDES WITH ALKENES	7
1.4 STAUDINGER LIGATION	8
1.5 PHOTOINDUCED REACTION OF TRIAZOLES WITH ALKENES	8
1.6 REACTIONS OF KETONES AND ALDEHYDES	10
1.7 DIELS-ALDER REACTIONS	11
1.8 CONCLUSION	14
1.9 REFERENCES	17

CHAPTER 2 REGIOSELECTIVE INVERSE DIELS-ALDER REACTION OF UNSYMMETRICAL TETRAZINES WITH ALDEHYDES AND KETONES.....	25
2.1 INTRODUCTION.....	25
2.2 RESULTS AND DISCUSSION	27
2.3 CONCLUSION	44
2.4 EXPERIMENTAL SECTION	44
2.5 REFERENCES.....	57
CHAPTER 3 QUARTZ CRYSTAL MICROBALANCE SENSOR FOR DETECTION OF CELLULAR SIALIC ACIDS.....	60
3.1 INTRODUCTION.....	60
3.2 RESULTS AND DISCUSSION	65
3.3 CONCLUSION	73
3.4 EXPERIMENTAL SECTION	73
3.5. REFERENCES.....	76
CHAPTER 4 PYRENE-FUNCTIONALIZED BORONIC ACID SENSORS FOR LABELING GLYCANS ON CELLS.....	81
4.1 INTRODUCTION.....	81
4.2 RESULTS AND DISCUSSION	83
4.3 CONCLUSION	87
4.4 EXEPERIMENTAL SECTION	89
4.5 REFERENCES.....	102

LIST OF FIGURES

Figure 1.1 Schematic of the dominant transition state interaction of orbitals of dienes and dienophiles, and their representative energy levels during Diels-Alder reactions.....	15
Figure 2.1 Tetrazines tested for iDA reactions	27
Figure 2.2. NMR spectra showing regioselectivity in iDA reaction of 3-methyl-6-phenyl-1,2,4,5-tetrazine with acetone (a) and propionaldehyde (b)	31
Figure 2.3 (a) The amine-catalyzed iDA reaction of 3-methyl-6-phenyl-1,2,4,5-tetrazine with phenylpropionaldehyde (b) Single crystal structures of the sole product obtained...	32
Figure 2.4 Combinatorial screening of amine-catalyzed iDA reaction of tetrazine with aldehydes and ketones.....	36
Figure 2.5 (a, b) Absorption spectra of tetrazines 2.5 showing maximum absorption at 514 nm, (a), and 2.4 showing maximum absorption at 534 nm (b). (c) The fluorescence emission spectrum of naphthalimide dye 2.10	39
Figure 2.6 Emission spectra of naphthalimide-tetrazine 2.11 (10 μ M) and the corresponding iDA product 2.12 in CH ₂ Cl ₂) (b) Emission spectra of naphthalimide-amide tetrazine 2.13 (10 μ M) and the corresponding iDA product 2.14	39
Figure 2.7 Application of fluorogenic tetrazine 2.13 in imaging aldehyde-containing molecules in cells.....	43
Figure 3.1 (a) Conformation of N-acetylneuraminic acid (Neu5AC, left) and N-glycolylneuraminic acid (Neu5Gc, right) (b) The family of naturally occurring sialic acids	61
Figure.3.2 (a) Schematic of QCM chip showing one of its two same sides (b) Assembly of DAN on graphene via μ - μ interaction.	68
Figure 3.3 Frequency shift in response to sequential binding of graphene, DAN and sialic acid to QCM chip. (b) Frequency shift in response to sequential binding of graphene, DAN and glucose.....	69

Figure 3.4 (a) Plot of frequency shift with time for binding of sialic acid (1mg/mL) pretreated with sodium periodate (0.1 M, 300 μ L) to QCM-DAN sensing platform. (b) Frequency shifts observed for introducing QCM-DAN chips into different concentrations of sialic acid	70
Figure 3.5 QCM response for fetuin from bovine serum after treatment with sodium periodate.....	71
Figure 3.6 Frequency shifts in response to binding of cell surface sialic acid to QCM chips modified with DAN for 20 k cells and 40 k cells at 0,7, 14 and 21 days	72
Figure 4.1 Structure of pyrene-derivatized boronic acid dyes for imaging cell surface glycans	84
Figure 4.2 Fluorescence images of BMSCs labeled with different pyrene-derivatized boronic acids (4.1-4.7) and pyrene (4.8).....	85
Figure 4.3.Fluorescence images of BMSCs labeled with dyes 4.1 , 4.2 and 4.8 and the corresponding fluorescent intensities.....	86
Figure 4.4 Fluorescence images of BMSCs labeled with naphthalimide-derivatized boronic acid dyes 4.9 and 4.10	88

LIST OF SCHEMES

Scheme 1.1 (a) Copper-Catalyzed azide-alkyne cyclization (CuAAC) reaction (b) Ligands of CuAAC reactions.....	3
Scheme 1.2 (a) Strained-promoted azide-alkyne reaction (b) Typical strained cyclooctynes and their second order rate constants for reaction with azides	6
Scheme 1.3 Reaction of azide with oxanorbornadiene	7
Scheme 1.4 (a) Mechanism of Classical Staudinger reaction (b) Mechanism of Staudinger ligation of azides with triarylphosphine.....	9
Scheme 1.5 Photoinduced reaction of diaryltetrazole with alkene.	10
Scheme 1.6 Reactions of aldehydes/ketones with α -effect amines	12
Scheme 1.7. The inverse electron demand Diels-Alder reaction of tetrazines with alkenes.....	16
Scheme 2.1. Reaction pathway of secondary amine-catalyzed iDA reaction between ketones/aldehydes and tetrazines	26
Scheme 2.2 Proposed mechanism of the regioselective reaction of unsymmetrical tetrazine with aldehydes/ketones	33
Scheme 2.3 One pot oxidation of diols to aldehydes, enamine formation and iDA reactions	34
Scheme 2.4 Synthesis of fluorogenic naphthalimide-tetrazine dyes 2.11 and 2.13	40
Scheme 2.5 Expected reaction for of biotin-aldehyde (2.18) with tetrazine 2.13	42
Scheme 3.1 Covalent labeling of sialic acids on cell surface with α -effect amines.	63
Scheme 3.2 Reaction of 1,8-diaminonaphthalene (DAN) with sialic acid pretreated with sodium periodate	66

CHAPTER 1

INTRODUCTION TO BIOCONJUGATION REACTIONS

1.1 Bioconjugation and Click Chemistry

Bioconjugation is the process of forming a stable covalent linkage between two or more molecules of which at least one is a biomolecule, or an engineered biomolecule.¹ However, the complex nature of biological environments, such as in the cell, makes selectively targeting a biomolecule for conjugation to another molecule daunting. To achieve selective bioconjugation in cells, the chemistry for linking a biomolecule to another, or to an organic molecule, ought to be inert to the myriad of reactive species within the cellular environment. Therefore, only very few known reactions have proved adaptable for such purpose.^{2,3}

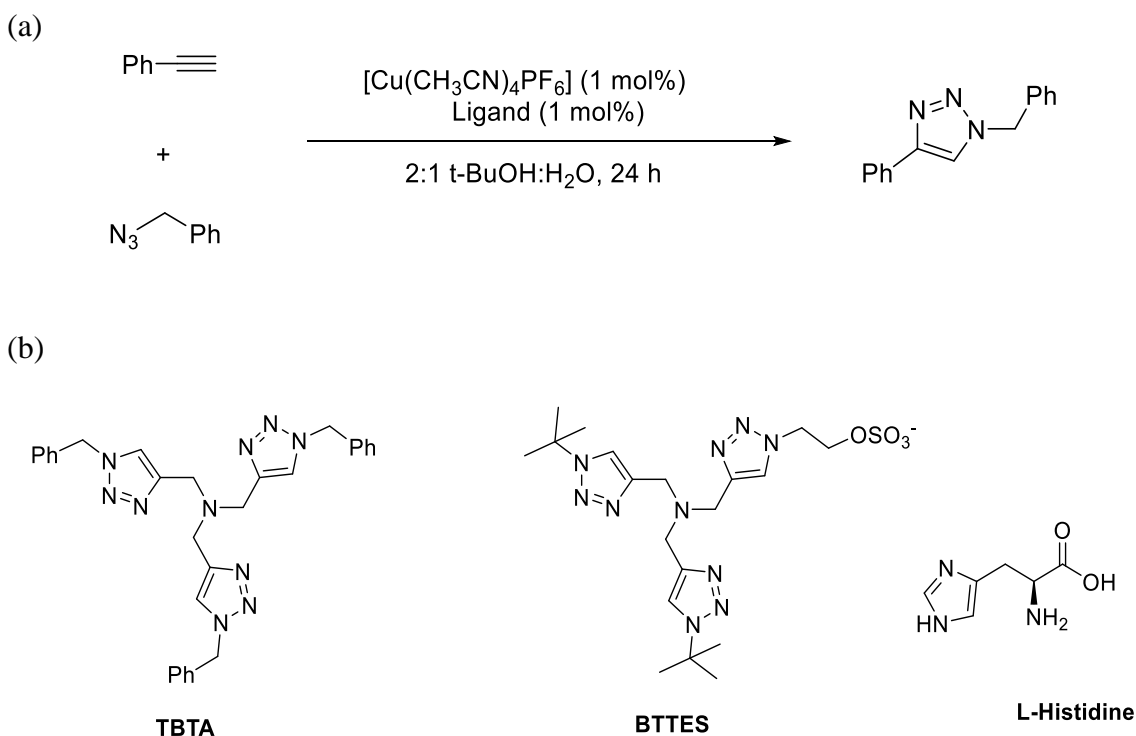
Since functional groups required for selective or bioorthogonal reactions are mostly not in the list of functionalities found in biomolecules, the method of biolabeling requires the introduction of a functional group into the biomolecule. This is often achieved by metabolic incorporation of an unnatural substrates. The modified substrates can subsequently be ligated using their complimentary functional groups.

In 2001, Sharpless introduced the term “Click Chemistry”, and defined a set of stringent criteria that reactions must meet to be included in the scope⁴ He averred that such reactions must be modular, wide in scope, give very high yields, generate only inoffensive

by products that can be removed by nonchromatographic methods, and be stereospecific. In addition, the reaction must proceed in no solvents or easily removable and benign solvents, including water; and must be compatible with physiological conditions.⁴ The quintessential click reaction, the copper (I)-catalyzed azide-alkyne reaction, was discovered concurrently and independently by the groups of Sharpless/Fokin and Mendel.^{5,6} The reaction was a modification and an improvement of the Huisgen 1,3-dipolar cycloaddition reaction discovered in the early 1960s.⁷ Whereas the original Huisgen's reaction requires high temperatures to occur and affords both 1,4- and 1,5-disubstituted-1,2,3-triazole,^{7,8} the copper(I)-catalyzed azide-alkyne reaction, proceeds at room temperature and gives only the 1,4-disubstituted-1,2,3-triazole. However, the thermodynamic instability of Cu(I) was a major drawback for the reaction as its easily oxidizes to Cu(II) or disproportionates to Cu (0), limiting the reaction to inert environments and anhydrous solvents for optimal yield. To circumvent this, copper(I)-stabilizing ligands were developed to improve the process. Fokin, Sharpless and coworkers designed oligotriazole ligands for stabilizing the Cu(I), and tested them using a model reaction between phenylacetylene and benzyl azide with 1 mol% Cu(I) and 1 mol% ligand in 2:1 *t*-BuOH:H₂O (Scheme 1). Improved reactivity was observed for the ligand-stabilized Cu(I) reactions, with tris((1-benzyl-1H-1,2,3-triazol-4-yl)methyl)amine (**TBTA**) being the best ligand. The **TBTA** appeared to tightly bind Cu(I), thereby stabilizing it from oxidation to Cu(II) as confirmed by cyclic voltammetry.⁹

The excellent reaction profiles of the ligand-stabilized Cu(I) mediated azide-alkyne reaction has made the reaction an important tool in bioconjugation. Many elegant “click” ligation of biomolecules in *vitro* and in cell lysates have been reported, but the toxicity of

copper-ligand complexes have for most part precluded the applications *in vivo*. For example, *E. coli* cells that incorporated azidohomoalanine in their outer membrane protein *ompC* were labeled using 100 μM CuBr for 16 h and survived, but were no longer able to divide afterwards.^{10,11} Similarly, mammalian cells survived treatment with 500 μM of Cu(I) for 1 h, but greater than 90% of the cells underwent apoptosis when Cu(I) concentration was increased to 1 mM under optimized conditions.^{1,12} Zebra fish embryos also displayed similar sensitivity to Cu(I). All the embryos were dead within 15 minutes after treatment with 1 mM CuSO₄, 1.5 mM sodium ascorbate and 0.1 mM **TBTA** ligand.¹ Although copper-binding ligands were later discovered, such as the **BTES** by Wu and coworkers,¹³ and L-Histidine by Pezacki and coworkers,¹⁴ which render the copper benign to cells, a lot more researchers prefer metal-free methods for bioconjugation



Scheme 1.1. (a) Copper(I)-catalyzed azide-alkyne cyclization (CuAAC) reaction. (b) Ligands of CuAAC reactions.

1.2 Strained alkynes

The strain-promoted azide-alkyne cycloaddition (SPAAC) reaction was developed to meet the demand for a metal-free alternative to the CuAAC reaction. This became imperative at the time when the existing copper-ligand complexes were considered toxic to cells. Inspired by the work of Wittig and Krebs who reported that cyclooctyne, the smallest stable cycloalkyne reacted “like an explosive” with phenyl azides (Scheme 1.2a).¹⁵ Bertozzi and coworkers synthesized biotin conjugates with cyclooctynes and reported that it labeled azides efficiently within cell-surface glycans without any apparent toxicity to the cells.¹⁶ The improved reactivity of the azide with cyclooctyne over that of linear alkynes is due to the release of ~ 18 kcal/mol ring strain associated with the cyclooctyne in the transition state of the cycloaddition. However, the second order reaction rate of the strain-promoted azide-alkyne [3+2] cycloaddition of this first generation cyclooctyne was only $0.0024 \text{ M}^{-1} \text{ s}^{-1}$, which is lower than that of normal CuAAC reaction.¹⁷ Additionally, the compound also had limited water solubility.

The lowest unoccupied orbital (LUMO) of the cyclooctyne is lower in energy relative to the linear alkynes due to the intrinsic ring strain of the former. This leads to a better overlap between the LUMO of the alkyne and the highest occupied molecular orbital (HOMO) of the azide.^{18,19} To further lower the LUMO of the alkynes and improve the reaction rates, Bertozzi and coworkers synthesized and investigated the reactivity of cyclooctynes substituted with electron-withdrawing fluorines on the propargyl carbon (Scheme 1.2b). Relative to the first generation unsubstituted cyclooctynes, monofluorinated cyclooctyne (MOFO) demonstrated a 4-fold increase in reactivity with azides,¹⁸ while the gem-difluorinated (DIFO) had a dramatic 60-fold increase.¹⁹ The *gem*-

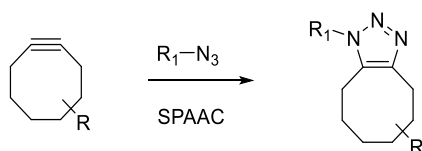
difluorinated DIFO also has a good water solubility and a second order rate constant similar to CuAAC reaction in biomolecule labeling, earning it the name “Copper-free click reaction”.¹⁹

These findings inspired investigations into other substituted cyclooctynes. Boons and co-workers reported that fusing two aryl rings to the cyclooctyne core resulted in a highly strained cyclooctyne (DIBO,) with a rate constant similar to that of DIFO,²⁰ while Bertozzi group reported another magnitude increase in the reaction rate by addition of amide bond to the DIBO scaffold to afford biarylazacyclooctyne (BARAC $k = 0.96 \text{ M}^{-1}\text{s}^{-1}$).²¹ Other substituted cyclooctynes developed with remarkable second order rate constants include, DIBAC or ADIBO,^{22,23} photocaged DIBO (PDIBO)²⁴ and tetramethoxy versions of DIBO (TMDIBO).²⁵

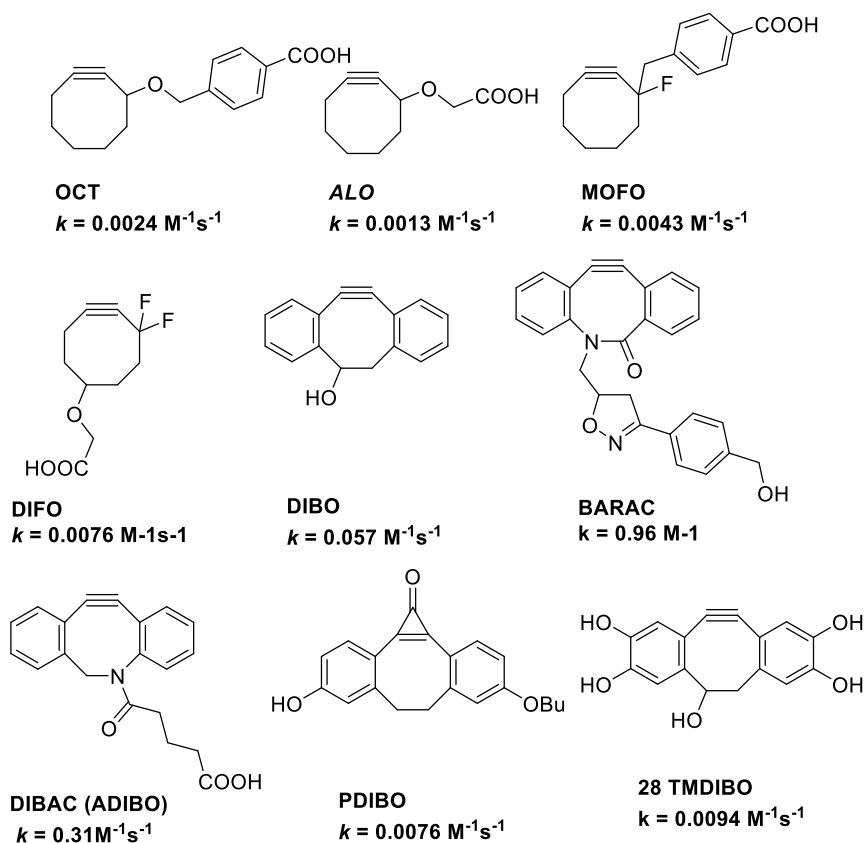
The excellent reactivity of SPAAC and its nontoxicity spurred its application *in vivo*. Bertozzi and coworkers employed DIFO-Alexa Fluor conjugates to label azido sugars on cell surface of developing embryos²⁶ and *Caenorhabditis elegans*.²⁷ This was achieved by first metabolically incorporating peracylated N-azidoacetylgalactosamine (Ac₄GalNAZ) into the zebra fish embryo or the *C. elegans*' glycans. The peracylated glycans passively diffused into the cells where they were deacylated by cellular esterases. Consequently, the free sugars were processed and incorporated into newly synthesized glycans, some of which were displayed on cell-surface glycoconjugates. The azido sugars on the cell surface were then imaged by SPAAC chemistry using the cyclooctyne probes, enabling visualization of the glycans *in vivo*. The developing zebra fish embryos were imaged between 60 to 73 hpf, and dynamic labeling was monitored in the pectoral fins, olfactory pit, and jaw. Glycan trafficking between 60 and 73 h was also analyzed through

pulse-chase experiments with spectrally distinct glycoconjugates. Similar labeling was observed in the pharynx, vulva, and anus when *C. elegans* were treated with DIFO-Alexa Fluor conjugates after the incorporation of azido-glycans.²⁷ Comparative study of a number of cyclooctynes *in vivo* showed that the reactivity of the cyclooctynes *in vivo* depends on the combined influence of intrinsic reactivity and bioavailability.²⁸

(a)



(b)

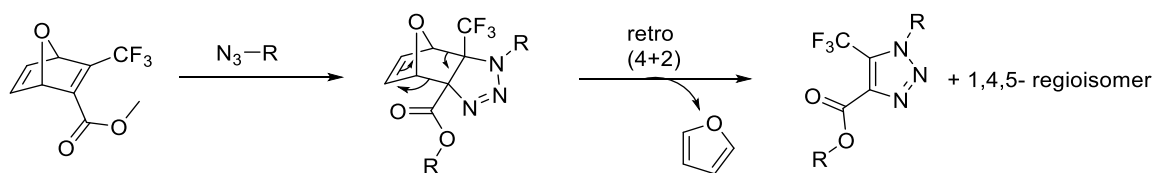


Scheme 1.2. (a) Strained-promoted azide-alkyne reaction. (b) Typical strained cyclooctynes and their second order rate constants for reaction with azides

1.3 Reaction of azides with alkenes

Alkenes react with azides in a similar way as alkynes. However, the reactions of azides with alkenes produce triazolines, which unlike the triazoles are unstable. The azide-alkene reaction dates back to the 1930s when Alder and Stein reported that strain alkenes such as norbornene and dicyclopentadiene reacted over hundred times faster than unstrained alkenes.^{29,30} As expected, the low stability of the product, the triazolines, precludes most strained alkenes from being used in bioorthogonal reactions with azides.

Nonetheless, Rutjes and coworkers reported that the use of oxanorbornadiene to react with the azides produced stable aromatic triazoles (Scheme 1.3), and were able to apply the reaction to selectively label an oxanorbornadiene-functionalized protein that had been incorporated into a hen egg white lysoszyme. The reaction between azides and oxanorbornadiene occurred at the electron poor double bond to form a triazoline, which further underwent a retro-Diels-Alder reaction to extrude furan, to produce a stable aromatic triazole.



Scheme 1.3. Reaction of azide with oxanorbornadiene.

1.4 Staudinger ligation

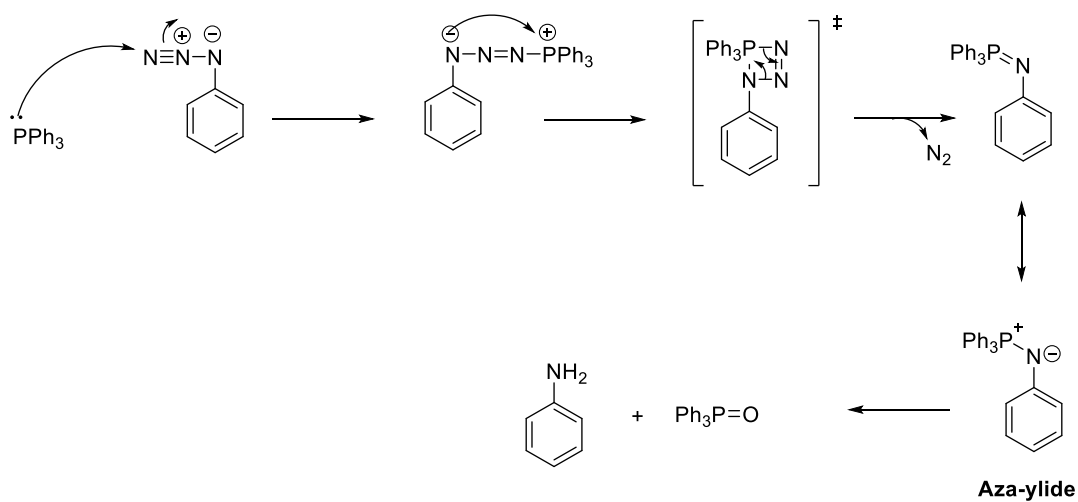
Staudinger ligation is a modification of an earlier discovered reaction, the Staudinger reduction, which involves the reduction of azides with triphenylphosphine to obtain amines and triphenylphosphine oxides (Schemes 1.4a).³¹ In Staudinger ligation, an ester group is strategically placed on an arylphosphine or phosphonothioester to allow an aza-ylide formed to undergo intramolecular reaction with the ester to form an amide bond (Scheme 1.4b). The reaction of the aza-ylide with the ester is critical; otherwise, the aza-ylide would hydrolyze to form the corresponding amine and triaryllphosphine.³²

The reaction has been successfully used in labeling biomolecules *in vitro* and *in vivo* with no adverse effects.³³⁻³⁵ However, the Staudinger ligation suffers from slow reaction kinetics and limited water solubility,^{32,36} which limits the scope of its application.

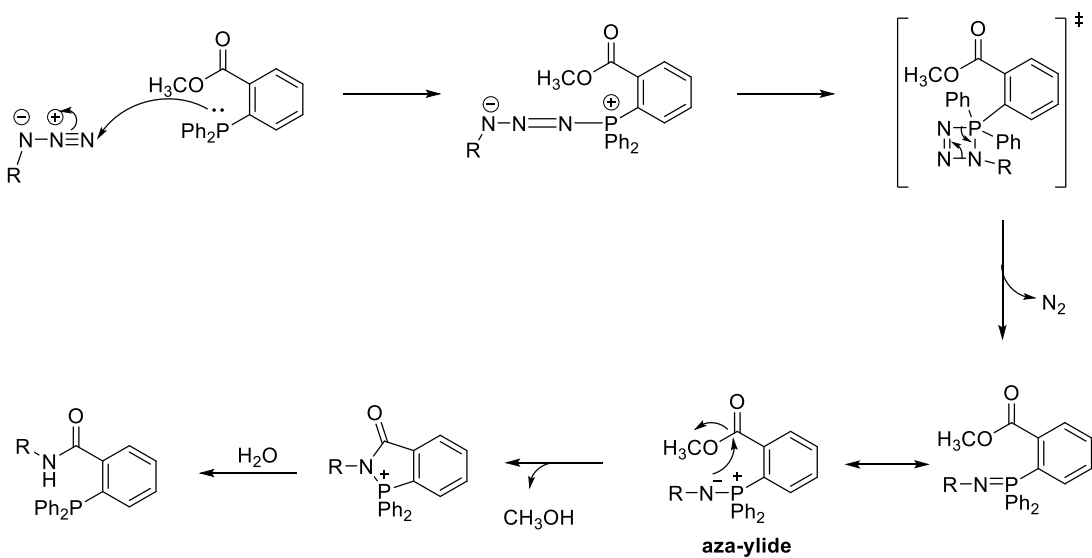
1.5 Photoinduced reaction of tetrazoles with alkenes

The photoinduced cycloaddition reaction between tetrazole and alkenes to form pyrazolines takes advantage of the nitrile imine dipole generated during reverse-cycloaddition of diaryltetrazole to form a [3+2] cycloadduct with alkenes (Scheme 1.5). This phenomenon was also first reported by Huisgen and coworkers. They observed that 2,5-diphenyltetrazole reacted with methylcrotonate under photoactivation to form a pyrazoline.³⁷ However, Lin and coworkers were the first to apply this reaction in bioconjugation by incorporating *o*-allyl tyrosine into a protein in *E. coli* and “clicking” with tetrazole under 302 nm of light.³⁸ The small size of the alkenes relative to norbornene or cyclooctynes is the advantage of this method, but the irradiations at 302 nm is toxic to cells. To circumvent this, new diaryltetrazoles were developed that can be activated by 365 nm of UV light,³⁹ and 405 nm laser light.⁴⁰

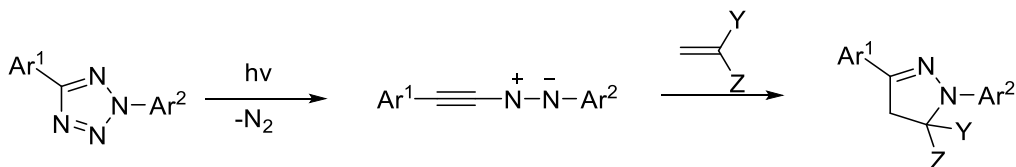
(a)



(b)



Scheme 1.4. (a) Mechanism of Classical Staudinger reaction. (b) Mechanism of Staudinger ligation of azides with triarylphosphine.



Scheme 1.5. Photoinduced reaction of diaryltetrazole with alkene.

1.6 Reactions of ketones and aldehyde

Aldehydes and ketones are, as a matter of fact, not exogenous to cells, as aldehydes can be found in glucose and intracellular metabolites, and ketones in mammalian hormones. Nonetheless, they have found utility in bioconjugation, and remain functional groups of choice for bioconjugation reactions.^{2,41} They are absent from endogenous biopolymers and are unreactive to functional groups found in protein, lipids and glycans. The reaction of aldehydes or ketones with amines produces Schiff base. In aqueous medium, the reaction is reversible, and in the case of primary amines the equilibrium favors the carbonyl.³⁵ To avoid rapid hydrolysis of the Schiff base, researchers have used α -effect amines – hydrazines and aminoxy compounds – to ligate biomolecules tagged with aldehydes or ketones.^{42,43} The reactions of hydrazines and aminoxy (also called hydroxylamines) produce hydrazones and oximes respectively (Scheme 1.6a). Although these are more stable than imines, they still have limitations as far as applications *in vivo* is concerned. The reactions of the α -effect nitrogen with aldehydes or ketones is optimum at slightly acid conditions (pH 5-6) due to the protonation of the carbonyl step involved before the reaction with the amines. But lowering of the pH of the reaction mixture also protonates the amines, rendering them less nucleophilic. High concentrations of the amines have been used to circumvent the reactivity problem but quantitative labeling could not be

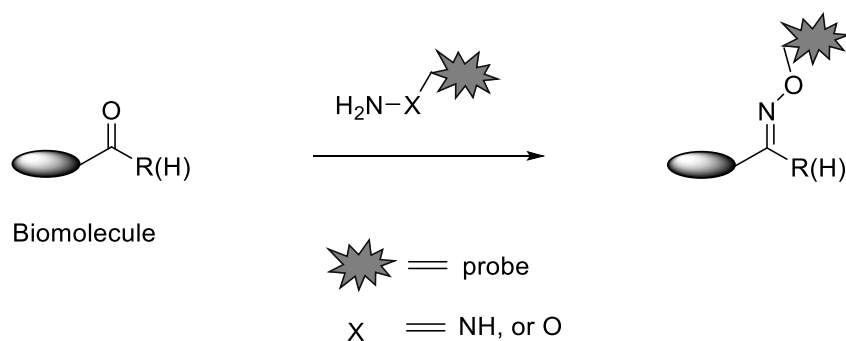
achieved. Other researchers have used aniline as the catalyst to improve the reactivity via transamination.⁴⁴⁻⁴⁶ The aniline reacts with the protonated carbonyls to form imines, which remains protonated at the pH of the reaction, and consequently reacting with the aminoxy or hydrazine reagent to form an oxime or hydrazone (Scheme 1.6b).

Another method of bioconjugation involving aldehydes is based on the Pictet-Spengler reaction between aldehydes and tryptamines.⁴⁷ This method, which forms an irreversible C-C bond between tryptamine and an aldehyde or a ketone was recently applied to the ligation of biomolecules by Bertozzi and coworkers.⁴⁷ In order to increase the rate of the reaction, an alkoxyamine (α -effect amine) was used to react with an aldehyde to form an intermediate oxyiminium ion, which subsequently underwent intramolecular reaction with indole nucleophiles to form a stable oxacarboline product (Scheme 1.6c).

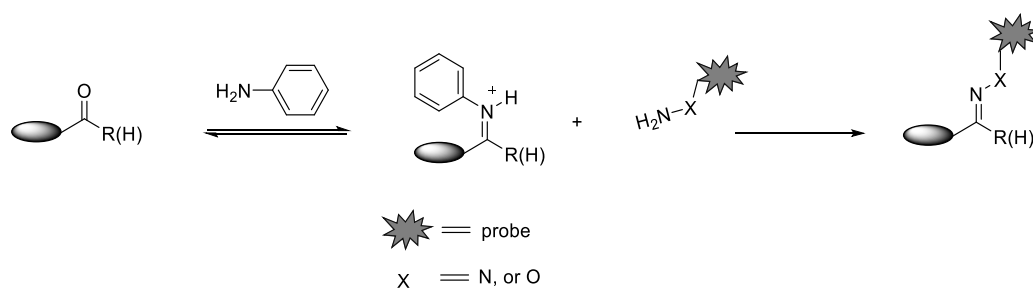
1.7 *Diels-Alder reactions*

Diels-Alder reaction is one of the methods that has been extensively used in bioconjugation due to its efficiency, selectivity and compatibility with water. It typically involves reacting an alkene (or a dienophile) with a diene. Alkenes and dienes are absent from biological systems, except in lipids, and few hormones. Electron poor alkenes such as maleimides have been used in bioconjugation reactions with dienes.⁴⁸⁻⁵⁰ However, this reaction is not bioorthogonal since bio-thiols can react with maleimide via Michael addition.^{51,52} Protection of thiol groups is therefore required to achieve selectivity with these reactions. For example, Walder and his coworkers have used Ellman's reagent to protect cysteine of Rab 7 before ligating the dienes on the Rab 7 protein with a maleimide via Diels-Alder reaction.⁵³ The kinetics of Diels-Alder reaction is, however, slow and

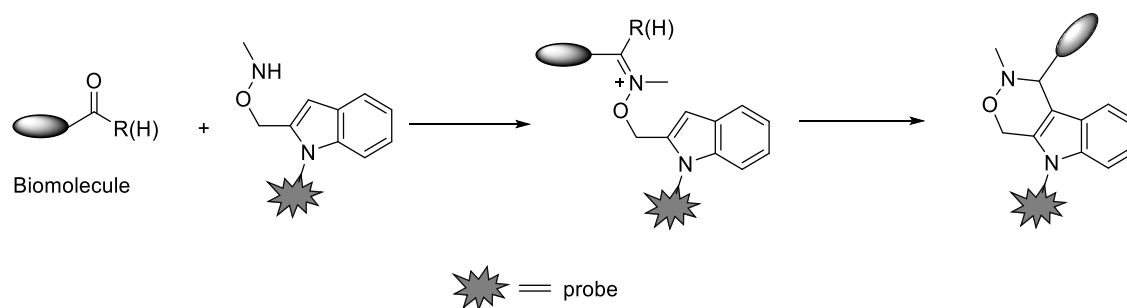
(a)



(b)



(c)



Scheme 1.6. Reactions of aldehydes/ketones with α -effect amines. (a) Reactions of aldehydes/ketones with hydroxylamine or hydrazine to produce oximes or hydrazine respectively. (b) Aniline-catalyzed oxime ligation. The aniline reacts with the carbonyl to form imine, which subsequently reacts with the α -effect amine to form an oxime. (c) Pictet–Spengler ligation of aldehydes with a modified tryptamine. The alkoxyamine reacted with the carbonyl to form an imine, which subsequently underwent intramolecular reaction with indole to form a stable product.

generally requires high concentration of the substrates (greater than 1 mM) for successful ligation.⁵⁴

Another type of Diels-Alder reaction, the inverse electron demand Diels-Alder reaction (iDA) with tetrazines as the diene, and alkenes or alkynes as the dienophiles has been extensively used in bioconjugation recently.^{1,55} The kinetics of Diels-Alder reaction of tetrazines with different alkenes and alkynes was extensively studied by Sauer and coworkers in 1998.⁵⁶ However, it was not until 2008 that Fox and coworkers reported the first applications of iDA reaction in bioconjugation.⁵⁷ By functionalizing the protein, thioredoxin (Trx) with *trans*-cyclooctene, and reacting with dipyridyltetrazine in aqueous medium, the iDA ligation product was obtained within 5 minutes. Subsequently Weisleder and coworkers demonstrated the utility of the reaction in live cell imaging by pretargeting cells with *trans*-cyclooctene bearing anti-EGFR antibody and labeling them with tetrazine tethered to a fluorophore.⁵⁸ They reported that the labeling was specific for cells treated with *trans*-cyclooctene bearing anti-EGFR antibody and occurred primarily on the surface of the cells where EGFR concentration is the highest.

In contrast to Diels-Alder reactions involving maleimides and dienes, the reaction of tetrazines with *trans*-cyclooctene is exceptionally fast, with a rate constant of 2000 to 22000 M.s⁻¹, which is far faster than SPAAC reactions.^{59,60} Other strained alkenes that have since been used in bioconjugation reactions with tetrazines include norbornene,⁶¹ and cyclopropane.⁶² However, the kinetics of these cycloalkenes are many orders of magnitude lower than that of *trans*-cyclooctene.⁶³

The Diels-Alder reactions of tetrazines, or other electron poor heteroatom dienes with alkenes is known as inverse electron demand Diels- Alder reaction (iDA) because the

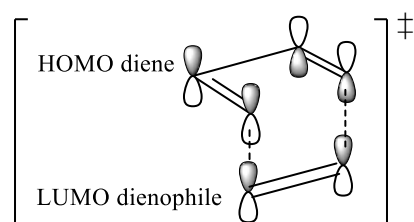
dominant orbital interactions in the transition state (TS) of Diels-Alder reaction is reversed for reactions involving electron poor dienes such as tetrazines. For normal Diels-Alder reactions, the dominant interaction is between the HOMO of the diene and the LUMO of the dienophiles. But for tetrazines and other electron poor dienes, it is the HOMO of the dienophile (i.e. alkene) that interacts with the LUMO of the diene (i.e. tetrazine) Figure (1.1).^{64,65} The iDA reaction with tetrazines proceeds in two steps: an inverse electron-demand Diels- Alder reaction, followed by a retro Diels-Alder reaction, which extrude nitrogen to give the product (Scheme 1.7).

1.8 Conclusion

The reactions discussed herein represent key chemical transformations that have been applied in bioconjugation. They have been used in direct labeling of biomolecules such as nucleic acids, proteins, carbohydrates and lipids inside cells, and also in target identification of bioactive small molecules, leading to great insights and fundamental discoveries. Nonetheless, the biocompatibility of these chemical tags, such as toxicity, selectivity, sensitivity and stability when they are present in biological environment still needs further improvement. For example, the use of Cu(I) catalyst in CuAAC makes the reaction unsuitable for animal studies and SPAAC was developed to meet the needs for catalyst-free labeling. However, the size of the cyclooctynes used in SPAAC could lead to perturbation of certain biomolecules. Tetrazine ligation with strained alkenes is also achieved without catalyst, but the stability of the most reactive strained alkenes, *trans*-cyclooctene in biological media is not good enough. There is therefore a need to develop new bioorthogonal reactions with improved reactivity and stability in biological media to

add to the tool kit of reactions available for bioconjugation. This thesis discusses my efforts in developing new reactions and methods for labeling biomolecules in cells.

(a) Normal Diels-Alder reaction



(b) Inverse Demand Diels-Alder reaction

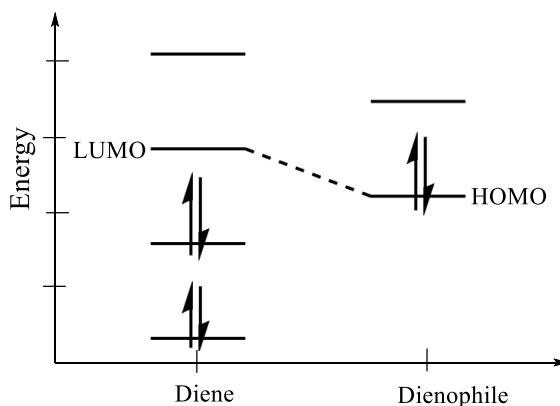
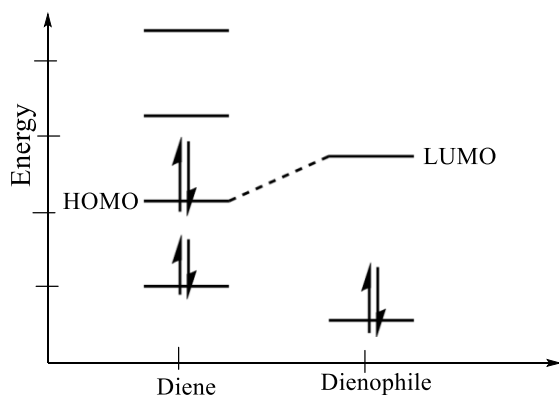
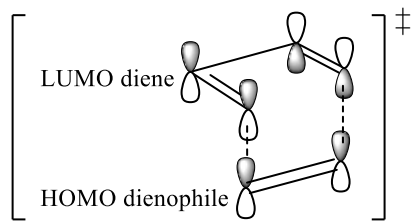
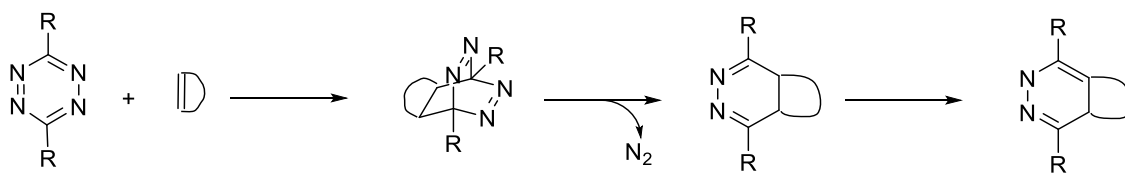


Figure 1.1. Schematic of the dominant transition state interaction of orbitals of dienes and dienophiles (up) and their representative energy levels (down) during Diels-Alder reactions (a) Normal Diels-Alder reaction. The HOMO of the diene interacts with the LUMO of the dienophile (b) Inverse Diels-Alder reaction. The HOMO of the dienophile interacts with the LUMO of the diene.



Scheme 1.7. The inverse electron demand Diels-Alder reaction of tetrazines with alkenes. The reaction proceeds in two steps: an inverse electron-demand Diels-Alder reaction, followed by a retro Diels-Alder reaction, which extrude nitrogen to give the product.

1.9 REFERENCES

- (1) Sletten, E. M.; Bertozzi, C. R.: Bioorthogonal Chemistry: Fishing for Selectivity in a Sea of Functionality. *Angew. Chem. Int. Ed.* **2009**, *48*, 6974-6998.
- (2) Gong, Y.; Pan, L.: Recent advances in bioorthogonal reactions for site-specific protein labeling and engineering. *Tetrahedron Letters* **2015**, *56*, 2123-2132.
- (3) Debets, M. F.; Van Berkel, S. S.; Dommerholt, J.; Dirks, A. J.; Rutjes, F.; Van Delft, F. L.: Bioconjugation with Strained Alkenes and Alkynes. *Accts. Chem. Res.* **2011**, *44*, 805-815.
- (4) Kolb, H. C.; Finn, M. G.; Sharpless, K. B.: Click chemistry: Diverse chemical function from a few good reactions. *Angew. Chem. Int. Ed.* **2001**, *40*, 2004-2021.
- (5) Rostovtsev, V. V.; Green, L. G.; Fokin, V. V.; Sharpless, K. B.: A stepwise Huisgen cycloaddition process: Copper(I)-catalyzed regioselective "ligation" of azides and terminal alkynes. *Angew. Chem. Int. Ed.* **2002**, *41*, 2596-2599.
- (6) Tornøe, C. W.; Christensen, C.; Meldal, M.: Peptidotriazoles on Solid Phase: [1,2,3]-Triazoles by Regiospecific Copper(I)-Catalyzed 1,3-Dipolar Cycloadditions of Terminal Alkynes to Azides. *J. Org. Chem.* **2002**, *67*, 3057-3064.
- (7) Huisgen, R.: 1.3-Dipolare Cycloadditionen - Ruckschau Und Ausblick. *Angew. Chem. Int. Ed.* **1963**, *75*, 604-606.
- (8) Huisgen, R.: 1.3-Dipolare Cycloadditionen - Ruckschau Und Ausblick. *Angew. Chem., Int. Ed. Engl.* **1963**, *2*, 565-632.
- (9) Chan, T. R.; Hilgraf, R.; Sharpless, K. B.; Fokin, V. V.: Polytriazoles as Copper(I)-Stabilizing Ligands in Catalysis. *Org. Lett.* **2004**, *6*, 2853-2855.

- (10) Link, A. J.; Tirrell, D. A.: Cell Surface Labeling of Escherichia coli via Copper(I)-Catalyzed [3+2] Cycloaddition. *J. Am. Chem. Soc.* **2003**, *125*, 11164-11165.
- (11) Link, A. J.; Vink, M. K. S.; Tirrell, D. A.: Presentation and Detection of Azide Functionality in Bacterial Cell Surface Proteins. *J. Am. Chem. Soc.* **2004**, *126*, 10598-10602.
- (12) Speers, A. E.; Adam, G. C.; Cravatt, B. F.: Activity-Based Protein Profiling in Vivo Using a Copper(I)-Catalyzed Azide-Alkyne [3 + 2] Cycloaddition. *J. Am. Chem. Soc.* **2003**, *125*, 4686-4687.
- (13) Soriano Del Amo, D.; Wang, W.; Jiang, H.; Besanceney, C.; Yan, A. C.; Levy, M.; Liu, Y.; Marlow, F. L.; Wu, P.: Biocompatible copper(I) catalysts for in vivo imaging of glycans. *J. Am. Chem. Soc.* **2010**, *132*, 16893-9.
- (14) Kennedy, D. C.; McKay, C. S.; Legault, M. C. B.; Danielson, D. C.; Blake, J. A.; Pegoraro, A. F.; Stolow, A.; Mester, Z.; Pezacki, J. P.: Cellular Consequences of Copper Complexes Used To Catalyze Bioorthogonal Click Reactions. *J. Am. Chem. Soc.* **2011**, *133*, 17993-18001.
- (15) Wittig, G.; Krebs, A.: Zur Existenz Niedergliedriger Cycloalkyne I *Chem. Ber. Recl.* **1961**, *94*, 3260-3275.
- (16) Agard, N. J.; Prescher, J. A.; Bertozzi, C. R.: A Strain-Promoted [3 + 2] Azide-Alkyne Cycloaddition for Covalent Modification of Biomolecules in Living Systems. *J. Am. Chem. Soc.* **2004**, *126*, 15046-15047.
- (17) Rodionov, V. O.; Fokin, V. V.; Finn, M. G.: Mechanism of the Ligand-Free CuI-Catalyzed Azide-Alkyne Cycloaddition Reaction. *Angew. Chem. Int. Ed.* **2005**, *44*, 2210-2215.

- (18) Agard, N. J.; Baskin, J. M.; Prescher, J. A.; Lo, A.; Bertozzi, C. R.: A comparative study of bioorthogonal reactions with azides. *ACS Chem. Biol.* **2006**, *1*, 644-648.
- (19) Baskin, J. M.; Prescher, J. A.; Laughlin, S. T.; Agard, N. J.; Chang, P. V.; Miller, I. A.; Lo, A.; Codelli, J. A.; Bertozzi, C. R.: Copper-free click chemistry for dynamic in vivo imaging. *Proc. Natl. Acad. Sci. U.S.A.* **2007**, *104*, 16793-16797.
- (20) Ning, X. H.; Guo, J.; Wolfert, M. A.; Boons, G. J.: Visualizing metabolically labeled glycoconjugates of living cells by copper-free and fast Huisgen cycloadditions. *Angew. Chem. Int. Ed.* **2008**, *47*, 2253-2255.
- (21) Jewett, J. C.; Sletten, E. M.; Bertozzi, C. R.: Rapid Cu-Free Click Chemistry with Readily Synthesized Biarylazacyclooctynones. *J. Am. Chem. Soc.* **2010**, *132*, 3688-3690.
- (22) Debets, M. F.; van Berkel, S. S.; Schoffelen, S.; Rutjes, F.; van Hest, J. C. M.; van Delft, F. L.: Aza-dibenzocyclooctynes for fast and efficient enzyme PEGylation via copper-free (3+2) cycloaddition. *Chem. Commun.* **2010**, *46*, 97-99.
- (23) Kuzmin, A.; Poloukhine, A.; Wolfert, M. A.; Popik, V. V.: Surface Functionalization Using Catalyst-Free Azide-Alkyne Cycloaddition. *Bioconjugate Chem.* **2010**, *21*, 2076-2085.
- (24) Poloukhine, A. A.; Mbua, N. E.; Wolfert, M. A.; Boons, G.-J.; Popik, V. V.: Selective Labeling of Living Cells by a Photo-Triggered Click Reaction. *J. Am. Chem. Soc.* **2009**, *131*, 15769-15776.
- (25) Stockmann, H.; Neves, A. A.; Stairs, S.; Ireland-Zecchini, H.; Brindle, K. M.; Leeper, F. J.: Development and evaluation of new cyclooctynes for cell surface glycan imaging in cancer cells. *Chem. Sci.* **2011**, *2*, 932-936.

- (26) Laughlin, S. T.; Baskin, J. M.; Amacher, S. L.; Bertozzi, C. R.: In vivo imaging of membrane-associated glycans in developing zebrafish. *Science* **2008**, *320*, 664-667.
- (27) Laughlin, S. T.; Bertozzi, C. R.: In Vivo Imaging of *Caenorhabditis elegans* Glycans. *ACS Chem. Biol.* **2009**, *4*, 1068-1072.
- (28) Chang, P. V.; Prescher, J. A.; Sletten, E. M.; Baskin, J. M.; Miller, I. A.; Agard, N. J.; Lo, A.; Bertozzi, C. R.: Copper-free click chemistry in living animals. *Proc. Natl. Acad. Sci. U.S.A.* **2010**, *107*, 1821-1826.
- (29) Alder, K.; Stein, G.: The graduated capability of addition of unsaturated circular systems. *Justus Liebigs Annalen Der Chemie* **1931**, *485*, 211-222.
- (30) Alder, K.; Stein, G.: About the graduated addition ability of unsaturated ring systems. II. *Justus Liebigs Annalen Der Chemie* **1933**, *501*, 1-48.
- (31) Staudinger, H.; Meyer, J.: On new organic phosphorus bonding III Phosphine methylene derivatives and phosphinimine. *Helv. Chim. Acta* **1919**, *2*, 635-646.
- (32) Saxon, E.; Bertozzi, C. R.: Cell surface engineering by a modified Staudinger reaction. *Science* **2000**, *287*, 2007-2010.
- (33) Saxon, E.; Luchansky, S. J.; Hang, H. C.; Yu, C.; Lee, S. C.; Bertozzi, C. R.: Investigating Cellular Metabolism of Synthetic Azidosugars with the Staudinger Ligation. *J. Am. Chem. Soc.* **2002**, *124*, 14893-14902.
- (34) Prescher, J. A.; Dube, D. H.; Bertozzi, C. R.: Chemical remodelling of cell surfaces in living animals. *Nature* **2004**, *430*, 873-877.
- (35) Prescher, J. A.; Bertozzi, C. R.: Chemistry in living systems. *Nat. Chem. Biol.* **2005**, *1*, 13-21.

- (36) Lin, F. L.; Hoyt, H. M.; van Halbeek, H.; Bergman, R. G.; Bertozzi, C. R.: Mechanistic Investigation of the Staudinger Ligation. *J. Am. Chem. Soc.* **2005**, *127*, 2686-2695.
- (37) Clovis, J. S.; Eckell, A.; Huisgen, R.; Sustmann, R.: 1,3-Dipolare Cycloadditionen XXV Der Nachweis Des Freien Diphenylnitrilimins Als Zwischenstufe Bei Cycloadditionen. *Chem. Ber. Recl.* **1967**, *100*, 60-70.
- (38) Yu, Z.; Ho, L. Y.; Wang, Z.; Lin, Q.: Discovery of new photoactivatable diaryltetrazoles for photoclick chemistry via 'scaffold hopping'. *Bioorg. Med. Chem. Lett.* **2011**, *21*, 5033-5036.
- (39) Wang, Y.; Hu, W. J.; Song, W.; Lim, R. K. V.; Lin, Q.: Discovery of Long-Wavelength Photoactivatable Diaryltetrazoles for Bioorthogonal 1,3-Dipolar Cycloaddition Reactions. *Org. Lett.* **2008**, *10*, 3725-3728.
- (40) An, P.; Yu, Z.; Lin, Q.: Design of oligothiophene-based tetrazoles for laser-triggered photoclick chemistry in living cells. *Chem. Commun.* **2013**, *49*, 9920-9922.
- (41) Cornish, V. W.; Hahn, K. M.; Schultz, P. G.: Site-Specific Protein Modification Using a Ketone Handle. *J. Am. Chem. Soc.* **1996**, *118*, 8150-8151.
- (42) Shao, J.; Tam, J. P.: Unprotected Peptides as Building Blocks for the Synthesis of Peptide Dendrimers with Oxime, Hydrazone, and Thiazolidine Linkages. *J. Am. Chem. Soc.* **1995**, *117*, 3893-3899.
- (43) Dirksen, A.; Dawson, P. E.: Rapid Oxime and Hydrazone Ligations with Aromatic Aldehydes for Biomolecular Labeling. *Bioconjugate Chem.* **2008**, *19*, 2543-2548.
- (44) Dirksen, A.; Hackeng, T. M.; Dawson, P. E.: Nucleophilic Catalysis of Oxime Ligation. *Angew. Chem. Int. Ed.* **2006**, *45*, 7581-7584.

- (45) Zeng, Y.; Ramya, T. N. C.; Dirksen, A.; Dawson, P. E.; Paulson, J. C.: High-efficiency labeling of sialylated glycoproteins on living cells. *Nat. Methods* **2009**, *6*, 207-209.
- (46) Key, J. A.; Li, C.; Cairo, C. W.: Detection of Cellular Sialic Acid Content Using Nitrobenzoxadiazole Carbonyl-Reactive Chromophores. *Bioconjugate Chem.* **2012**, *23*, 363-371.
- (47) Stöckigt, J.; Antonchick, A. P.; Wu, F.; Waldmann, H.: The Pictet–Spengler Reaction in Nature and in Organic Chemistry. *Angew. Chem. Int. Ed.* **2011**, *50*, 8538-8564.
- (48) Willems, L. I.; Verdoes, M.; Florea, B. I.; van der Marel, G. A.; Overkleeft, H. S.: Two-Step Labeling of Endogenous Enzymatic Activities by Diels-Alder Ligation. *ChemBioChem* **2010**, *11*, 1769-1781.
- (49) Marchán, V.; Ortega, S.; Pulido, D.; Pedroso, E.; Grandas, A.: Diels-Alder cycloadditions in water for the straightforward preparation of peptide–oligonucleotide conjugates. *Nucleic Acids Res.* **2006**, *34*, e24.
- (50) Houseman, B. T.; Mrksich, M.: Carbohydrate Arrays for the Evaluation of Protein Binding and Enzymatic Modification. *Chemistry & Biology* **2002**, *9*, 443-454.
- (51) Fontaine, S. D.; Reid, R.; Robinson, L.; Ashley, G. W.; Santi, D. V.: Long-Term Stabilization of Maleimide–Thiol Conjugates. *Bioconjugate Chem.* **2015**, *26*, 145-152.
- (52) Kim, Y.; Ho, S. O.; Gassman, N. R.; Korlann, Y.; Landorf, E. V.; Collart, F. R.; Weiss, S.: Efficient Site-Specific Labeling of Proteins via Cysteines. *Bioconjugate Chem.* **2008**, *19*, 786-791.

- (53) de Araujo, A. D.; Palomo, J. M.; Cramer, J.; Kohn, M.; Schroder, H.; Wacker, R.; Niemeyer, C.; Alexandrov, K.; Waldmann, H.: Diels-Alder ligation and surface immobilization of proteins. *Angew. Chem. Int. Ed.* **2006**, *45*, 296-301.
- (54) Hill, K. W.; Taunton-Rigby, J.; Carter, J. D.; Kropp, E.; Vagle, K.; Pieken, W.; McGee, D. P. C.; Husar, G. M.; Leuck, M.; Anziano, D. J.; Sebesta, D. P.: Diels-Alder Bioconjugation of Diene-Modified Oligonucleotides. *J. Org. Chem.* **2001**, *66*, 5352-5358.
- (55) Chen, W.; Wang, D.; Dai, C.; Hamelberg, D.; Wang, B.: Clicking 1,2,4,5-tetrazine and cyclooctynes with tunable reaction rates. *Chem. Commun.* **2012**, *48*, 1736-1738.
- (56) Sauer, J.; Heldmann, D. K.; Hetzenegger, J.; Krauthan, J.; Sichert, H.; Schuster, J.: 1,2,4,5-tetrazine: Synthesis and reactivity in 4+2 cycloadditions. *Eur. J. Org. Chem.* **1998**, 2885-2896.
- (57) Blackman, M. L.; Royzen, M.; Fox, J. M.: Tetrazine Ligation: Fast Bioconjugation Based on Inverse-Electron-Demand Diels-Alder Reactivity. *J. Am. Chem. Soc.* **2008**, *130*, 13518-13519.
- (58) Devaraj, N. K.; Upadhyay, R.; Hatin, J. B.; Hilderbrand, S. A.; Weissleder, R.: Fast and Sensitive Pretargeted Labeling of Cancer Cells through a Tetrazine/trans-Cyclooctene Cycloaddition. *Angew. Chem. Int. Ed.* **2009**, *48*, 7013-7016.
- (59) Blackman, M. L.; Royzen, M.; Fox, J. M.: Tetrazine ligation: Fast bioconjugation based on inverse-electron-demand Diels-Alder reactivity. *J. Am. Chem. Soc.* **2008**, *130*, 13518-13519.
- (60) Taylor, M. T.; Blackman, M. L.; Dmitrenko, O.; Fox, J. M.: Design and Synthesis of Highly Reactive Dienophiles for the Tetrazine-trans-Cyclooctene Ligation. *J. Am. Chem. Soc.* **2011**, *133*, 9646-9649.

- (61) Devaraj, N. K.; Weissleder, R.; Hilderbrand, S. A.: Tetrazine-Based Cycloadditions: Application to Pretargeted Live Cell Imaging. *Bioconjugate Chem.* **2008**, *19*, 2297-2299.
- (62) Cole, C. M.; Yang, J.; Seckute, J.; Devaraj, N. K.: Fluorescent Live-Cell Imaging of Metabolically Incorporated Unnatural Cyclopropene-Mannosamine Derivatives. *ChemBioChem* **2013**, *14*, 205-208.
- (63) Thalhammer, F.; Wallfahrer, U.; Sauer, J.: Reactivity of simple open-chain and cyclic dienophiles in inverse-type diels-alder reactions. *Tetrahedron Letters* **1990**, *31*, 6851-6854.
- (64) Liang, Y.; Mackey, J. L.; Lopez, S. A.; Liu, F.; Houk, K. N.: Control and Design of Mutual Orthogonality in Bioorthogonal Cycloadditions. *J. Am. Chem. Soc.* **2012**, *134*, 17904-17907.
- (65) Grossman, R. B.; The Art of Writing Reasonable Organic Reaction Mechanisms. Second edition, *Springer-Verlag New York Inc*, **2003**, pp 173-174.
- .

CHAPTER 2

REGIOSELECTIVE INVERSE DIELS-ALDER REACTION OF UNSYMMETRICAL TETRAZINES WITH ALDEHYDES AND KETONES

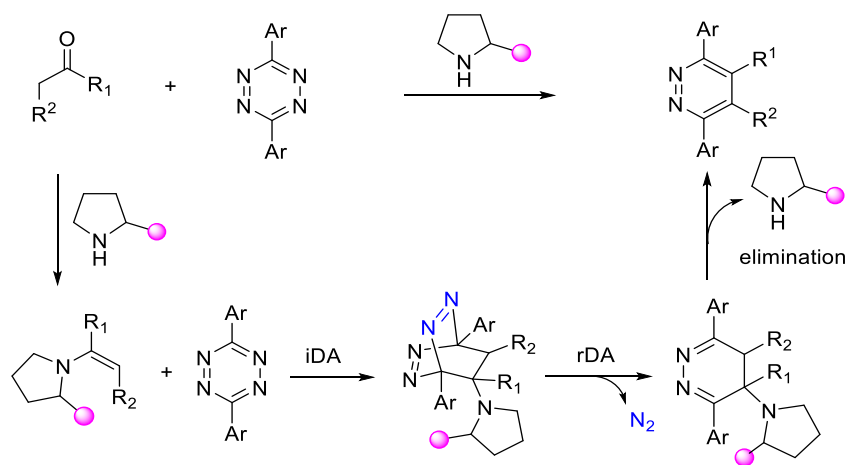
2.1. INTRODUCTION

The reactivity of tetrazines and alkenes in inverse electron demand Diels-Alder reactions (iDA) depends on the differences in energies between the lowest unoccupied molecular orbital of the diene ($\text{HOMO}_{\text{diene}}$) and the highest occupied molecular orbital of the dienophile ($\text{LUMO}_{\text{dienophile}}$).^{1,2} Thus, one can easily improve the kinetics of the reaction by either placing electron withdrawing groups on the 3,6-position of the tetrazine, or having electron donating groups on the α -position of the dienophile. Most of the bioconjugation reactions performed to date using iDA reactions have relied on strained alkenes or alkynes since angle strains increase the HOMO energy level of the dienophiles and consequently improve the kinetics of the iDA reactions.³⁻⁵ Each of the strained alkenes or alkynes used for the reaction has its unique advantages, but *trans*-cyclooctene remains the most used dienophile for iDA ligations due to its exceptional reactivity.¹

Although *trans*-cyclooctene is very reactive and could easily react with most tetrazines at room temperature with kinetics fast enough for biolabeling, it is unstable and thus requires storage at subzero temperatures.⁷ Other strained alkenes such as norbornene, *cis*-cyclooctene and cyclooctyne are more stable at room temperature but have low reactivity relative to *trans*-cyclooctene, and in some instances do not react with some

tetrazines at mild conditions needed for bioconjugation.⁸ There is therefore the need to develop more reactive dienophiles for tetrazines ligation using reagents that are both stable and having reactivity that is fast enough for bioconjugation

Sauer and coworkers studied the reaction of 1,2,4,5-tetrazine and electron rich dienophiles, such as enamines, ynamines and enol ethers and found that enamines display the fastest kinetics among non-strained dienophiles.² However, the low stability of enamines, especially in water greatly compromises their reactivity and potential applications in bioconjugation. To circumvent this, Wang and coworkers used proline as a catalyst to promote direct iDA reactions of ketones with tetrazines via the *in situ* formation of the enamine intermediate (Scheme 2.1).⁹ The enamines underwent iDA reaction with tetrazine followed by retro Diels-Alder reaction, which resulted in the loss of nitrogen molecules. However, only symmetric tetrazines were tested in that study. In this work, we report the regioselectivity of the direct iDA reaction of aldehydes and ketones with unsymmetrical tetrazines as well as the potential application of the reaction in bioimaging.



Scheme 2.1. Reaction Pathway of secondary amine-catalyzed iDA reaction between ketones/aldehydes and tetrazines.

2.2 RESULTS AND DISCUSSION

2.2.0 Reactivity of tetrazines with *in situ* generated enamines.

Tetrazines, **2.1** - **2.4**, (Figure 2.1) were synthesized according to the method by Deveraj and coworkers with little modifications.¹⁰ whiles tetrazine **2.5** was synthesized by first making dichlorotetrazine using procedure by Clavier and coworkers,¹¹ followed by reaction of the dichlorotetrazine with *n*-butylamine to obtain compound **2.5**.¹² Initial screening of the iDA reaction of the tetrazines with *in situ* generated enamines using hexanaldehyde and pyrrolidine showed that whiles tetrazines, **2.1**, **2.2** and **2.4** reacted easily leading to the disappearance of the purple color of the tetrazines, tetrazines **2.3** and **2.5** remained unreactive, even after stirring at 100 °C for 24 hours.

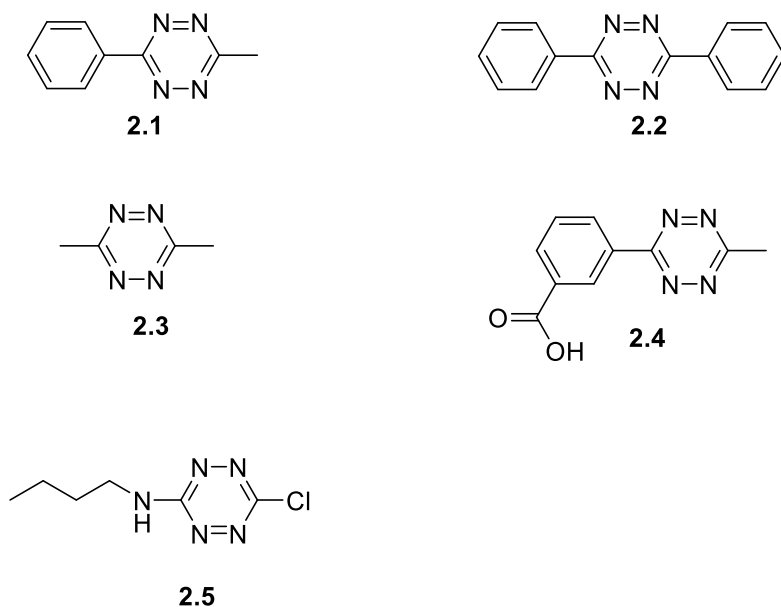


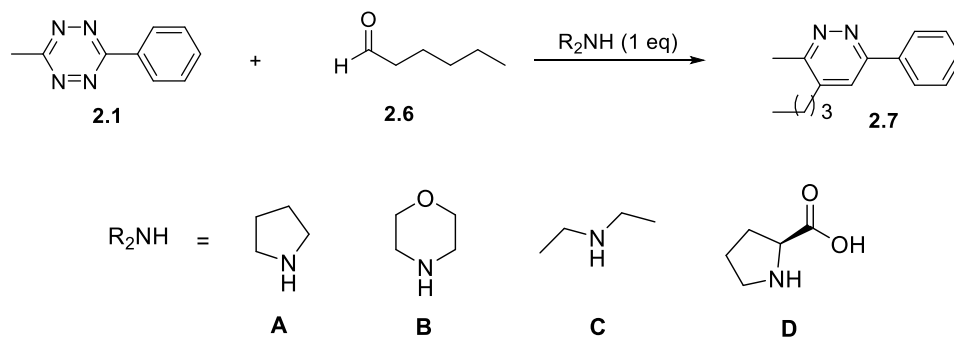
Figure 2.1. Tetrazines tested for iDA reactions.

To further investigate the reactivity and regioselectivity of the secondary amine-catalyzed iDA reactions of unsymmetrical tetrazines with aldehydes and ketones, a selection of secondary amines (**A-D**) was screened as catalysts for the reaction of 3-methyl-6-phenyl-1,2,4,5-tetrazine (**2.1**) with hexanaldehyde (**2.6**). All the reactions proceeded smoothly at room temperature to produce a single cycloadduct **2.7**, in 45-95% yield. The use of pyrrolidine or morpholine in acetonitrile or dichloromethane furnished the product in 89-95% yield within 5 minutes (Table 2.1, Entries 1, 2, 4); whereas using diethylamine took 15 minutes (Entry 5). When we replaced the secondary amines with proline, similar yields were observed in DMSO (Entry 9-10), but no products were observed when other solvents were used, even with heating. The use of acetonitrile and water (1:1) resulted in a 45% yield (Entry 3), and a significant amount of unidentified by-products. As control reactions, by mixing the tetrazine with secondary amines in the absence of aldehydes or ketones, we observed no product formation, but a gradual degradation of the starting material over 24 hours. This was also confirmed by NMR, and by observing the disappearance of the purple color of the tetrazine.

Using pyrrolidine as the catalyst, we studied the reactivity and regioselectivity of a number of aldehydes and ketones with asymmetric tetrazines (**2.1**). NMR analysis of the crude products taken after each reaction unambiguously confirmed the formation of a sole isomeric product in each case (Table 2.2). Upon purification, single crystal analysis of some of the products were obtained to further confirm their regioselectivity. Figure 2.2 shows the NMR spectra of the sole products obtained by reaction of the tetrazine with (a) acetone and (b) propionaldehyde. Figure 2.3 shows the crystal structure of the product

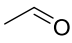
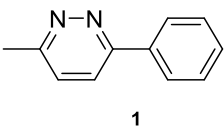
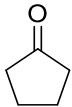
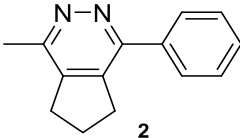
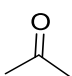
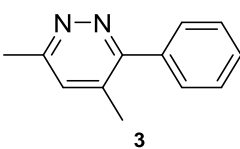
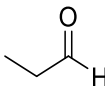
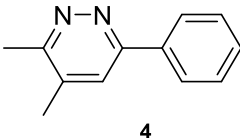
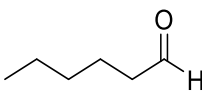
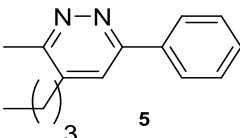
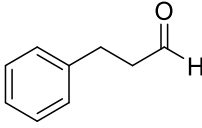
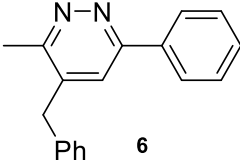
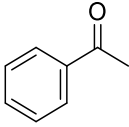
obtained by the reaction of the tetrazine with 3-phenylpropionaldehyde (Table 2.2, Entry 6).

Table 2.1. Regioselectivity of secondary amine-catalyzed iDA reaction of hexanaldehyde with an unsymmetrical tetrazine.



Entry	R_2NH	Solvent	Temperature	Time	Yield (%)
1	A	CH_2Cl_2	rt	5 min	95
2	A	CH_3CN	rt	5 min	89
3	A	$CH_3CN:H_2O$ (1:1)	100 °C	24 h	45
4	B	CH_2Cl_2	rt	5 min	95
5	C	CH_2Cl_2	rt	15 min	94
6	D	CH_2Cl_2	rt	24 h	0
7	D	CH_3CN	rt	24 h	0
8	D	toluene	100 °C	24 h	0
9	D	DMSO	rt	24 h	94
10	D	DMSO	100 °C	10 min	95

Table 2.2. Pyrrolidine-catalyzed regioselective reaction of 3-methyl-6-phenyl-1,2,4,5-tetrazine (**2.1**) with aldehydes/ketones

Entry	Aldehyde/Ketone	Product	Yield (%)
1		 1	99
2		 2	99
3		 3	94
4		 4	98
5		 5	95
6		 6	89
7		No reaction	ND

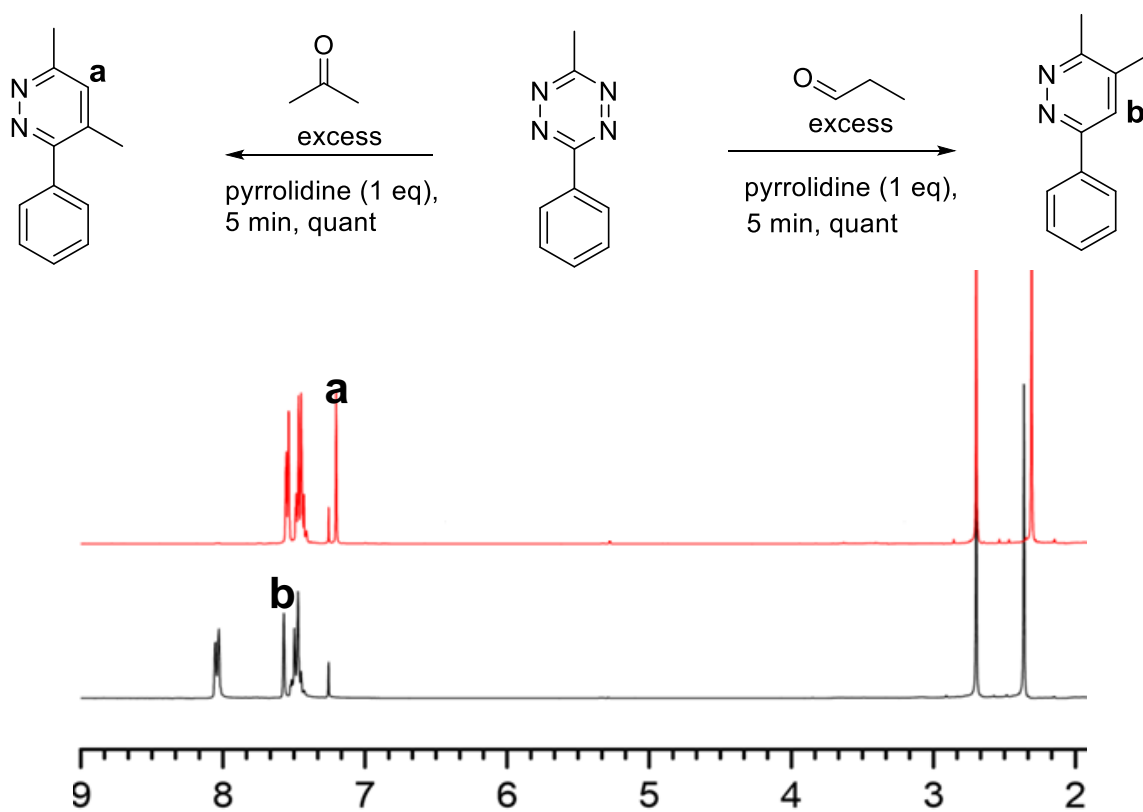


Figure 2.2. NMR spectra showing regioselectivity in iDA reaction of 3-methyl-6-phenyl-1,2,4,5-tetrazine with acetone (a) and propionaldehyde (b).

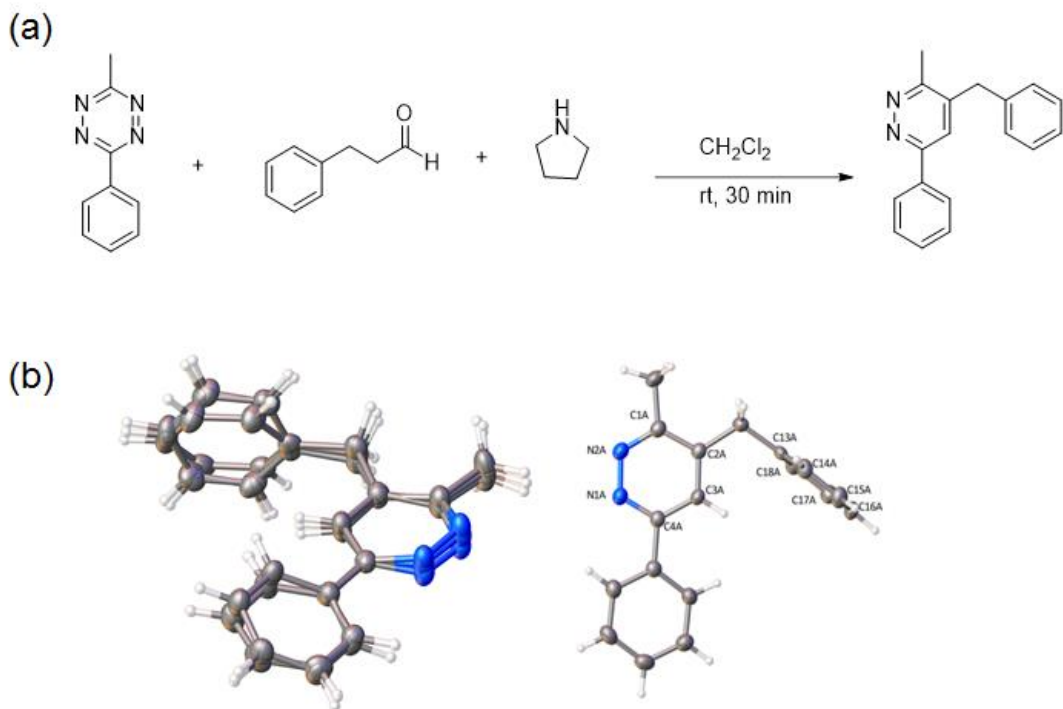
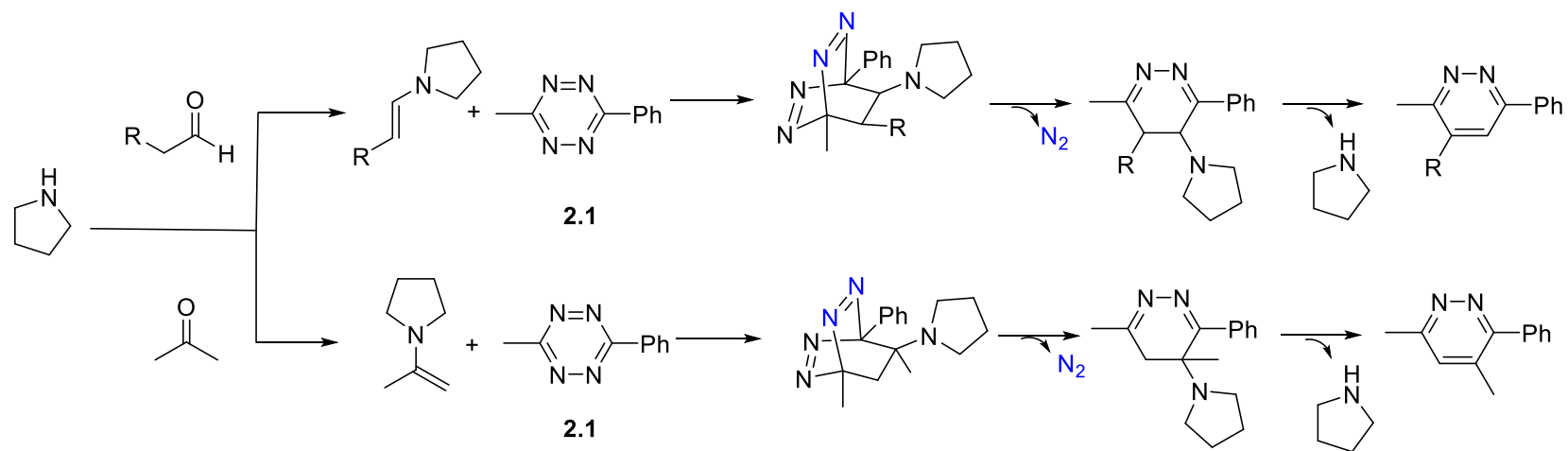


Figure 2.3. (a) The amine-catalyzed iDA reaction of 3-methyl-6-phenyl-1,2,4,5-tetrazine with phenylpropionaldehyde (b) Single crystal structures of the sole product obtained.

The regioselectivity of the products formed were consistent with what one would expect according to the zwitterionic models of alignment of dienophiles with unsymmetrical dienes during the Diels-Alder reaction.¹³ In this case, the transition state of the intermediate favors placement of the secondary amine and the phenyl substituent of the tetrazine on the same side (Scheme 2.2).

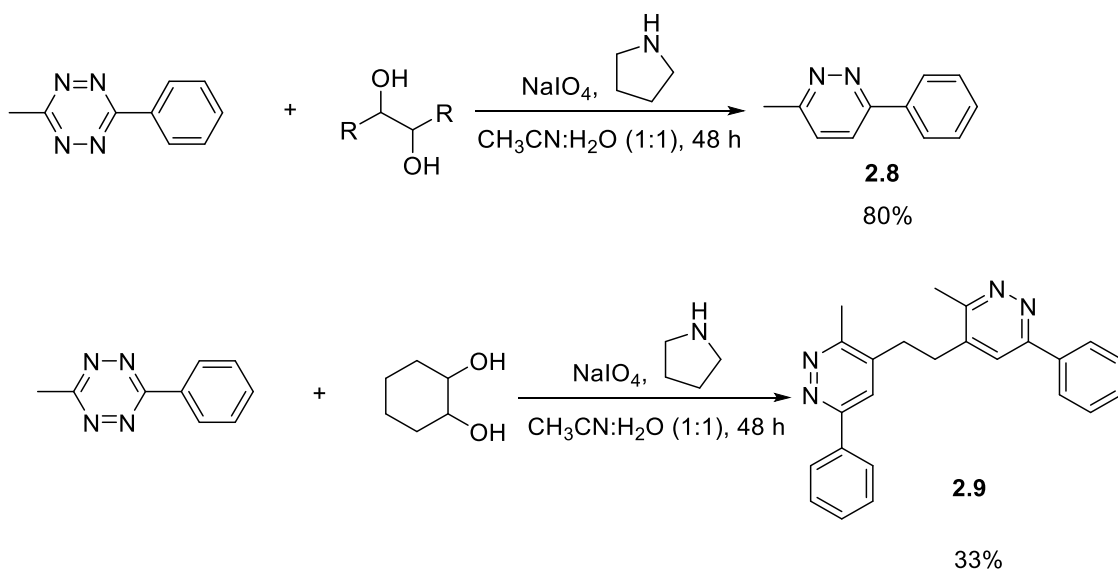
2.2.1 Oxidation of diols to aldehydes, enamine formation and iDA reaction in one pot

Since aldehydes can be generated from diols by oxidation with sodium periodate.¹⁴⁻¹⁶ We envisaged that the iDA reactions of tetrazines could be extended to vicinal diols, by first treating a mixture of tetrazine and a vicinal diol with sodium periodate, and immediately adding a secondary amine to the reaction mixture. This would generate an enamine that could subsequently undergo iDA reaction with the tetrazine. We selected two



Scheme 2.2. Proposed mechanism of the regioselective reaction of unsymmetrical tetrazine with aldehydes/ketones.

diols for the initial screening; 2,3-butanediol and 1,2-cyclohexanediol, and the reaction was carried out in 50% acetonitrile in water. The reaction with 1,2-butanediol proceeded smoothly to afford the desired pyridazine **2.8** in 80% yield after 18 hours of stirring at room temperature, whereas the reaction with 1,2-cyclohexanediol afforded the desired product **2.9** in 33% after 48 hours of stirring (Scheme 2.3). However, the reaction did not work with sialic acid and estriol, two known biomolecules containing diols.



Scheme 2.3. One pot oxidation of diols to aldehydes, enamine formation and iDA reactions.

2.2.3 Screening for stability of tetrazine and the reactivity of the amine-catalyzed iDA reaction in water

Having advanced our standing on the reactivity of the tetrazines in base-catalyzed iDA reactions, we proceeded to test the compatibility of our reactants in aqueous media. Methylphenyltetrazine (**2.1**) was dissolved in 1-5 mM solutions of pyrrolidine in DMSO:H₂O (10%). After 48 hours, the purple color of tetrazines in pyrrolidine solution of

3 mM or more disappeared while those in 1-2 mM solutions of tetrazine did not show any change. This shows that the methylphenyltetrazine degrades in solutions at pyrrolidine concentrations higher than 2 mM.

We further proceeded to screen the iDA reaction of the tetrazine with a number of aldehydes or ketones, and different amines as shown in Figure 2.4. After 24 hours, the wells with diethylamine or pyrrolidine showed complete conversion whereas morpholine did not show any conversion when mixed with glucose and galactose. The iDA reactions catalyzed by proline only showed conversion for hexanaldehyde and propionaldehyde, but not the ketones, glucose or galactose. We therefore concluded that proline is the least reactive of the secondary amines. We were however unable to characterize the product of the reactions involving glucose and galactose.

2.2.4 Synthesis of fluorogenic tetrazines for bioimaging

Tetrazines are chromophores with absorption wavelengths between 500 and 600 nm.¹⁷ However, upon reaction with dienophiles, the absorption band within this wavelength disappears.¹⁷ This unique property, coupled with its exceptional reactivity makes tetrazine both a quencher and a bioorthogonal reactor. Weisleder and coworkers have demonstrated that this ability of a tetrazine to modulate fluorescence of dyes is due mainly to Förster resonance energy transfer (FRET) between the fluorophore and tetrazine, as only green- and red- emitting dyes show significant fluorescence quenching when functionalized with tetrazines.¹⁸ The quenching effect is truncated once the tetrazine undergoes iDA reaction to furnish the desired product, leading to restoration of the fluorescence.^{19,20}

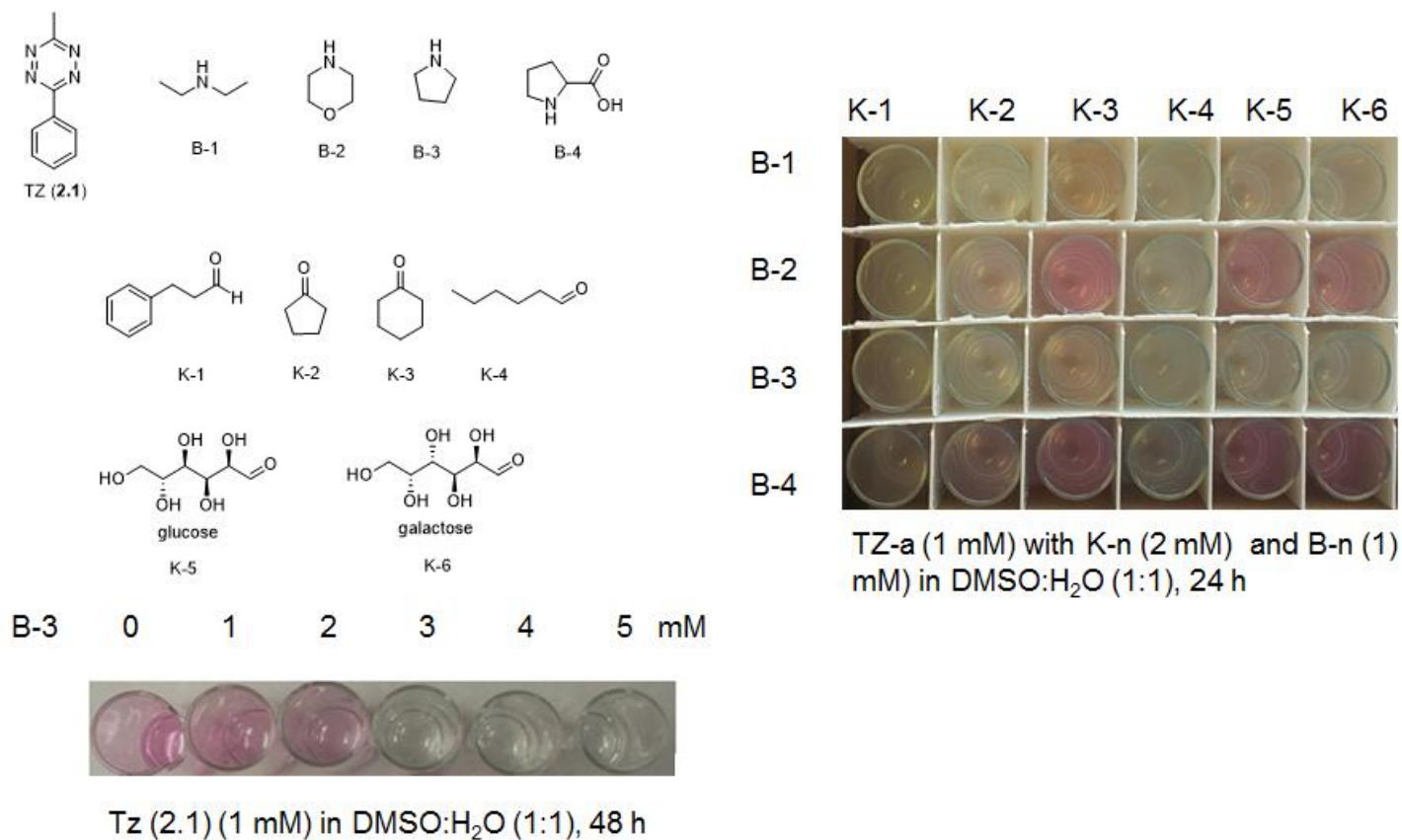


Figure 2.4. Combinatorial screening of amine-catalyzed iDA reaction of tetrazine with aldehydes and ketones. Aldehyde (K-1 and K-4) worked better than ketone. Concentration of bases higher than 2 mM causes destruction of tetrazine.

To choose the appropriate dye for our fluorogenic tetrazines, the absorption spectra for the tetrazine to be outfitted on a fluorophore were measured. Compound **2.4** showed maximum absorption at 534 nm (Figure 2.5a) whereas compound **2.5** showed a maximum absorption at 514 nm (Figure 2.5b). We therefore chose to synthesize naphthalimide-tetrazine conjugates as our bioorthogonal fluorogenic reactors since naphthalimide dyes have maximum emissions at wavelengths within the range of our tetrazines (Figure 2.5c). They also have large Stokes shifts, and high photostability, making them fluorophores of choice for biolabeling experiments.²¹

Fluorogenic naphthalimide-tetrazine dyes **2.11** and **2.13** were therefore prepared. Naphthalimide-tetrazine, **2.11** was synthesized by addition of dichlorotetrazine to the amine terminal of naphthalimide dye **2.10** (scheme 2.4a) while **2.13** was synthesized by EDCI and NHS mediated coupling of **2.4** to the amine terminal of **2.10** (Scheme 2.4b). Significant quenching of the naphthalimide dye was observed after functionalization with each of the tetrazine compounds.

Upon addition of stoichiometric amounts of phenylpropionaldehyde and diethylamine to each dye in dichloromethane, the naphthalimide-tetrazine dyes underwent iDA reactions to furnish fluorescent compounds. The fluorescence turn on ratios for **2.11** was 600 folds, while that of **2.13** was only 18 folds (Figure 2.5). This observation is most likely due to the fact that, the *n*-butylchlorotetrazine dye's (**2.5**) maximum absorption wavelength of 514 nm is closer to the naphthalimide dye's maximum emission wavelength of 507 nm than the tetrazine benzoic acid (**2.4**). Another factor that could have influenced the quenching efficiency of the dyes by the tetrazines is the distance between the naphthalimide and tetrazines linked together. Since the distance between the dye and

tetrazine for **2.11** is shorter than that of **2.13**, it is expected that a more effective quenching effect, and a higher turn on ratio would be observed for **2.11** than **2.13**.

NMR and MS analysis of the product of the iDA reaction of phenylpropionaldehyde with **2.11** showed the elimination of the amine to produce pyridazine did not occur in this instant, which could be due to relative stability of the dihydropyridazine of **2.12** over that of **2.14** and the methylphenyltetrazine (**2.1**).

2.2.5 Application of the fluorogenic naphthalimide-tetrazine dye in bioimaging

To evaluate the utility of the fluorogenic naphthalimide-tetrazine dyes in imaging aldehyde containing biomolecules in cells, biotin aldehyde (50 μ M), base (proline or pyrrolidine) (100 μ M) were incubated with bone marrow stroma cells (BMSCs) in primary media for 2 hours, after which the cells were washed and the dye, **2.13** (10 μ M) added to the cells in a new media. After 1 hour, the cells were washed again to remove non-binding dyes and visualized under fluorescence microscope. Scheme 2.5 shows the expected iDA reaction of the naphthalimide tetrazine (**2.13**) and biotin-aldehyde (**2.18**)

Nonspecific binding of the dye to the cells, leading to high fluorescence images were observed in the cells, including those without biotin and a base. Nonetheless, comparing the fluorescence intensity of the six different wells containing different combinations of the dye **2.13**, a base and a biotin aldehyde (**2.18**) showed the wells with all the three reagents (Figure 2.7, Exp 2 and Exp 3) showed 30-35% increase in fluorescence intensity relative to the wells with **2.13** but lacking either the base or the biotin aldehyde **2.18**. The increase in the fluorescence intensity is a confirmation of ligation of **2.13** to the biotin aldehyde. It is expected that an appropriate dye, and a longer reaction time will show a higher turn on ratio for the amine-catalyzed iDA ligation.

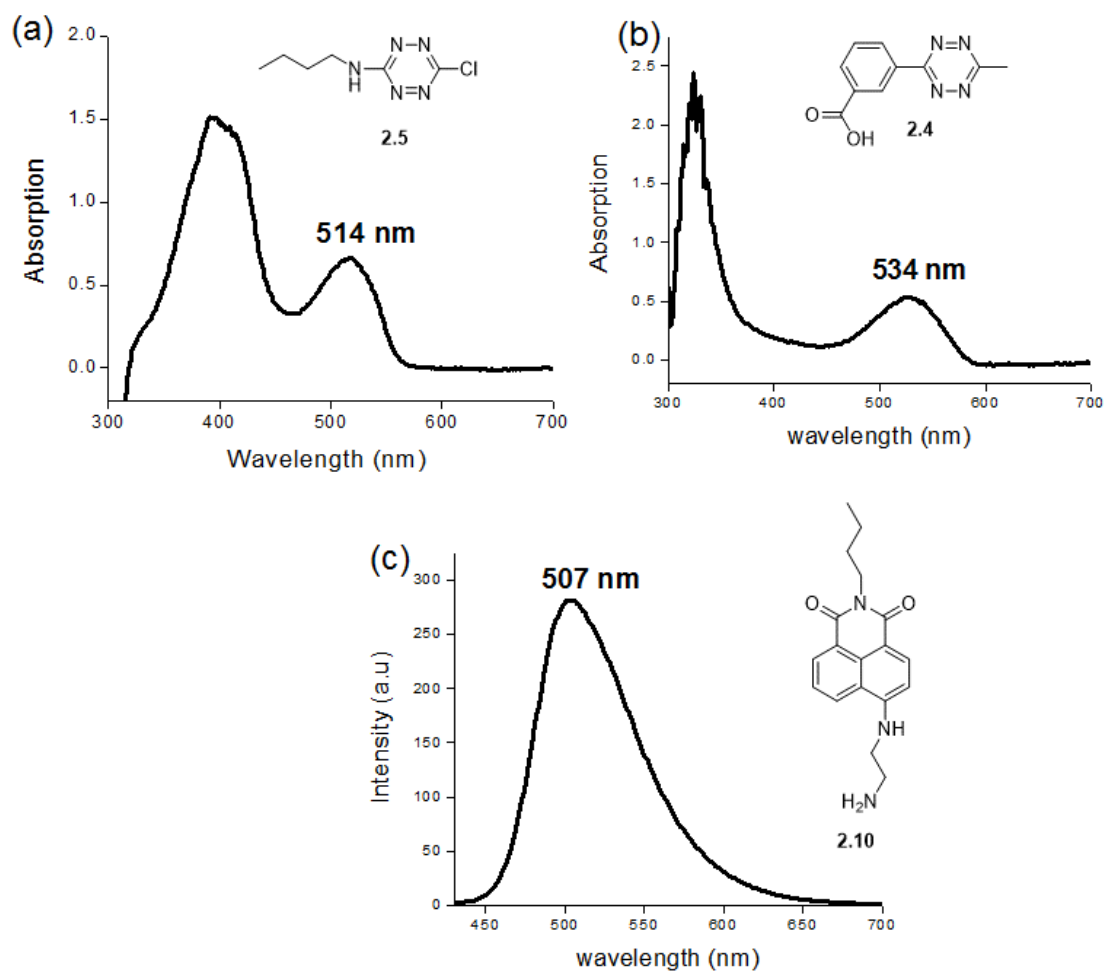
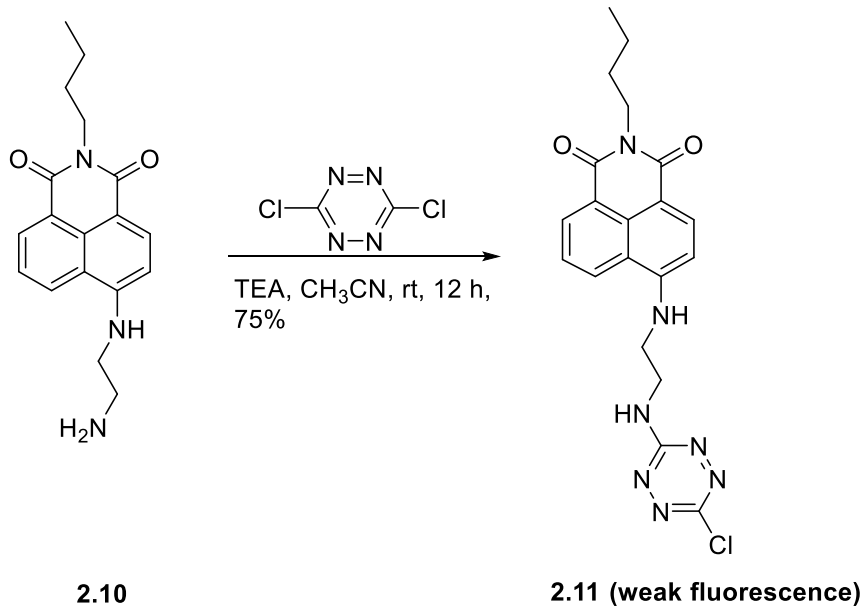
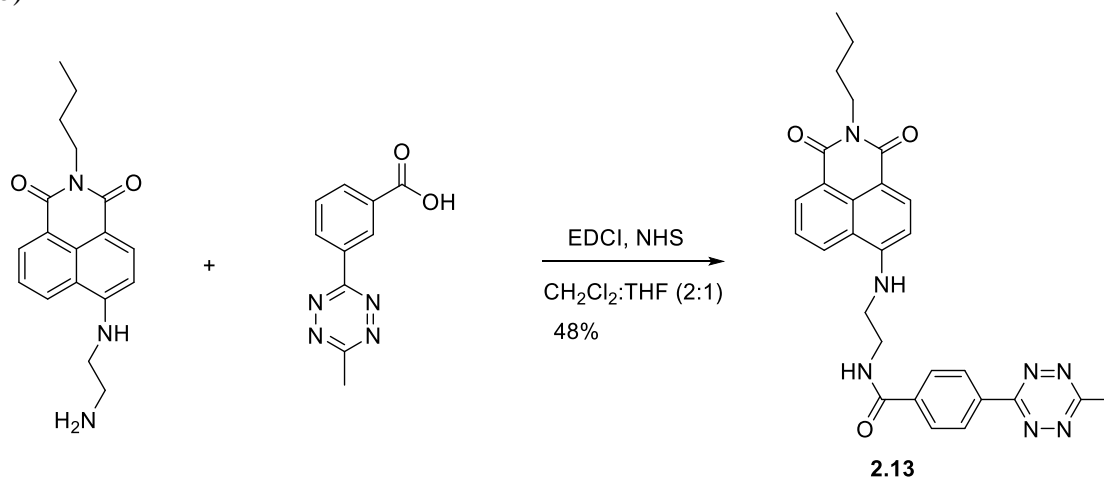


Figure 2.5. (a, b) Absorption spectra of tetrazines **2.5** showing maximum absorption at 514 nm, (a), and **2.4** showing maximum absorption at 534 nm (b). (c) The fluorescence emission spectrum of naphthalimide dye **2.10**.

(a)

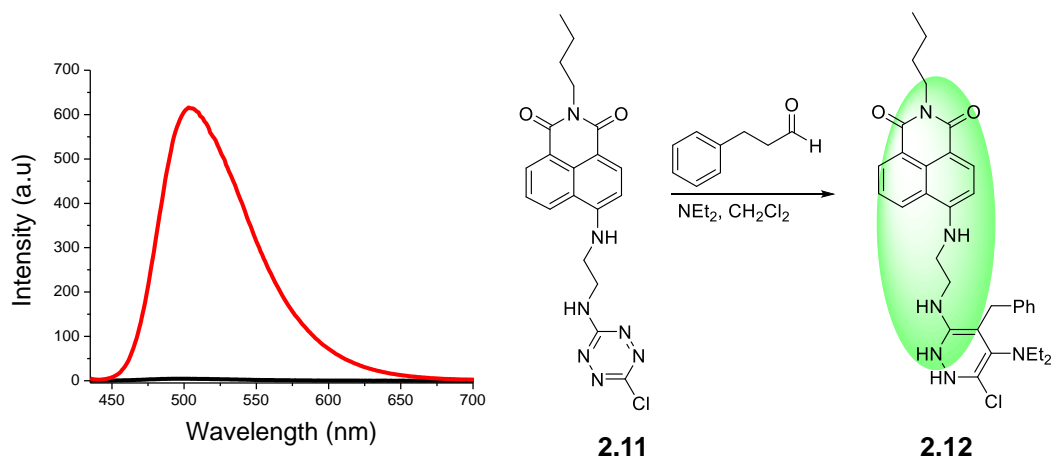


(b)



Scheme 2.4. Synthesis of fluorogenic naphthalimide-tetrazine dyes **2.11** and **2.13**.

(a)



(b)

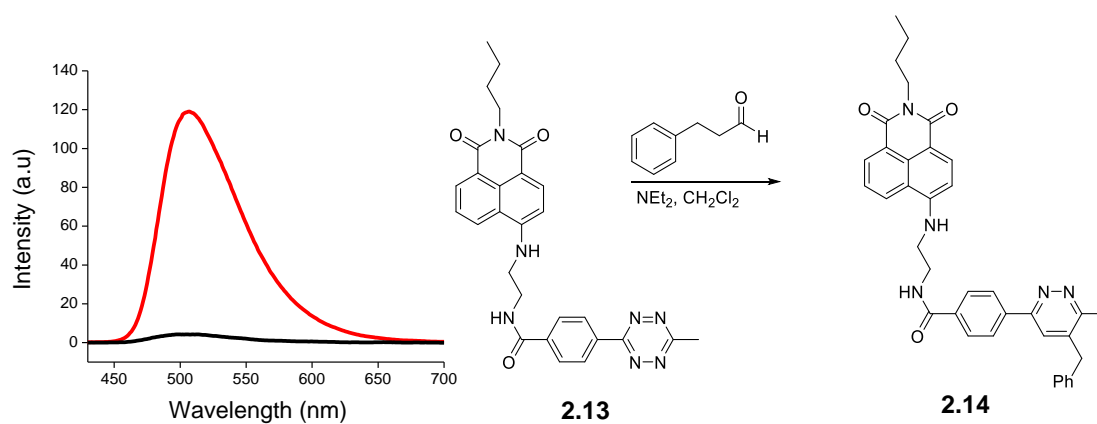
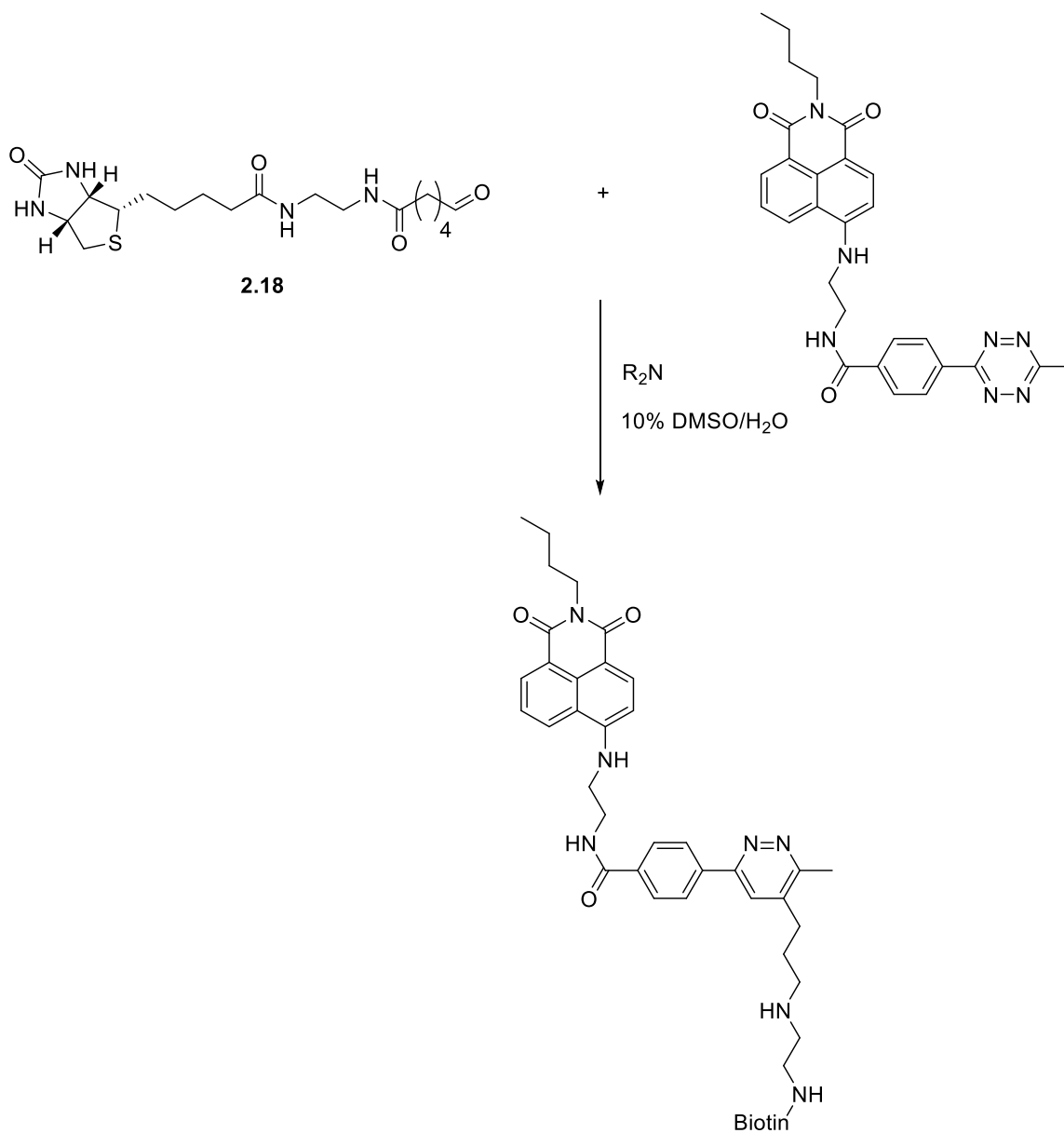


Figure 2.6. (a) Emission spectra of naphthalimide-tetrazine **2.11** (10 μM) (black) and the corresponding iDA product, **2.12** (red) in CH_2Cl_2 (b) Emission spectra of naphthalimide-amide tetrazine **2.13** (10 μM) (black) and the corresponding iDA product **2.14** (red).



Scheme 2.5. Expected reaction of biotin-aldehyde (**2.18**) with tetrazine **2.13**.

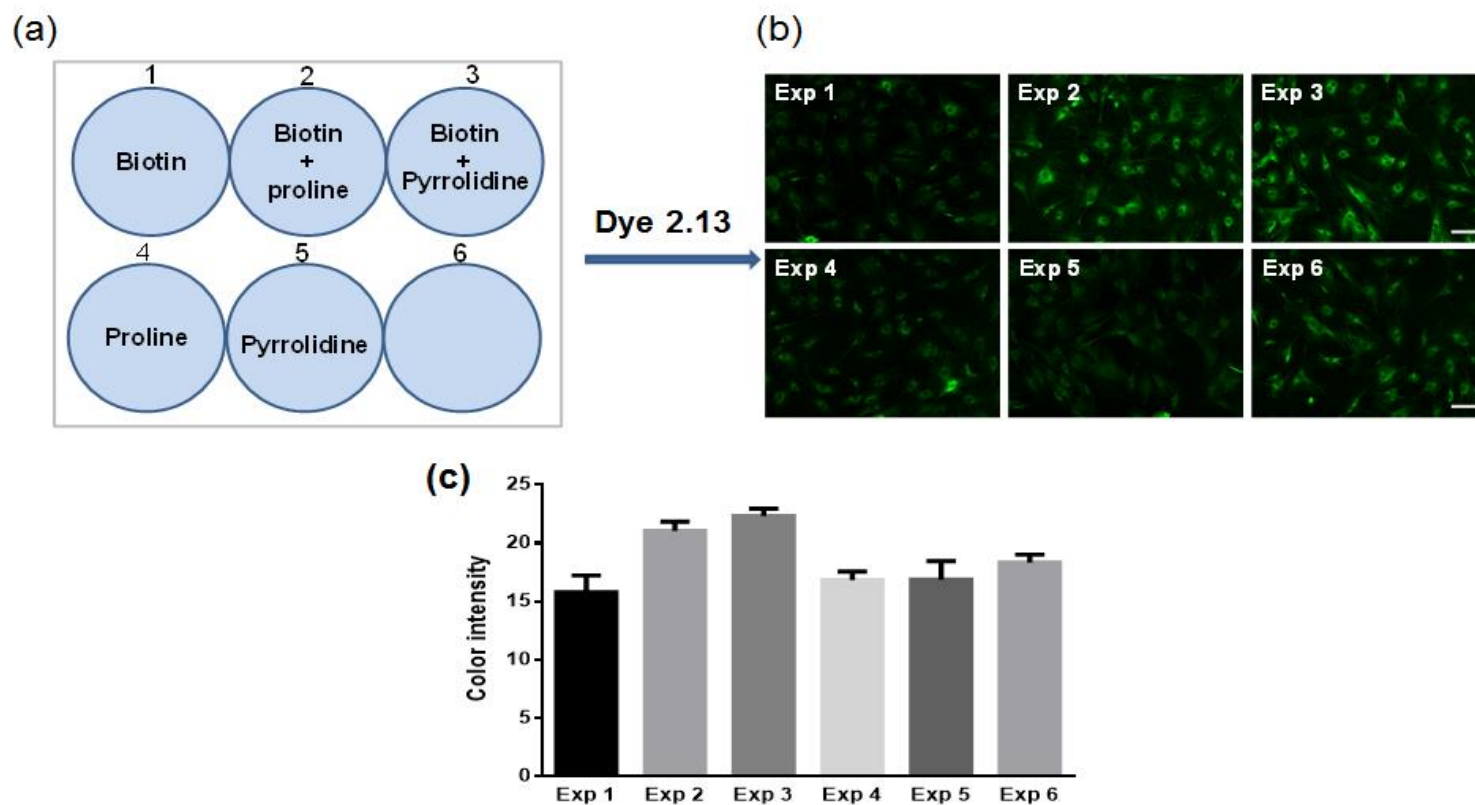


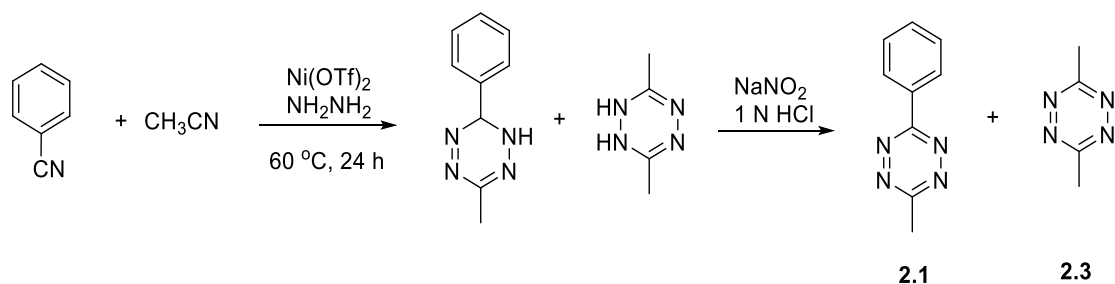
Figure 2.7. Application of fluorogenic tetrazine **2.13** in imaging aldehyde-containing molecules in cells. (a) Cells incubated with biotin aldehyde (50 μ M) and/or an amine (100 μ M); (b) Fluorescent confocal micrograph of cells after addition of dye, **2.13** (10 μ M) (c) Corresponding fluorescent intensity of cells after treatment with **2.13**. Cells incubated with biotin aldehyde and proline (Exp 2); and biotin aldehyde with pyrrolidine (Exp 3) showed higher fluorescent intensity than cells incubated with only biotin (Exp 1), proline (Exp 4) or pyrrolidine (Exp 5). Cells in Exp 6 were incubated without biotin or base prior to addition of **2.13**.

2.3 CONCLUSION

We have established the regioselectivity of secondary amine-catalyzed iDA reaction with unsymmetrical tetrazines such as 3-methyl-6-phenyl-1,2,4,5-tetrazine. The mechanism for the regioselectivity was established to be directed by the alignment of the tetrazine and the enamine formed *in-situ* at the transition state of the iDA reaction; a model which could be used to predict the regioselectivity of the reaction with other unsymmetrical tetrazines. The iDA reaction of tetrazines with vicinal diols was also demonstrated, but this reaction was slow and may not be applicable in cells. The application of the reaction in tuning the fluorescence of fluorogenic dyes having a tetrazine motif was demonstrated, as well as the potential for bioconjugation and imaging molecules containing aldehydes or ketones. The labeling of aldehyde in cells resulted in high background fluorescence. We surmised that this could be due to the hydrophobicity of the dye. It is expected that the use of a hydrophilic dye will result in very low or no unspecific labeling, which will make the reaction more suitable for cell imaging.

2.4 EXPERIMENTAL SECTION

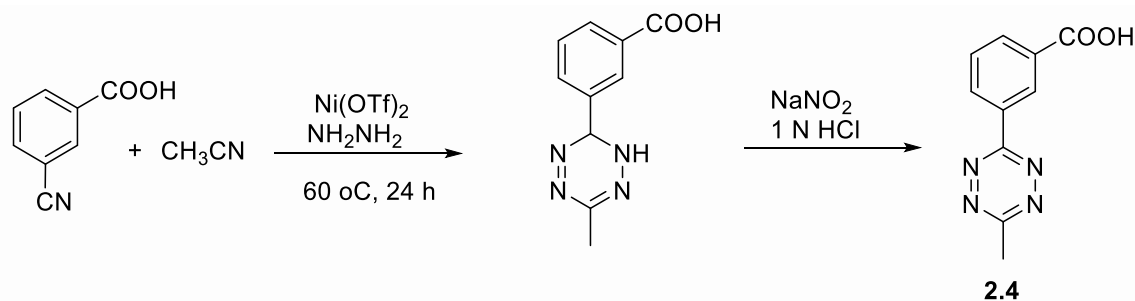
General. Unless otherwise specified all reagents and solvents were of commercial grade. NMR spectra were recorded on Bruker 300 or 400 instruments. Flash column chromatography was performed with silica gel (32-63 μm). High resolution mass spectrometry (HRMS) was obtained using a magnetic sector mass spectrometer.



To a 10 mL sealed tube equipped with a stir bar was added Nickel(II) trifluoromethanesulfonate (100 mg, 0.3 mmol), benzo nitrile (103 mg, 1.0 mmol), acetonitrile (0.52 mL, 10.0 mmol) and anhydrous hydrazine (1.6 mL, 50 mmol). The vessel was sealed and the mixture was stirred in an oil bath at 60° C for 24 hours. After reaction, the mixture was cooled to room temperature and the seal was removed. Sodium nitrite (1.3 g, 20 mmol) in water (10 mL) was slowly added to the solution and followed by slow addition of 1 N HCl during which the solution turned bright red in color and gas evolved. Addition of 1 N HCl continued until gas evolution ceased and pH ~ 3. The mixture was extracted with ethyl acetate (20 x 2) and the organic phase dried over sodium sulfate. The solvent was removed using rotary evaporation and the residue purified using silica column chromatography with dichloromethane:hexane (1:1) as eluent to obtain 3-methyl-6-phenyltetrazine (**2.1**) (85mg, 49%) and a trace amount of dimethyltetrazine (**2.3**) (<5%)

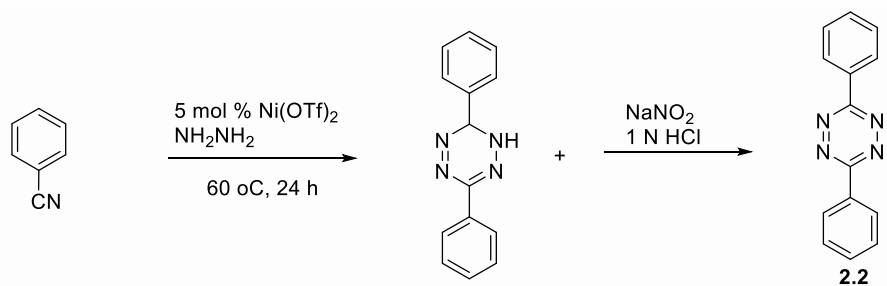
3-Methyl-6-phenyltetrazine (2.1). ¹H NMR (300 MHz, CDCl₃): δ 8.70–8.45 (m, 2H), 7.73–7.50 (m, 3H), 3.10 (s, 3H). ¹³C NMR NMR (75 MHz, CDCl₃): 167.2, 164.2, 132.5, 131.7, 129.2, 127.8, 21.1

3,6-Dimethyltetrazine (2.3). ¹H NMR (300 MHz, CDCl₃): δ 3.04 (s, 6H)



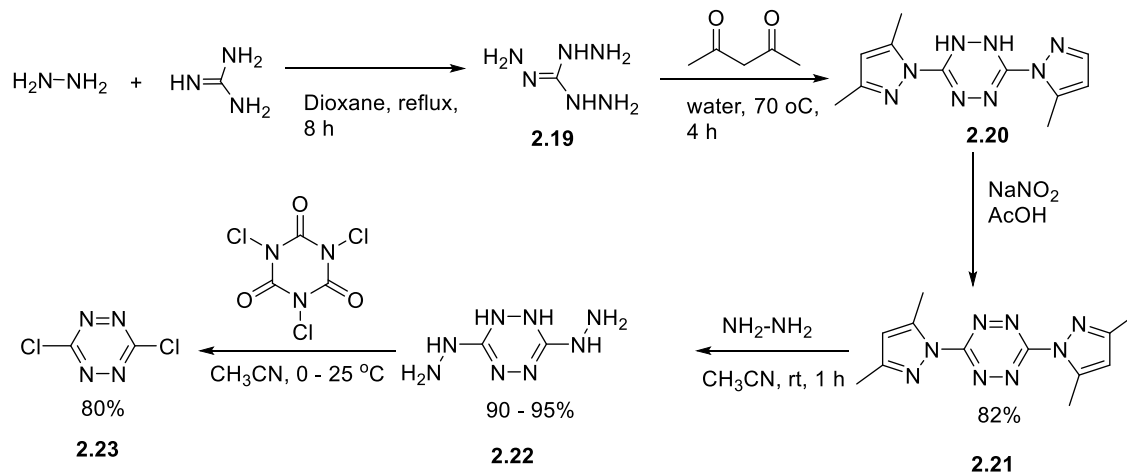
To a 10 mL sealed tube equipped with a stir bar was added Nickel(II) trifluoromethanesulfonate (100 mg, 0.3 mmol), 3-cyanobenzoic acid (103 mg, 1.0 mmol), acetonitrile (0.52 mL, 10.0 mmol) and anhydrous hydrazine (1.6 mL, 50 mmol). The vessel was sealed and the mixture was stirred in an oil bath at 60 °C for 24 hours. After reaction, the mixture was cooled to room temperature and the seal was removed. Sodium nitrite (1.3 g, 20 mmol) in water 10 mL was slowly added to the solution and followed by slow addition of 1N HCl during which the solution turned bright red in color and gas evolved. Addition of 1 N HCl continued until gas evolution ceased and pH ~ 3. The mixture was extracted with ethyl acetate (20 x 2) and the organic phase dried over sodium sulfate. The solvent was removed using rotary evaporation and the residue purified using silica column chromatography to obtain titled compound **2.4** (200 mg, 46%)

¹H NMR (400 MHz, DMSO): δ 13.34 (s, 1H), 9.00 (d, *J* = 12.5 Hz, 1H), 8.68 (d, *J* = 7.9 Hz, 1H), 8.22 (d, *J* = 7.9 Hz, 1H), 7.93–7.71 (m, 1H), 3.11–2.90 (m, 2H). ¹³C NMR (101 MHz, DMSO): δ 167.84, 167.07, 133.30, 132.84, 132.34, 131.87, 130.40, 128.47, 21.33.



To a 10 mL sealed tube equipped with a stir bar was added Nickel(II) trifluoromethanesulfonate (100 mg, 0.3 mmol), benzo nitrile (103 mg, 1.0 mmol), anhydrous hydrazine (1.6 mL, 50 mmol). The vessel was sealed and the mixture was stirred in an oil bath at 60° C for 24 hours. After reaction, the mixture was cooled to room temperature and the seal was removed. Sodium nitrite (1.3 g, 20 mmol) in water 10 mL was slowly added to the solution and followed by slow addition of 1N HCl during which the solution turned bright red in color and gas evolved. Addition of 1 N HCl continued until gas evolution ceased and pH ~ 3. The mixture was extracted with ethyl acetate (20 x 2) and the organic phase dried over sodium sulfate. The solvent was removed using rotary evaporation and the residue purified on silica column chromatography using dichloromethane:hexane (1:1) as eluent to obtain to obtain compound **2.2** (95 mg, 41%) ¹H NMR (300 MHz, CDCl₃): δ 8.85–8.6 (m, 2H), 7.78–7.58 (m, 3H). ¹³C NMR (75 MHz, CDCl₃): 163.9, 132.7, 131.8, 129.3, 127.9.

Synthesis of dichlorotetrazine¹¹



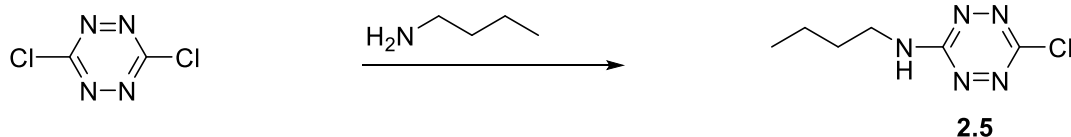
Triaminoguanidine hydrochloride (2.19). To a slurry of guanidine hydrochloride (19.1g, 0.20mol) in 1,4-dioxane (100mL) was added hydrazine monohydrate (34.1g, 0.68mol) with stirring. The mixture was heated under reflux for 2 hours. After the mixture cooled to ambient temperature, the product was collected by filtration, washed with 1,4-dioxane, and dried to give (27 g, quantitative) of pure triaminoguanidine monohydrochloride. ^{13}C NMR (D_2O , 75MHz) δ = 160.5 ppm.

3,6-Bis(3,5-dimethyl-1-H-pyrazol-1-yl)-1,2-dihydro-s-tetrazine (2.20). To a solution of triaminoguanidine monohydrochloride (27.0g, 0.19 mol) in water (150 mL) was added 2,4-pentanedione (39.4 mL, 0.38 mol) dropwise with stirring at room temperature for 0.5 h. The mixture is then heated to 70 °C and stirred for 4 hours, during which time solid precipitated from solution. The mixture was cooled to room temperature, filtered, washed with cold water and dried to obtain the product as a yellow solid (10.1 g, 20%) 3,6-Bis(3,5-dimethylpyrazol-1-yl)-1,2-dihydro-s-tetrazine. ^1H NMR (300 MHz, CDCl_3): δ 8.09 (br s, 2H), 5.95 (s, 2H), 2.47 (s, 6H), 2.21 (s, 6H). ^{13}C NMR (75MHz, CDCl_3): δ 14.9, 148.5, 1, 142.3, 109.8, 13.7, 13.4.

3,6-Bis(3,5-dimethyl-1H-pyrazol-1-yl)-s-tetrazine (2.21). Sodium nitrite (7.1 g, 0.1 mol) was dissolved in water (100 mL) and CH₂Cl₂ (20 mL) was added. The mixture was kept on ice and 3,6-bis(3,5-dimethylpyrazol-1-yl)-1,2-dihydro-s-tetrazine (10.1g, 0.036 mol) was added in batches. Acetic acid (9.3 mL, 0.16 mol) was added dropwise. Gas evolution occurred, after which the organic layer was separated and the aqueous layer was extracted with CH₂Cl₂ (3 x 20mL). The organic layers were combined, washed to neutrality with a 5% aqueous solution of potassium carbonate, dried over anhydrous sodium sulfate and filtered. The solvent was removed *in vacuo* to obtain a dark red solid, which was washed several times with diethyl ether to obtain a brick red solid (8.2g 82%) as the titled compound. ¹H NMR (300 MHz, CDCl₃): δ 2.39 (s, 6H), 2.72 (s, 6H), 6.20 (s, 2H). ¹³C NMR (75 MHz, CDCl₃): δ 13.9, 14.7, 111.9, 143.8, 154.5, 159.3.

3,6-Dihydrazinyl-s-tetrazine (2.22). To a slurry of 3,6-bis(3,5-dimethylpyrazol-1-yl)-s-tetrazine (8.2 g, 0.03 mole) in acetonitrile (50 mL), was added hydrazine monohydrate (2.4 mL, 0.06 mol) dropwise at room temperature. The mixture was refluxed for 30 minutes and cooled to room temperature. The mixture was filtered and washed with acetonitrile to provide a black powder, 4 g, which was used for the next step without further purification.

3,6-Dichloro-s-tetrazine (2.23). To a slurry of 3,6-di(hydrazino)-1,2,4,5-tetrazine (3.5 g, 0.025 mol) in acetonitrile (100 mL) at 0 °C was added in batches trichloroisocyanuric acid (11.4 g, 0.05 mol) over 30 minutes. After the addition, the mixture was allowed to warm to room temperature and stirred further for 30 minutes. White insoluble precipitate formed was removed by filtration and the solvent removed *in vacuo* to give crude 3,6-dichloro-s-tetrazine which was purified on silica column using hexane to obtain orange crystals (1.05 g,). ¹³C NMR (75MHz, CDCl₃): δ 168.1.



6-Butylamino-3-chlorotetrazine (2.5).¹² Dichlorotetrazine (442.5 mg, 2.95 mmol) was dissolved in CH₂Cl₂ (30 mL) and stirred before *N*-butylamine (0.5 mL, 5.06 mmol) was added dropwise over 2 h. The resultant mixture was stirred at room temperature for another 2 h. The solvent was removed and the residue purified on flash column using CH₂Cl₂:hexane (1:2-2:1) gradient to obtain a red product (425 mg, 77%). ¹H NMR (300MHz, CDCl₃): 3.60 (q, *J* = 6.0 Hz, 2H), 1.77-1.63 (m, 2H), 1.52-1.38 (m, 2H) 0.97 (t, *J* = 7.5, 3H) ¹³C NMR (CDCl₃, 300MHz): 161.1, 160.0, 41.4, 30.9, 19.9, 13.6.

Typical procedure for secondary amine catalyzed inverse electron-demand Diels-Alder reactions with aldehyde or ketones (Table 2.2).

A mixture of 3-methyl-6-phenyl-1,2,4,5-tetrazine (20 mg, 0.12 mmol), aldehyde or ketone (0.24 mmol) and pyrrolidine (0.6 mg, 0.12 mmol) in CH₂Cl₂ (5 mL) was stirred at room temperature for 30 minutes. After removal of the solvent *in vacuo*, the crude product was purified by chromatography on silica to afford the desired product.

3-Methyl-6-phenylpyridazine (1).²⁶ ¹H NMR (400 MHz, CDCl₃): δ 8.06 – 8.04 (m, 2H), 7.75 (d, *J* = 8.7 Hz, 1H), 7.53–7.46 (m, 3H), 7.38 (d, *J* = 8.7 Hz, 1H), 2.73 (s, 1H). ¹³C NMR (100 MHz, CDCl₃): δ 158.6, 157.2, 136.5, 129.8, 128.9, 127.2, 126.9, 123.9, 22.1; HRMS (EI): *m/z* calcd for C₁₁H₁₀N₂: 170.0846; found: 170.0844.

1-Methyl-4-phenyl-6,7-dihydro-5H-cyclopenta(d)pyridazine (2). Oil. ¹H NMR (300 MHz, CDCl₃): δ 7.81 (d, *J* = 7.3, 2H), 7.52-7.39 (m, 3H), 3.13 (t, *J* = 7.2, 2H), 2.96 (t, *J* = 7.2, 2H), 2.6 (s, 3H), 2.21-2.07 (m, 2H). ¹³C NMR (100 MHz, CDCl₃): δ 156.4, 155.7,

143.9, 141.6, 137.3, 128.9, 128.5, 128.4, 32.9, 31.0, 29.7, 23.9, 19.9. HRMS (EI): calcd for C₁₄H₁₄N₂: 211.1235; found: 211.1231.

4,6-Dimethyl-3-phenylpyridazine (3). Off white solid. mp 80-82 °C. ¹H NMR (400 MHz, CDCl₃): δ 7.57-7.53 (m, 2 H), 7.50-7.42 (m, 2H), 7.21 (s, 1H), 2.70 (s, 1H), 2.31 (s, 1H). ¹³C NMR (100 MHz, CDCl₃): δ 160.1, 158.3, 137.1, 135.7, 219.1, 128.6, 128.4, 128.3, 21.8, 19.6; HRMS (EI): *m/z* calcd for C₁₂H₁₂N₂: 184.100; found: 184.0995.

3,6-Dimethyl-6-phenylpyridazine (4).²⁷ ¹H NMR (300 MHz, CDCl₃): δ 8.04 (dd, *J* = 7.0, 0.6 Hz, 2H), 7.57 (s, 1H), 7.53-7.44 (m, 3H), 2.70 (s, 3H), 2.36 (s, 3H). ¹³C NMR (100 MHz, CDCl₃): δ 160.1, 158.2, 137.2, 135.7, 129.1, 128.7, 128.5, 128.3, 21.8, 19.6; HRMS(EI): *m/z* calcd for C₁₂H₁₂N₂: 184.100; found: 184.0995.

4-Butyl-3-methyl-6-phenylpyridazine (5). Light yellow oil. ¹H NMR (400 MHz, CDCl₃): δ 8.04 (dd, *J* = 7.2, 0.7 Hz, 2H), 7.54 (s, 1H), 7.51-7.42 (m, 3H), 2.71 (s, 3H), 2.64 (t, *J* = 7.0 Hz, 2H), 1.68-1.58 (m, 2H), 1.50-1.38 (m, 2H), 0.98 (t, 7.3 Hz, 3H). ¹³C NMR (100 MHz, CDCl₃): δ 158.1, 157.7, 140.9, 136.7, 129.5, 128.9, 126.9, 123.1, 31.8, 30.6, 22.5, 19.7, 13.9; HRMS (EI): *m/z* calcd for C₁₂H₁₂N₂: 226.1470; found: 226.1466.

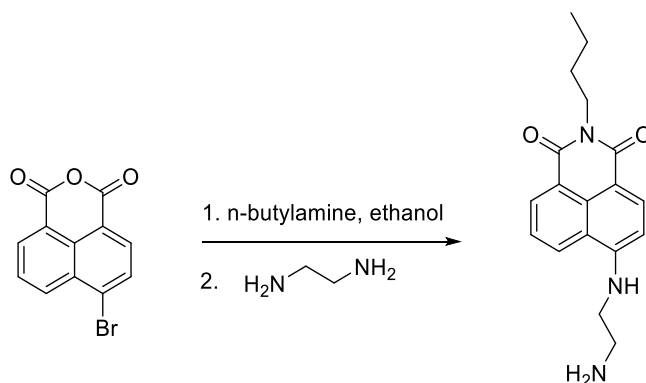
4-Benzyl-3-methyl-6-phenylpyridazine (6). Off white solid. mp 128-133 °C. ¹H NMR (400 MHz, CDCl₃): δ 7.99 (d, *J* = 6.3 Hz, 2H), 7.52-7.42 (m, 4H), 7.38-7.29 (m, 3H), 7.15 (d, *J* = 7.2, 2H), 4.02 (s, 2H), 2.7 (s, 3H). ¹³C NMR (100 MHz, CDCl₃): δ 158.2, 157.7, 140.89, 136.7, 129.5, 128.8, 126.9, 123.1, 31.7, 30.6, 22.5, 19.74, 13.9; HRMS (EI): *m/z* calcd for C₁₈H₁₆N₂: 260.1316; found: 260.1313.

General procedure oxidation of the diols to aldehydes, enamine formation and IDA reaction in one pot.

To a mixture of 3-methyl-6-phenyl-1,2,4,5-tetrazine (40.0 mg, 0.24 mmol), a 1,2-diol (0.24 mmol) in CH₃CN:H₂O was added NaIO₄ (1 M, 300 μ L). The mixture was stirred at room temperature for 5 minutes, and pyrrolidine (0.6 mg, 0.12 mmol) was added. The mixture was further stirred for 24 hours, diluted with water and extract into dichloromethane. The organic layer was dried over sodium sulfate anhydrous and the solvent removed *in vacuo*. The crude was purified by chromatography on silica to afford the desired product.

2.9 ¹H NMR (300 MHz, CDCl₃): δ 8.14–7.93 (m, 4H), 7.58–7.44 (m, 8H), 3.03 (s, 6H), 2.87–2.72 (m, 4H). HRMS (EI): *m/z* calcd for C₂₄H₂₂N₄: 366.1844; found: 366.1837.

Synthesis of naphthalimide dye 2.10



2.10. Following the literature procedure,^{22,23} a mixture of naphthalimide anhydride (1.0 g, 3.6 mmol) in ethanol (10 mL) and *n*-butylamine (1 mL, excess) was stirred at room temperature overnight. A precipitate was formed, which was filtered, washed with ethanol and dried in vacuo to obtain a white solid (725.0 mg, 60%). The intermediate (331 mg, 1.1 mmol) was refluxed in ethylenediamine (5 mL, excess) and heated to 80 °C for 6 h. The mixture was cooled to room temperature, poured slowly unto ice and allowed to warm to room temperature. A precipitate formed was filtered and dried to obtain a yellow solid

(300.5 mg, 92%). ^1H NMR (300 MHz, DMSO): δ 8.68 (d, J = 8.5 Hz, 1H), 8.40 (d, J = 7.2 Hz, 1H), 8.23 (d, J = 8.5 Hz, 1H), 7.65 (t, J = 7.8 Hz, 1H), 6.78 (d, J = 8.5 Hz, 1H), 3.99 (t, J = 7.3 Hz, 2H), 3.39 (dd, J = 26.4, 20.0 Hz, 5H), 2.83 (dd, J = 23.5, 17.1 Hz, 3H), 1.68 – 1.46 (m, 2H), 1.43 – 1.17 (m, 2H), 0.90 (t, J = 7.3 Hz, 3H).

NT-tetrazine 2.11. To compound **2.10** (104.6 mg, 0.34 mmol) in acetonitrile (10 mL) dichlorotetrazine (50.5 mg, 0.34 mmol) and TEA (100 μL) were added. The reaction was stirred at room temperature for 12 h. The product was poured in water (30 mL) and filtered to obtain a dark red solid, which was purified by chromatography on silica using CH_2Cl_2 : CH_3OH (10:0.1-10:0.5) gradient to obtain **10** as dark red solid (106 mg, 75%). mp 221-223 $^\circ\text{C}$. ^1H NMR (400 MHz, CDCl_3): δ 8.44 (d, J = 8.0 Hz, 1H), 8.33 (d, J = 8.0 Hz, 1H), 8.02 (d, J = 8.0 Hz, 1H), 7.51 (t, J = 8.0 Hz, 1H), 7.07 (br s, 1H), 6.66 (d, J = 8.0 Hz, 1H), 6.63 (br s, 1H), 4.13-4.04 (m, 4H), 3.77 (t, J = 7.1 Hz, 2H), 1.70-1.60 (m, 2H), 1.46-1.35 (m, 2H), 0.94 (t, J = 7.1 Hz, 3H). ^{13}C NMR (100 MHz, CDCl_3): δ 164.5, 164.1, 161.9, 161.1, 148.9, 134.1, 131.2, 129.5, 126.0, 125.0, 122.9, 120.2, 110.8, 104.1, 43.7, 40.6, 40.1, 30.9, 30.2, 20.4, 13.9; HRMS (ESI): m/z ($\text{M}+\text{H}$) calcd for $\text{C}_{20}\text{H}_{20}\text{ClN}_7\text{O}_2$: 426.1445; found: 426.1451.

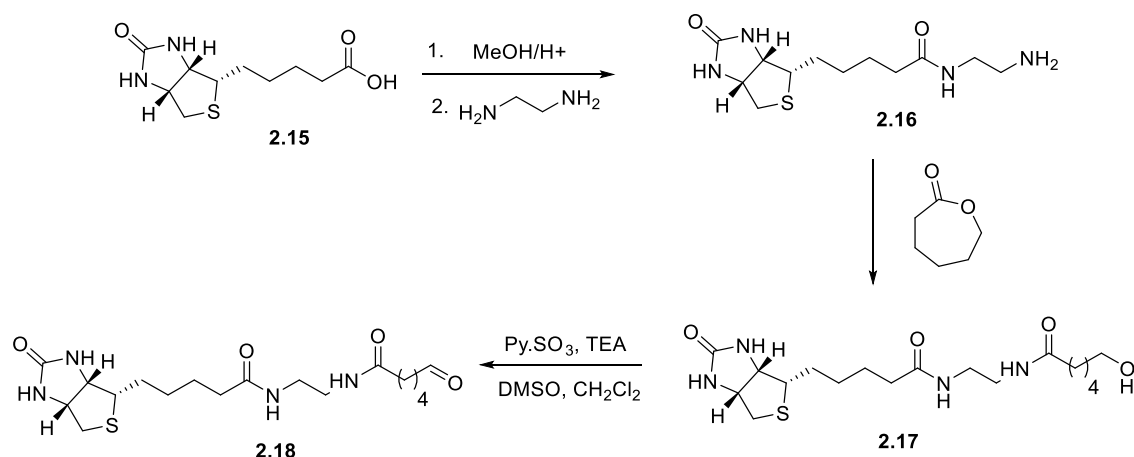
NT-diazine (2.12). NT-tetrazine **2.11** (50.0 mg, 0.18 mmol) in dry CH_2Cl_2 (50.0 mg, 0.18 mmol) was mixed with phenylpropionaldehyde (15.8 mg, 0.18 mmol) and diethylamine (18 μL , 0.18 mmol). The mixture was stirred at room temperature for 24 h and the solvent removed *in vacuo*. The crude green fluorescent mixture was purified on silica gel column with CH_2Cl_2 : CH_3OH (20:1) to obtain **2.11** as yellow solid (25 mg, 38%). mp 103-106 $^\circ\text{C}$ ^1H NMR (400 MHz, CDCl_3): δ 8.57 (d, J = 8.3 Hz, 1H), 8.42 (d, J = 8.3 Hz, 1H), 8.32 (d, J = 8.3 Hz, 1H), 8.21 (br s, 1H), 7.65 (t, J = 7.7 Hz, 1H), 7.14 (d, J = 7.0 Hz, 2H), 7.11-

7.01 (m, 3H), 6.48 (d, $J = 8.3$ Hz, 1H), 4.15 (t, $J = 7.5$ Hz, 2H), 3.87 (s, 2H), 3.50 (brs, 2H), 3.29 (s, 1H), 3.06-2.95 (m, 1H), 2.89-2.80 (m, 1H), 2.55-2.45 (m, 2H), 2.41-2.29 (m, 2H), 2.19-2.04 (m, 2H), 1.77-1.64 (m, 2H), 1.52-1.37 (m, 2H), 0.96 (t, $J = 7.1$ Hz, 3H), 0.64 (t, $J = 8.0$ Hz, 6H). ^{13}C NMR (CDCl_3 , 100 MHz). δ 164.8, 164.4, 157.9, 150.4, 135.9, 134.4, 134.1, 129.7, 129.1, 128.8, 128.0, 127.3, 124.9, 122.6, 120.4, 109.5, 102.7, 43.1, 40.8, 39.7, 35.7, 30.1, 20.5, 13.9, 13.4; HRMS (ESI): m/z (M+H) calcd for $\text{C}_{20}\text{H}_{20}\text{ClN}_7\text{O}_2$: 587.2901; found: 587.2896.

Naphthalimide-amidotetrazine 2.13: To tetrazine **2.4** (70.1 mg, 0.32 mmol) in CH_2Cl_2 (10 mL) was added EDCI (50.2 mg, 0.32 mmol) and *N*-hydroxysuccinimide (37.3 mg, 0.32 mmol). After 15 minutes of stirring, naphthalimide ethylenediamine (100.0 mg, 0.32 mmol) was added. THF (5 mL) was added to dissolve the dye and the reaction stirred at room temperature for 20 h. The reaction mixture was further diluted with dichloromethane and washed with water. The organic layer was dried over anhydrous sodium sulfate and purified on silica column using dichloromethane to obtain the product (71.9 mg, 48%).

^1H NMR (400 MHz, DMSO): δ 9.0-9.03 (br s, 1H), 8.96-8.93 (br s, 1H), 8.74–8.56 (m, 2H), 8.41 (d, $J = 6.8$ Hz, 1H), 8.24 (d, $J = 8.4$ Hz, 1H), 8.16 (d, $J = 6.8$ Hz, 1H), 7.95 (s, 1H), 7.79 – 7.64 (m, 2H), 6.94 (d, $J = 8.2$ Hz, 1H), 4.03-3.94 (m, 2H), 3.69–3.60 (m, 4H), 3.02 (s, 3H), 1.61–1.51 (m, 2H), 1.37–1.23 (m, 2H), 0.91 (t, $J = 7.2$ Hz, 3H). ^{13}C NMR (101 MHz, DMSO): δ 167.83, 166.46, 164.14, 163.35, 151.06, 135.73, 134.57, 132.56, 131.46, 131.14, 130.46, 130.06, 129.82, 128.86, 126.55, 124.84, 122.30, 120.60, 108.27, 104.99, 104.23, 42.74, 38.59, 30.25, 21.35, 20.28, 14.20. HRMS (ESI): m/z calcd for $\text{C}_{18}\text{H}_{16}\text{N}_2$: 510.2248; found: 510.2248.

Synthesis of biotin-aldehyde



To a suspension of biotin **2.15** (244.0 mg, 1.0 mmol) in methanol (10 mL) was added a drop of concentrated H_2SO_4 . The mixture was stirred at room temperature till all the biotin dissolved (72 h). The methanol was removed under vacuum to obtain a white precipitate as the biotin ester (255 mg, quantitative).

To the biotin ester (258.5 mg, 1.0 mmol) in 10 mL of methanol was added ethylenediamine (5 mL, excess) and the mixture stirred at 60 °C for 24 h. The methanol was removed under vacuum and the remaining diamine removed by azeotropic distillation under vacuum using methanol and toluene to obtain **2.16** as a yellow solid.²⁴ ^1H NMR (300 MHz, CD_3OD) δ 4.57–4.42 (m, 1H), 4.38–4.24 (m, 1H), 3.7–3.30 (m, 4H), 3.04–2.96 (m, 2H), 2.71 (d, J = 12.7 Hz, 1H), 2.39–2.14 (m, 2H), 1.84–1.55 (m, 4H), 1.52–1.34 (m, 2H).

2.17. To compound **2.16** (230 mg, 0.76 mmol) in dioxane 10 mL was added caprolactone (86.6 mg, 0.7 mmol). The mixture was refluxed for 24 h and the solvent removed to obtain a brown oil which was precipitate in diethyl ether and filtered to obtain **2.17** as brown solid, which was used for the next step without further purification.

2.18. To compound **2.17** (300.0 mg, 0.75 mmol) in CH_2Cl_2 (4 mL) and DMSO (1 mL) was added TEA (1 mL) followed by SO_3 .pyridine (190.0 mg, 1.5 mmol) in 4 portions over 20

minutes. The mixture was stirred at room temperature for 2 h, then poured into diethyl ether. A yellow precipitate formed was filtered, washed with diethyl ether and dried to obtain a brown solid (250.0 mg). ^1H NMR (300 MHz, CDCl_3) δ 9.39 (s, 1H), 4.36-4.01 (m, 2H), 3.47 (d, J = 6.9, 1H), 3.38-3.08 (m, 7H), 2.75 (t, J = 7.5 Hz 2H), 1.73-1.58 (m, 2H), 1.54-1.12 (m, 12H).

2.5 REFERENCES

- (1) Chen, W.; Wang, D.; Dai, C.; Hamelberg, D.; Wang, B.: Clicking 1,2,4,5-tetrazine and cyclooctynes with tunable reaction rates. *Chem. Commun.* **2012**, 48, 1736-1738.
- (2) Sauer, J.; Heldmann, D. K.; Hetzenegger, J.; Krauthan, J.; Sichert, H.; Schuster, J.: 1,2,4,5-tetrazine: Synthesis and reactivity in 4+2 cycloadditions. *Eur. J. Org. Chem.* **1998**, 2885-2896.
- (3) Taylor, M. T.; Blackman, M. L.; Dmitrenko, O.; Fox, J. M.: Design and Synthesis of Highly Reactive Dienophiles for the Tetrazine–trans-Cyclooctene Ligation. *J. Am. Chem. Soc.* **2011**, 133, 9646-9649.
- (4) Blackman, M. L.; Royzen, M.; Fox, J. M.: Tetrazine ligation: Fast bioconjugation based on inverse-electron-demand Diels-Alder reactivity. *J. Am. Chem. Soc.* **2008**, 130, 13518-13519.
- (5) Debets, M. F.; Van Berkel, S. S.; Dommerholt, J.; Dirks, A. J.; Rutjes, F.; Van Delft, F. L.: Bioconjugation with Strained Alkenes and Alkynes. *Accts. Chem. Res.* **2011**, 44, 805-815.
- (6) Sletten, E. M.; Bertozzi, C. R.: Bioorthogonal Chemistry: Fishing for Selectivity in a Sea of Functionality. *Angew. Chem. Int. Ed.* **2009**, 48, 6974-6998.
- (7) Darko, A.; Wallace, S.; Dmitrenko, O.; Machovina, M. M.; Mehl, R. A.; Chin, J. W.; Fox, J. M.: Conformationally strained trans-cyclooctene with improved stability and excellent reactivity in tetrazine ligation. *Chem. Sci.* **2014**, 5, 3770-3776.
- (8) Thalhammer, F.; Wallfaher, U.; Sauer, J.: Reactivity of simple open-chain and cyclic dienophiles in inverse-type Diels-Alder reactions. *Tetrahedron Letters* **1990**, 31, 6851-6854.

- (9) Xie, H.; Zu, L.; Oueis, H. R.; Li, H.; Wang, J.; Wang, W.: Proline-Catalyzed Direct Inverse Electron Demand Diels–Alder Reactions of Ketones with 1,2,4,5-Tetrazines. *Org. Lett.* **2008**, *10*, 1923-1926.
- (10) Yang, J.; Karver, M. R.; Li, W.; Sahu, S.; Devaraj, N. K.: Metal-Catalyzed One-Pot Synthesis of Tetrazines Directly from Aliphatic Nitriles and Hydrazine. *Angew. Chem. Int. Ed.* **2012**, *51*, 5222-5225.
- (11) Gong, Y.-H.; Miomandre, F.; Méallet-Renault, R.; Badré, S.; Galmiche, L.; Tang, J.; Audebert, P.; Clavier, G.: Synthesis and Physical Chemistry of s-Tetrazines: Which Ones are Fluorescent and Why? *Eur. J. Org. Chem.* **2009**, *2009*, 6121-6128.
- (12) Novak, Z.; Bostai, B.; Csekei, M.; Lorincz, K.; Kotschy, A.: Selective nucleophilic substitutions on tetrazines. *Heterocycles* **2003**, *60*, 2653-2668.
- (13) Jurberg, I. D.; Chatterjee, I.; Tannert, R.; Melchiorre, P.: When asymmetric aminocatalysis meets the vinylogy principle. *Chem. Commun.* **2013**, *49*, 4869-4883.
- (14) Kohler, J. J.: Aniline: A Catalyst for Sialic Acid Detection. *ChemBioChem* **2009**, *10*, 2147-2150.
- (15) Zeng, Y.; Ramya, T. N. C.; Dirksen, A.; Dawson, P. E.; Paulson, J. C.: High-efficiency labeling of sialylated glycoproteins on living cells. *Nat Meth* **2009**, *6*, 207-209.
- (16) Jourdian, G. W.; Dean, L.; Roseman, S.: The Sialic Acids: XI. A Periodate-Resorcinol Method For The Quantitative Estimation Of Free Sialic Acids And Their Glycosides. *J. Biol. Chem.* **1971**, *246*, 430-435.
- (17) Dumas-Verdes, C.; Miomandre, F.; Lepicier, E.; Galangau, O.; Vu, T. T.; Clavier, G.; Meallet-Renault, R.; Audebert, P.: BODIPY-Tetrazine Multichromophoric Derivatives. *Eur. J. Org. Chem.* **2010**, 2525-2535.

- (18) Gong, Y.; Pan, L.: Recent advances in bioorthogonal reactions for site-specific protein labeling and engineering. *Tetrahedron Letters* **2015**, *56*, 2123-2132.
- (19) Devaraj, N. K.; Hilderbrand, S.; Upadhyay, R.; Mazitschek, R.; Weissleder, R.: Bioorthogonal Turn-On Probes for Imaging Small Molecules inside Living Cells. *Angew. Chem. Int. Ed.* **2010**, *49*, 2869-2872.
- (20) Wang, C.; Xie, F.; Suthiwangcharoen, N.; Sun, J.; Wang, Q.: Tuning the optical properties of BODIPY dye through Cu(I) catalyzed azide-alkyne cycloaddition (CuAAC) reaction. *Science China-Chemistry* **2012**, *55*, 125-130.
- (21) Qian, X.; Xiao, Y.; Xu, Y.; Guo, X.; Qian, J.; Zhu, W.: "Alive" dyes as fluorescent sensors: fluorophore, mechanism, receptor and images in living cells. *Chem. Commun.* **2010**, *46*, 6418-6436.
- (22) Wang, J.; Xu, Z.; Zhao, Y.; Qiao, W.; Li, Z.: Synthesis and characterization of novel fluorescent surfactants. *Dyes Pigm.* **2007**, *74*, 103-107.
- (23) Sahin, O.; Yilmaz, M.: Synthesis and fluorescence sensing properties of a new naphthalimide derivative of calix 4 arene. *Tetrahedron Letters* **2012**, *53*, 2319-2324.
- (24) Tao, L.; Geng, J.; Chen, G.; Xu, Y.; Ladmiral, V.; Mantovani, G.; Haddleton, D. M.: Bioconjugation of biotinylated PAMAM dendrons to avidin. *Chem. Commun.* **2007**, 3441-3443.

CHAPTER 3

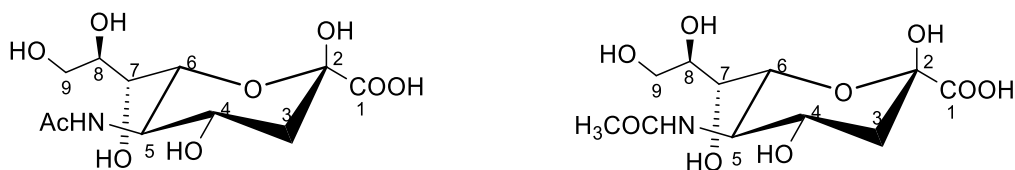
QUARTZ CRYSTAL MICROBALANCE SENSOR FOR DETECTION OF CELLULAR SIALIC ACIDS

3.1 INTRODUCTION

3.1.0 Sialic acids

Sialic acids represent a family of naturally occurring derivatives of the nine carbon sugar, neuraminic acids, attached to the surfaces of cells' proteins, glycans and lipids.¹⁻⁴ They contribute to the structure and functional diversity of glycoproteins, glycolipids and cells; and are important for a number of vital processes such as cell-cell interaction, cell morphology, embryogenesis, development and in immune responses.^{5,6} Two classes of the neuraminic acids exist, the N-acylated forms called the N-acetylneuraminic acids (Neu5Ac), and the N-glycolated forms, known as the N-glycolylneuraminic acids (Neu5Gc) (Figure 3.1a). The N-acetylneuraminic acids are the most ubiquitous of the two groups, and almost the only ones found in humans, The N-glycolylneuraminic acids are common in many animal species but are not found in humans, except in the case of a particular kind of cancer. In addition to the N-substitutions, sialic acids can be O-substituted at C-4, -7, -8, -9, linking acetyl, methyl, sulfate and phosphate groups onto the molecule (Figure 3.1).⁷ On cell surfaces, sialation and desialation of glycoproteins are controlled by sialyltransferases and sialidases (also known as neuraminidases) respectively to create equilibrium for proper cell functioning.⁸ A shift in this equilibrium has been associated with various diseases such as cancer, cardiovascular and neurological diseases.²

(a)



(b)

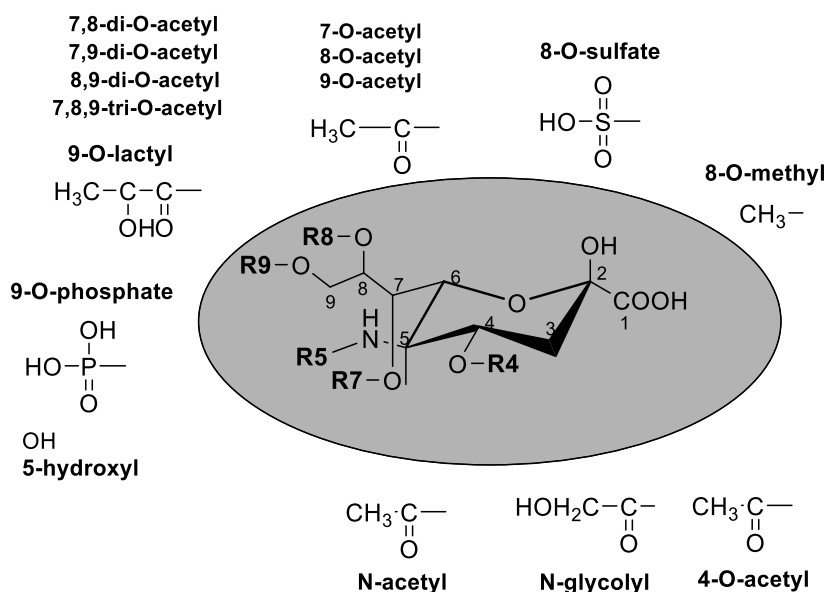


Figure 3.1. (a) Conformation of N-acetylneuraminic acid (Neuc5AC, left) and N-glycolylneuraminic acid (Neu5Gc, right) (b) The family of naturally occurring sialic acids.⁷

3.1.1 Detection of Sialic acids

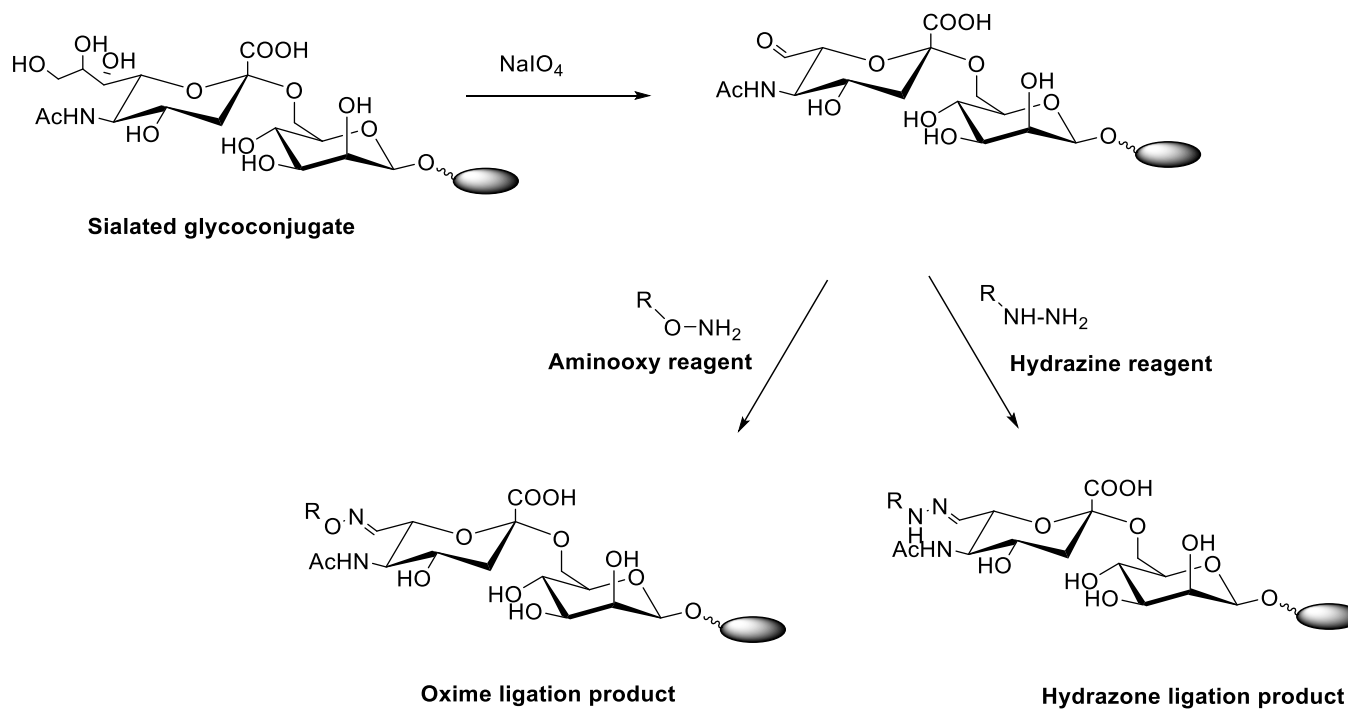
The importance of sialic acids on cell surfaces makes development of methods for identify and studying them, for possible applications in clinical research and diagnosis attractive to chemists and biologists. Several successful methods developed rely on metabolic labeling of cells using analogues of glycan precursors that carry bioorthogonal reporters such as azides or alkynes, for ligation by fluorescent or biotin tags containing complementary functional groups.⁹⁻¹¹ The metabolic incorporation of the analogues

containing bioorthogonal functional groups is nonetheless not trivial, and makes the process inadaptatable for clinical purposes.

A number of methods were therefore developed for direct detection of sialic acids on cell surfaces. These include the use of boronic acid containing sensors that bind to diols of sialic acids,^{12,13} lectins,¹⁴ or aptamers.¹⁵

Another efficient approach involves exploiting the intrinsic reactivity of sialic acids to generate aldehydes on the surface of the cells.¹⁶ The glycerol side chain of sialic acids react with sodium periodate at mild conditions to form aldehydes, which could subsequently react with an amine to form a Schiff base. Hydrazine and hydroxylamines tethered to biotins or fluorescent molecules have been ligated with glycoproteins, glycolipids and glycopeptides containing sialic acid using this approach.^{17,18} Although this method could detect other carbohydrates, under suitably mild conditions, periodates selectively oxidize sialic acids to their C-7 aldehydes, while vicinal diols in the other carbohydrates remain intact (Scheme 3.1).^{16,19,20}

The absence of native aldehydes or ketones on cell surfaces makes the periodate-promoted ligation of amines to sialic acids on cell surfaces chemoselective. However, low reactivity of the α -effect amines makes its applications *in vivo* almost impractical. To circumvent that, aniline was used as a nucleophilic catalyst to catalyze the reaction of the α -effect amines to the sialic acids via transamination.²¹⁻²³ The introduction of aniline as a catalyst was observed not only to increase the kinetics of the reaction, but allowed the ligation to be carried out at neutral pH instead of the slightly acidic medium that only works for the non-catalyzed reactions.



Scheme 3.1. Covalent labeling of sialic acids on cell surface with α -effect amines. Mild periodate treatment selectively oxidizes the terminal glycol of sialic acids to aldehyde for oxime or hydrazone ligation by aminoxy reagents or hydrazine reagent respectively.

In light of the above discoveries, we envisioned that 1,8-diaminonaphthalene (DAN) could be assembled on a Quartz Crystal Microbalance (QCM) chip coated with a graphene and successfully used to detect sialic acids in solution and cell surfaces.

3.1.1 Quartz crystal microbalance

Quartz crystal microbalances (QCM) are ultrasensitive devices that utilize converse piezoelectric effect to determine the mass change from a change in frequency of a quartz crystal resonator.^{24,25} They are capable of measuring masses down to 1 ng/cm². The relationship between the frequency of the quartz crystal and the change in mass was first reported by Sauerbrey.²⁶ He observed that when a voltage is applied to a quartz crystal, it oscillates at a specific frequency. An increase in an elastic mass bound to the quartz surface causes the crystal's oscillation frequency to decrease, and vice versa. The relationship between the change in the mass (Δm) and the corresponding change in the frequency (Δf) was given by the Sauerbrey equation.

$$(\Delta f) = -2\Delta m f^2 / A (\mu \rho_q)^{0.5} = -C_f \Delta m \quad (1)$$

Where Δf is the measured frequency decrease in Hz, f is the intrinsic crystal frequency and Δm is the elastic mass in g. A is the electrode area cm², ρ_q is the density of quartz in g/cm³, μ is the shear modulus in dyn/cm² and C_f is the integrated QCM sensitivity in Hz/ng. The Sauerbrey equation is only valid for small elastic masses added to the crystal surface. When the change in mass is greater than 2% of the crystal mass, the equation becomes invalid.

The QCM chip is a shear mode device consisting of a thin quartz disk with coated electrodes. The electrodes can be made of a number of metals (e.g. gold, silver, platinum etc), and are connected by wires for transmitting the oscillatory signals to a transducer. The

quartz crystal plate must be cut to a specific orientation with respect to the crystal axes (i.e. AT or BT) so that acoustic wave propagates perpendicular to the crystal axes. The AT cuts (35°, 15') from the Z axis of the crystal are the most widely used.^{27,28} The sensitivity of the QCM is inversely proportional to thickness of the crystal: the thinner the crystal, the higher its resonance frequency and sensitivity. Quartz crystals are therefore polished to a hair-thin disc that supports resonance of 1-30 MHz. The diameter of the crystal usually is in the range of 0.3 – 0.5 inches. The temperature dependence of the AT cut is zero at room temperature.²⁸

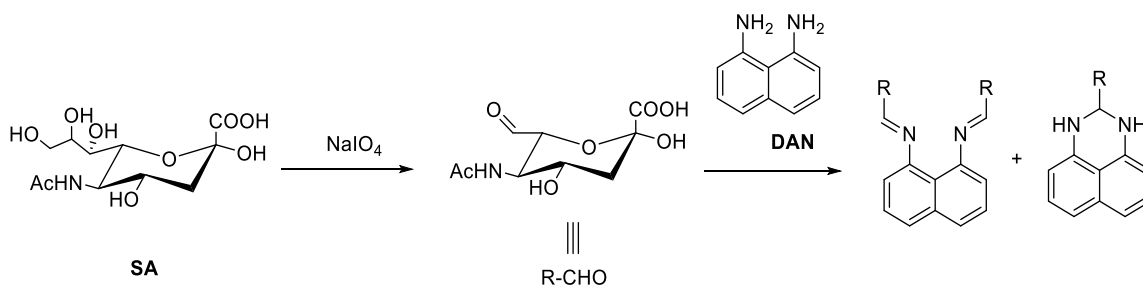
To make the QCM sensitive and specific to a particular analyte, a recognition motif is first adsorbed onto the electrode, followed by introduction of the analyte to the electrode-modified crystal chip. Binding of the analyte onto it recognition motif adsorbed on the quartz chip causes a change in mass, resulting in a change the quartz vibration frequency. This procedure has found utility in the detection and quantifying of a number of important analytes, spanning volatile organic compounds, inorganic molecules, biomolecules, cells and pathogens.^{29,30}

3.2 RESULTS AND DISCUSSION

2.2.0 Development of QCM sensors for sialic acid

The ability of graphene to assemble on QCM and subsequent adsorption of aromatic compounds onto graphene surfaces via π - π stacking has been previously reported.^{31,32} Since amines could react with sialic acids after treatment of the sialic acid with sodium periodate, which converts the terminal diols of the sialic acid into an aldehyde, we anticipated that, immobilizing 1,8-diaminonaphthalene (DAN) onto a QCM coated with graphenes could serve as a sensitive and facile method for detection of sialic acids in

solutions and on cell surfaces. Scheme 3.2 shows the proposed reaction scheme between DAN and sialic acid pretreated with sodium periodate. To this end, graphene was immobilized onto silver-coated QCM chips, followed by assembling of DAN on the graphene surfaces (Figure 3.2). The extent of addition of new materials onto the surface of the chip was determined by the change in the frequency of the QCM chip when the chip was connected to a QCM transducer. When a mass was added a decrease in frequency was observed.



Scheme 3.2. Reaction of 1,8-diaminonaphthalene (DAN) with sialic acid pretreated with sodium periodate.

Figure 3.3a shows the QCM responses for graphene adsorption, DAN assembly, and subsequent binding of sialic acid pretreated with sodium periodate to the functionalized QCM chip. The initial measurement of the QCM chip, which is about 9 MHz was taken after thoroughly washing the chip with ethanol, followed by water and blow-drying with nitrogen. A decrease in the QCM frequency was observed when the chip was later introduced into a suspension of graphenes in ethyl acetate for an hour. To ensure that the change in frequency is only due to the graphenes adsorbed onto the silver surface, the QCM chip was introduced into the graphene solution vertically, and afterwards, washed thoroughly with water and blow-dried with nitrogen to remove any non-binding graphenes

on the QCM surface. This process was repeated for DAN, dissolved in 50% acetonitrile in water, and resulted in further decrease in the frequency of the QCM chip. Subsequently, the QCM chip functionalized with layers of graphene and DAN was used as a sensing platform for sialic acids. As expected, binding of sialic acid, or any analyte resulted in a further decrease in the frequency, while in the cases where no binding occurred, no significant change in the QCM frequency was observed.

Contrary to previous reports that ligation of hydrazines and hydroxylamines to aldehydes only occur, or are at optimum in acidic buffers. The binding of DAN to sialic acid was equally significant at pH = 7.4, and also in deionized water, according to the change in frequencies we observed for the same concentration of sialic acids in three solutions (deionized water, sodium phosphate buffer, pH = 7.4 and sodium acetate buffer pH = 4.6). We therefore chose pH 7.4 for all our subsequent sensing experiments. No changes in frequency was observed when the experiment was repeated for sialic acids that had not been pretreated with sodium periodate. To establish that this method is selective for sensing sialic acids, the experiment was carried out on glucose, with or without treatment with sodium periodate. No frequency change was observed in both treated and untreated glucose as shown in (Figure 3.3 b)

When the binding of sialic acid (1 mg/mL) pretreated with sodium periodate (0.1 M, 300 μ M) to the modified QCM chip was measured with time, an increase in frequency was observed with time for up to about 50 minutes after which no significant change in the frequency was observed (Figure 3.4a). This was due to the fact that all the amines on the QCM surface had reacted with the aldehydes in solution. We further prepared different concentrations of the sialic acid, ranging from 1 mg/mL to 10^{-6} mg/mL and treated them

with sodium periodate for sensing with our QCM chips modified with DAN. Sensitivity of the QCM chips for sialic acid was observed down to 10^{-5} mg/mL. No significant frequency shift was observed for sialic acid concentrations below this concentration after introducing the sensors into the solutions for up to 20 minutes. As anticipated, above this critical sensing concentration, a decrease in frequency was observed with increasing concentration of the sialic acid (Figure 3.4b).

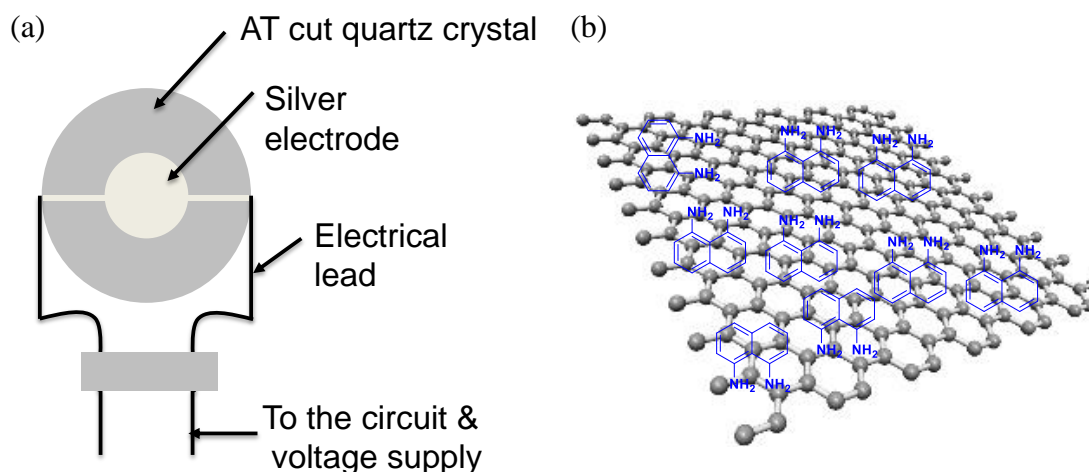


Figure 3.2. (a) Schematic of QCM chip showing one of its two same sides (b) Assembly of DAN on graphene via μ - μ interaction. The graphene is first adsorb onto the silver electrode on both sides of the QCM chip before the DAN assembly.

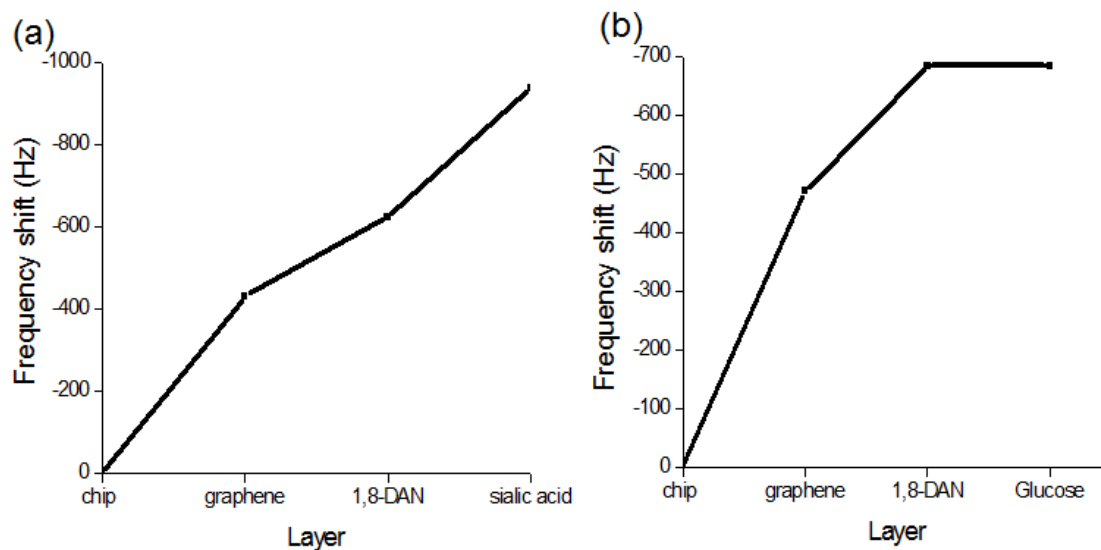


Figure 3.3. Frequency shift in response to sequential binding of graphene, DAN and sialic acid to QCM chip. (b) Frequency shift in response to sequential binding of graphene, DAN and glucose. No frequency change was observed for binding of glucose to DAN.

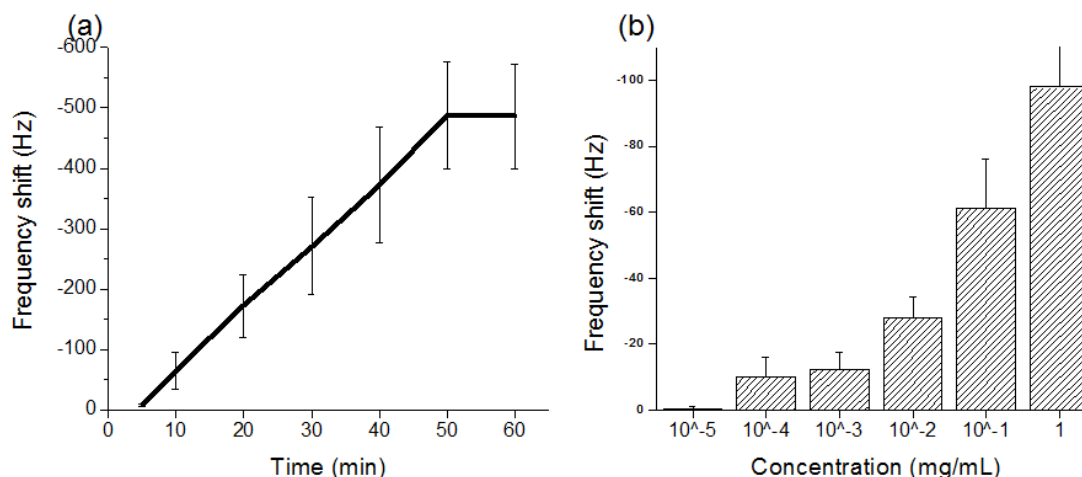


Figure 3.4 (a) Plot of frequency shift with time for binding of sialic acid (1mg/mL) pretreated with sodium periodate (0.1 M, 300 μ L) to QCM-DAN sensing platform. A steady decrease in frequency with time up to 50 minutes observed after which there was no significant change in the frequency. (b) Frequency shifts observed for introducing QCM-DAN chips into different concentrations of sialic acid pretreated with sodium periodate. The chips are immersed in the sialic acid solution for 20 minutes, rinsed with deionized water, blow-dried with nitrogen and the frequency measured on a transducer.

Having established the effectiveness of our probe for sensing sialic acids, we moved on to detect sialic acids on a sialo protein, fetuin from fetal bovine serum. Two different samples of the proteins were prepared in a sodium phosphate buffer (0.5 mg/mL, pH 7.4). One was treated with a neuraminidase and the other solution remained untreated. Neuraminidase are sialic acid cleaving enzymes. When a sialoprotein is treated with neuraminidase, the sialic acids on the proteins are expected to be cleaved from the protein. Sodium periodate solutions (0.1 M, 300 μ L) was later added to the two sialoprotein solutions at 0 $^{\circ}$ C and the solutions kept at the same temperature for 30 minutes. The QCM-modified chips that was introduced into the untreated sialo protein for 30 minutes showed an averaged frequency decrease of almost 270 Hz after three trials whiles the chips

introduced into proteins treated with the enzyme had only about 50 Hz of frequency shift (Figure 3.5). We surmise that there was more decrease in frequency for the untreated sialoprotein because the sialic acids are attached to a higher molecular weight proteins, whereas the treated sialoproteins had mostly free and low molecular weight sialic acid in solution.

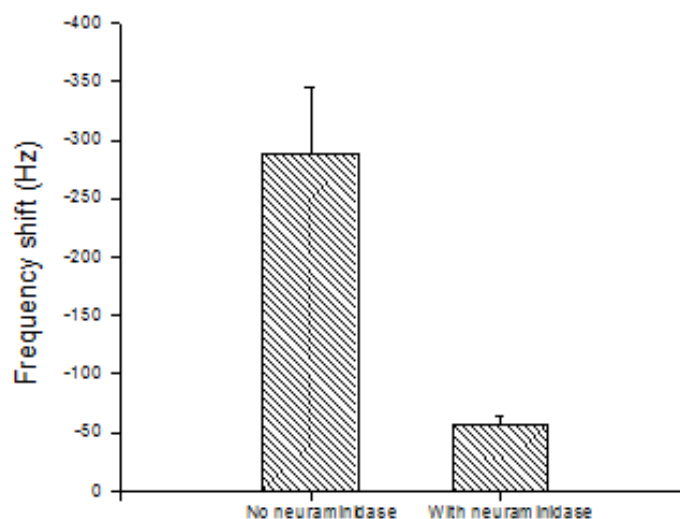


Figure 3.5 QCM response for fetuin from bovine serum after treatment with sodium periodate. The fetuin solution without neuraminidase showed a higher frequency shift than the one treated with neuraminidase.

3.2.1 Labeling of bone marrow stem cell sialic acids

We subsequently applied the method we have developed in detecting sialic acids on bone marrow stem cells that have been incubated and allowed to divide over 21 days. Stem cells are undifferentiated cells that have the ability divide, self-renew and differentiate into other types of cells. The differentiation of stem cells is associated with

antigens on the cell surface, which are made of glycoproteins or glycolipids.³³⁻³⁵ The terminal sugar residues of these glycoproteins or glycolipids are usually sialic acids and thus can be detected using the method developed above. To this end, cells that were incubated in a medium and allowed to divide were tested for the presence of sialic acids on their surfaces at 0,7,14 and 21 days. Using the procedure reported earlier for detecting sialic acids, the cells were subjected to mild periodate oxidation to selectively introduce aldehyde to the terminal sialic acids and subsequently tested for their ability to bind to our DAN-modified QCM chips. As shown in Fig. 3.5, no frequency shifts were observed at day zero, but frequency shift were observed in the subsequent measurements, increasing with the number of days of incubation. Also, the 40 k cells had higher frequency shifts than the 20 k cells for each measurement. Control reactions for the stem cell not treated with sodium periodate did not show any frequency shifts, indicating the binding was due to the introduction of aldehydes on the cell surface.

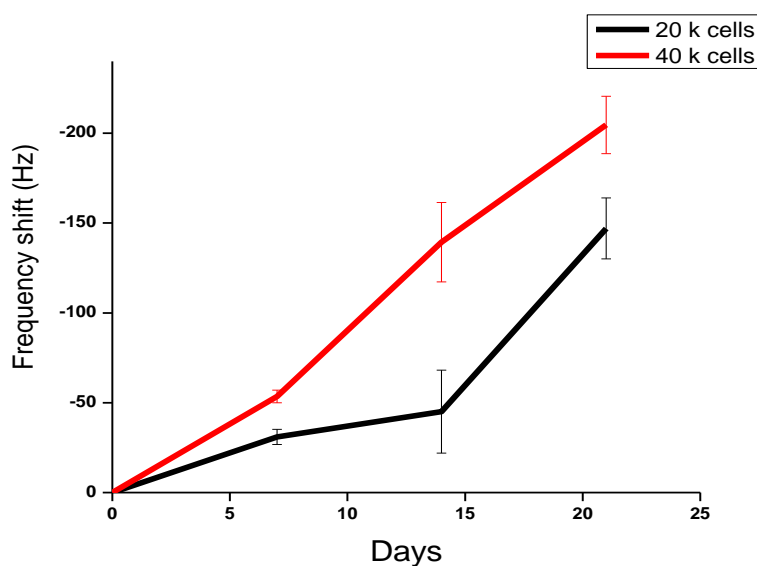


Figure 3.6 Frequency shifts in response to binding of cell surface sialic acid to QCM chips modified with DAN for 20 k cells (black) and 40k (cells) red, at 0, 7, 14 and 21 days.

3.3 CONCLUSION

A novel QCM-based method for detection of sialic acids in solutions and on cell surfaces has been developed. The method involves selective oxidation of the glycerol side chain of sialic acids to form an aldehyde and subsequent reaction with amines immobilized on QCM surface. A successful reaction of the amine with the oxidized sialic acid causes a decrease in the QCM's resonance frequency. The magnitude of the frequency shift is directly proportional to the mass of sialic acid that binds to the QCM surface. Unlike previous amine-based sialic acid sensors developed, which are effective only at slightly acid pH, the QCM-DAN sensor developed is effective at physiological pH and thus can be easily adapted for live cell sialic acid sensing.

3.4 EXPERIMENTAL SECTION

3.4.0 Materials

Proteck C3100 2.4 GHz programmable Universal Counter Quartz crystal microbalance was used for all measurements. Graphene dispersion in butyl acetate was purchased from Graphene Supermarket. All other reagents were of commercial grade and used without further purification. Stem cells were supplied by our group member, Panita Maturavongsadit.

Preparation of QCM sensors

The QCM chip were extensively cleaned with ethanol and water before being introduced into graphene solution (1 mg/mL) in ethyl acetate to allow for deposition of graphene onto the surface of the QCM chip. The chip was subsequently rinsed with water to allow, non-binding graphenes on the surface of the chip to be removed. After measuring the frequency

of the graphene-modified chip, the chip was introduced into a solution of 1,8-diaminonaphthalene (DAN) in acetonitrile and water (1:1), (0.5 mg/mL) for 30 minutes. The frequency of the QCM chip is again measured after rinsing the chip with water to remove non-binding DAN on the surface and blow-dried with nitrogen. Unless otherwise stated, sialic acid solutions were prepared in sodium phosphate buffer, pH 7.4., and experiments conducted in triplicates.

3.4.1 Measurement process

QCM measurement were carried out on a Protek C3100 2.4 GHz Programmable Universal Counter. The QCM chip was an AT-cut quartz crystal coated with silver on each side with a fundamental resonance frequency of 9 MHz. The principle of the QCM sensor is based on changes in the oscillating frequency of the QCM chip upon an analyte binding onto the silver-coated surface. For a small elastic object, there is a linear relationship between the amount of mass adsorbed onto the crystal surface (usually in the 1 ng cm⁻² range) and the frequency shift of the crystal in air or vacuum according to the Sauerbrey equation.^{36,37}

$$\Delta m = - C \Delta f_n / n$$

Where Δm is the mass change, C is the instrument constant, n is the vibrational mode number and Δf_n is the resonant frequency change for mode n . The instrument reports $\Delta f_n / n$ in Hz.

Cell isolation and culture

BMSCs were isolated from the bone marrow of young adult 160-180 g male Sprague-Dawley rats (Charles River Laboratories) as described in our previous reports.^{38,39} The procedures were performed in accordance with the guidelines for animal experimentation

by the Institutional Animal Care and Use Committee, School of Medicine, University of South Carolina. The cells were passaged no more than seven times after isolation and maintained in complete primary media (Dulbecco's Modified Eagle's Medium (DMEM) supplemented with 10% fetal bovine serum (FBS)), kept at 37 °C in a CO₂ incubator with 5% CO₂ : 95% air. The medium was replaced every 3-4 days.

Osteogenic differentiation of BMSCs

BMSCs were harvested from 80% confluent culture flask using 0.25% trypsin/EDTA for 5 min and counted and resuspended in complete primary media. A total of 20 or 40 × 10³ BMSCs were seeded per well. After 6 hours of an initial incubation, primary media were replaced with osteogenic media consisting of DMEM supplemented with 10% FBS, penicillin (100 U mL⁻¹), streptomycin (100 µg mL⁻¹), and amphotericin B (250 ng mL⁻¹), 10 × 10⁻³ M sodium β-glycerolphosphate, L -ascorbic acid 2-phosphate (50 µg mL⁻¹), and 10⁻⁸ M dexamethasone. Media were replenished every 3 days.

Detection of sialic acid on cell surfaces

After incubation, the cells were treated with sodium periodate (0.1 M, 300 µM) at 0 °C for 30 minutes to selectively introduce aldehyde to the terminal sialic acids. This was followed by introduction of DAN-modified QCM chips into the cell culture. The QCM chips were removed after 30 minutes, washed with water, blow-dried with nitrogen and the frequencies measured on the Protek C3100 2.4 GHz Programmable Universal Counter. The measurement were conducted in triplicates with separate DAN-modified QCM chip for each set of cells.

3.5 REFERENCES

- (1) Mahajan, V. S.; Pillai, S.: Sialic acids and autoimmune disease. *Immunol. Rev.* **2016**, 269, 145-161.
- (2) Varki, A.: Sialic acids in human health and disease. *Trends Mol. Med.* **2008**, 14, 351-360.
- (3) Kelm, S.; Schauer, R.: Sialic acids in molecular and cellular interactions. In *International Review of Cytology - a Survey of Cell Biology, Vol 175*; Jeon, K. W., Ed.; Elsevier Academic Press Inc: San Diego, 1997; Vol. 175; pp 137-240.
- (4) Wang, B.; Brand-Miller, J.: The role and potential of sialic acid in human nutrition. *Eur. J. Clin. Nutr.* **2003**, 57, 1351-1369.
- (5) Rabinovich, G. A.; van Kooyk, Y.; Cobb, B. A.: Glycobiology of immune responses. *Ann. N.Y. Acad. Sci.* **2012**, 1253, 1-15.
- (6) Dube, D. H.; Bertozzi, C. R.: Glycans in cancer and inflammation. Potential for therapeutics and diagnostics. *Nat. Rev. Drug Discovery* **2005**, 4, 477-488.
- (7) Schauer, R.: Sialic acids: fascinating sugars in higher animals and man. *Zoology* **2004**, 107, 49-64.
- (8) Bi, S.; Baum, L. G.: Sialic acids in T cell development and function. *Biochimica Et Biophysica Acta-General Subjects* **2009**, 1790, 1599-1610.
- (9) Chang, P. V.; Chen, X.; Smyrniotis, C.; Xenakis, A.; Hu, T.; Bertozzi, C. R.; Wu, P.: Metabolic Labeling of Sialic Acids in Living Animals with Alkynyl Sugars. *Angew. Chem. Int. Ed.* **2009**, 48, 4030-4033.
- (10) Laughlin, S. T.; Baskin, J. M.; Amacher, S. L.; Bertozzi, C. R.: In Vivo Imaging of Membrane-Associated Glycans in Developing Zebrafish. *Science* **2008**, 320, 664-667.

- (11) Hsu, T. L.; Hanson, S. R.; Kishikawa, K.; Wang, S. K.; Sawa, M.; Wong, C. H.: Alkynyl sugar analogs for the labeling and visualization of glycoconjugates in cells. *Proc. Natl. Acad. Sci. U.S.A.* **2007**, *104*, 2614-2619.
- (12) Zhang, X.; Chen, B.; He, M.; Zhang, Y.; Peng, L.; Hu, B.: Boronic acid recognition based-gold nanoparticle-labeling strategy for the assay of sialic acid expression on cancer cell surface by inductively coupled plasma mass spectrometry. *Analyst* **2016**, *141*, 1286-1293.
- (13) Qian, R. C.; Ding, L.; Yan, L. W.; Ju, H. X.: Fluorescence imaging for in situ detection of cell surface sialic acid by competitive binding of 3-(dansylamino)phenylboronic acid. *Anal. Chim. Acta* **2015**, *894*, 85-90.
- (14) Cao, H.; Yang, D.-P.; Ye, D.; Zhang, X.; Fang, X.; Zhang, S.; Liu, B.; Kong, J.: Protein-inorganic hybrid nanoflowers as ultrasensitive electrochemical cytosensing Interfaces for evaluation of cell surface sialic acid. *Biosens. Bioelectron.* **2015**, *68*, 329-335.
- (15) Cho, S.; Lee, B.-R.; Cho, B.-K.; Kim, J.-H.; Kim, B.-G.: In vitro selection of sialic acid specific RNA aptamer and its application to the rapid sensing of sialic acid modified sugars. *Biotechnol. Bioeng.* **2013**, *110*, 905-913.
- (16) Kohler, J. J.: Aniline: A Catalyst for Sialic Acid Detection. *ChemBioChem* **2009**, *10*, 2147-2150.
- (17) Zhang, Y.; Yuan, J.; Song, J.; Wang, Z.; Huang, L.: An efficient method for selectively imaging and quantifying in situ the expression of sialylated glycoproteins on living cells. *Glycobiology* **2013**, *23*, 643-653.

- (18) Zeng, Y.; Ramya, T. N. C.; Dirksen, A.; Dawson, P. E.; Paulson, J. C.: High-efficiency labeling of sialylated glycoproteins on living cells. *Nat. Meth* **2009**, *6*, 207-209.
- (19) Liao, T.-H.; Gallop, P. M.; Blumenfeld, O. O.: Modification of Sialyl Residues of Sialoglycoprotein(s) of the Human Erythrocyte Surface. *J. Biol. Chem.* **1973**, *248*, 8247-8253.
- (20) Jourdian, G. W.; Dean, L.; Roseman, S.: The Sialic Acids: XI. A Periodate-Resorcinol Method For The Quantitative Estimation Of Free Sialic Acids And Their Glycosides. *J. Biol. Chem.* **1971**, *246*, 430-435.
- (21) Key, J. A.; Li, C.; Cairo, C. W.: Detection of Cellular Sialic Acid Content Using Nitrobenzoxadiazole Carbonyl-Reactive Chromophores. *Bioconjugate Chem.* **2012**, *23*, 363-371.
- (22) Dirksen, A.; Hackeng, T. M.; Dawson, P. E.: Nucleophilic Catalysis of Oxime Ligation. *Angew. Chem. Int. Ed.* **2006**, *45*, 7581-7584.
- (23) Zeng, Y.; Ramya, T. N. C.; Dirksen, A.; Dawson, P. E.; Paulson, J. C.: High-efficiency labeling of sialylated glycoproteins on living cells. *Nat. Methods* **2009**, *6*, 207-209.
- (24) King, W. H.: Piezoelectric Sorption Detector. *Anal. Chem.* **1964**, *36*, 1735-1739.
- (25) Vashist, S. K.; Vashist, P.: Recent Advances in Quartz Crystal Microbalance-Based Sensors. *J. Sensors* **2011**.
- (26) Sauerbrey, G. Z.: Use of quartz vibration for weighing thin films on a microbalance. *Phys. J.* **1959**, *155*, 206-212.
- (27) Pavey, K. D.: Quartz crystal analytical sensors: the future of label-free, real-time diagnostics? *Expert Rev Mol Diagn* **2002**, *2*, 173-86.

- (28) Janshoff, A.; Galla, H.-J.; Steinem, C.: Piezoelectric Mass-Sensing Devices as Biosensors—An Alternative to Optical Biosensors? *Angew. Chem. Int. Ed.* **2000**, *39*, 4004-4032.
- (29) Juzeliunas, E.: Quartz crystal microgravimetry - fifty years of application and new challenges. *Chemija* **2009**, *20*, 218-225.
- (30) Cheng, C. I.; Chang, Y. P.; Chu, Y. H.: Biomolecular interactions and tools for their recognition: focus on the quartz crystal microbalance and its diverse surface chemistries and applications. *Chem. Soc. Rev.* **2012**, *41*, 1947-1971.
- (31) Tang, D.; Li, Q.; Tang, J.; Su, B.; Chen, G.: An enzyme-free quartz crystal microbalance biosensor for sensitive glucose detection in biological fluids based on glucose/dextran displacement approach. *Anal. Chim. Acta* **2011**, *686*, 144-149.
- (32) Zhu, Y.; Hao, Y.; Adogla, E. A.; Yan, J.; Li, D.; Xu, K.; Wang, Q.; Honea, J.; Lin, Q.: A graphene-based affinity nanosensor for detection of low-charge and low-molecular-weight molecules. *Nanoscale* **2016**, *8*, 5815-5819.
- (33) Draper, J. S.; Pigott, C.; Thomson, J. A.; Andrews, P. W.: Surface antigens of human embryonic stem cells: changes upon differentiation in culture. *J. Anat.* **2002**, *200*, 249-258.
- (34) Wright, A. J.; Andrews, P. W.: Surface marker antigens in the characterization of human embryonic stem cells. *Stem Cell Res.* **2009**, *3*, 3-11.
- (35) Yu, R. K.; Suzuki, Y.; Yanagisawa, M.: Membrane Glycolipids in Stem Cells. *FEBS Lett.* **2010**, *584*, 1694-1699.

- (36) Schneider, T. W.; Buttry, D. A.: Electrochemical quartz crystal microbalance studies of adsorption and desorption of self-assembled monolayers of alkyl thiols on gold. *J. Am. Chem. Soc.* **1993**, *115*, 12391-12397.
- (37) Ward, M. D.; Buttry, D. A.: In Situ Interfacial Mass Detection with Piezoelectric Transducers. *Science* **1990**, *249*, 1000-1007.
- (38) Kaur, G.; Wang, C.; Sun, J.; Wang, Q.: The synergistic effects of multivalent ligand display and nanotopography on osteogenic differentiation of rat bone marrow stem cells. *Biomaterials* **2010**, *31*, 5813-24.
- (39) Luckanagul, J.; Lee, L. A.; Nguyen, Q. L.; Sitasuwan, P.; Yang, X.; Shazly, T.; Wang, Q.: Porous alginate hydrogel functionalized with virus as three-dimensional scaffolds for bone differentiation. *Biomacromolecules* **2012**, *13*, 3949-58.

CHAPTER 4

PYRENE-FUNCTIONALIZED BORONIC ACID SENSORS FOR LABELING GLYCANS ON CELLS

4.1 INTRODUCTION

Glycans are one of the most abundant biomolecules found in cells.¹ They are involved in a wide array of biological processes, including cell-cell recognition, cell differentiation, growth, immune response and modulation.^{2,3} Changes in glycan expressions in cells have been linked to different cancers, and have been reported to regulate different aspects of tumor progression, including proliferation, invasion and metastasis.⁴⁻⁶ For example, overexpression of sialic acids have been linked to various disease states such as cancers,⁴ cardiovascular diseases⁷ and neurological diseases.⁸ Moreover, overexpression of mannose sugar has also been reported in breast cancer progression,⁹ and the overall level of fucose has been reported to be higher in ovarian and pancreatic cancer cells compared to their corresponding normal cells.¹⁰

Existing methods for detecting and analyzing glycans include, mass spectrometry,¹¹⁻¹³ nuclear magnetic resonance^{14,15} and high performance liquid chromatography.¹⁶ However, these methods involve first treating the cells with enzymes to release the saccharides from the protein before analysis, either with or without derivatization.¹¹ Another approach is based on metabolic incorporation of a bioorthogonal reporter into the cell by introducing synthetic analogues of natural monosaccharides

bearing the biorthogonal reporters into the cell.¹⁷⁻²¹ The unnatural sugars are utilized in the biosynthesis of glycans bearing the incorporated bioorthogonal reporters, which can be subsequently conjugated with a various kinds of probes. The reaction between the functionalized glycan and fluorescent probes allows visualization and monitoring of glycans in living cells by means of fluorescence microscopy, or other analytical methods, which is vital for elucidating protein glycosylation in the cell. Reporter groups such as azides, alkynes alkenes and ketones are some of the functional groups that are suitable for metabolic incorporation into the cell's glycans and subsequent labeling with affinity probes.^{20,22} However, bulky groups such as cyclooctynes could lead to perturbation of the pathways, and consequently, a dysregulation of the cellular activities.

Another method relies on the recognition and affinity binding of the polyhydroxy functional groups of the glycans *in situ* using lectins²³ or boronic acids²⁴. Lectins are class of carbohydrate binding proteins. Different lectins exist that are specific for different oligosaccharide sequences.²⁵ However, this method suffers from limited tissue penetration and toxicity. Boronic acids are synthetic recognition motif for glycans. They react rapidly and reversibly with 1,2 and 1,3-diols of the glycans to form five- and six-membered ring cyclic boronate esters respectively (Figure 4.1).²⁶⁻²⁸ The binding to glycans occurs at, or near physiological pH, and both the boronic acids and their boronate ester products are benign to cells, making this reaction suitable for biolabeling. The binding of boronic acid to cell surface glycans also enhances transport of molecules attached to the boronic acid into the cell. They are therefore employed in the delivery of polar molecules and drugs to cells. In this work, we synthesized a number of pyrene- and naphthalimide-derivatized boronic acids for glycan sensing. Pyrene is a versatile blue-fluorophore with high

fluorescence quantum yields,²⁹⁻³¹ and naphthalimide on the other hand are green-fluorescent emitting dyes.³² The spacers between pyrenes and boronic acids were varied to obtain the optimum spacing needed for higher fluorescence intensity.

4.2 RESULTS AND DISCUSSION

Figure 4.1 shows different pyrene-derivatized boronic acids that were synthesized for labeling glycans on cells. The boronic acid parts are the recognition motifs, while the pyrenes are the fluorescent parts, for visualization and tracking of the molecules in cells. The spacer length, and polarity of the sensors were varied to obtain the best design for imaging cellular glycans. Pyrene boronic acids (8 μ M) in 10% DMSO/H₂O were prepared and incubated with bone marrow stroma cells (BMSCs) in primary media at 37 °C for 30 minutes. The cells were subsequently washed three times with primary media, and fixed with 4% paraformaldehyde for 15 minutes at room temperature. Finally, images of the stained samples were collected using Olympus I \times 81 epi-fluor mode under 10 \times and 20 \times lens, exposure times 300 ms for DAPI and 700 ms for FITC channel. The cell imaging was performed by our group member, Panita Maturavongsadit.

Different fluorescence intensities were observed for the different dyes, **4.1-4.7** under a fluorescence microscope (Figure 4.2). Dyes **4.1** and **4.2**, which have ethyl and butyl spacers respectively, linking a pyrene and 3-amidophenylboronic acid showed the highest fluorescent labeling. When the amide in **4.2** was replaced by an amine to obtain **4.3**, no labeling was observed. The amphiphilic dyes **4.4** and **4.5** showed some labeling, but not as effective as those of **4.1**, and **4.2**; whereas **4.6**, which has a pentaethylene (PEG) linker

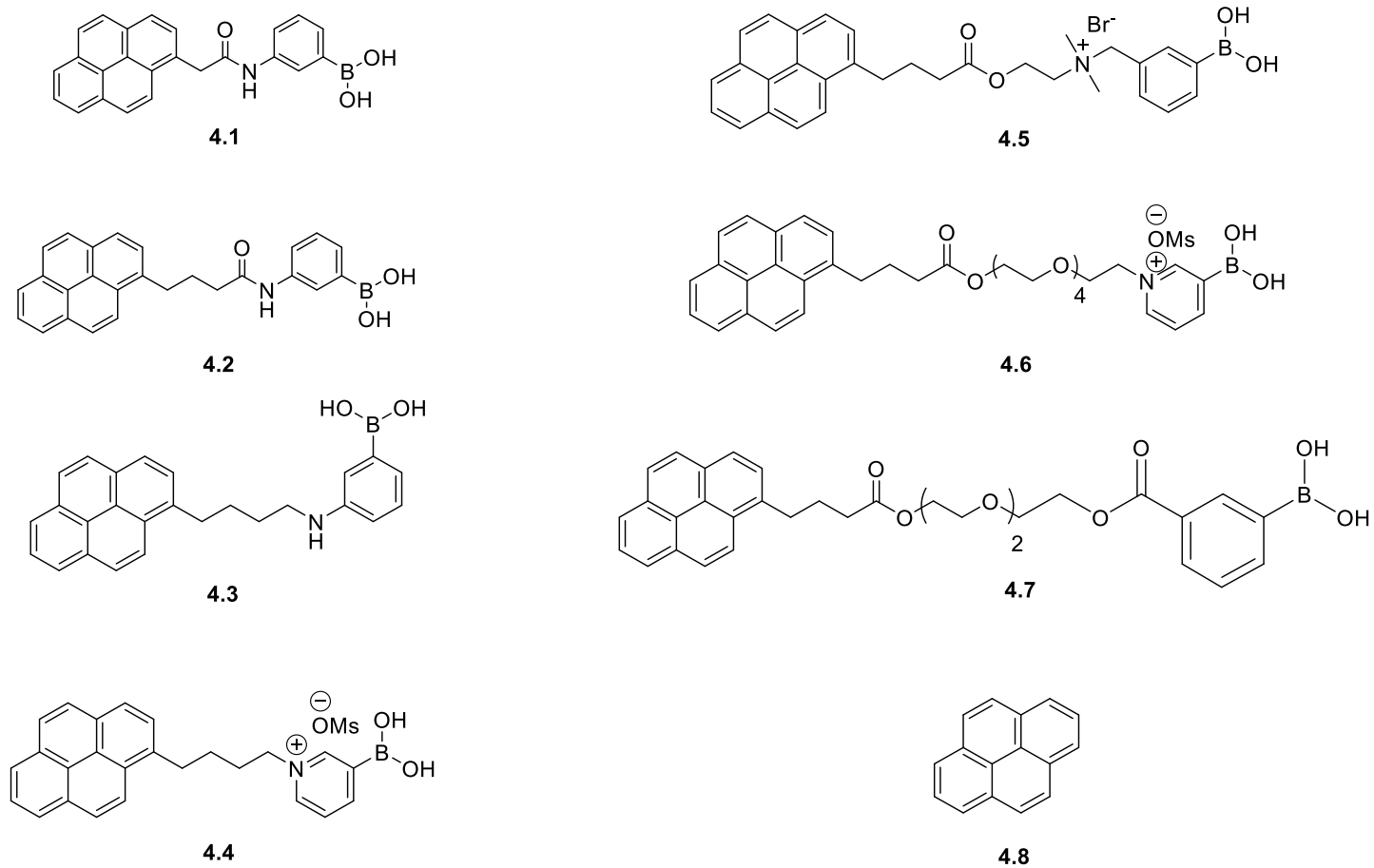


Figure 4.1 Structure of pyrene-derivatized boronic acid dyes for imaging cell surface glycans.

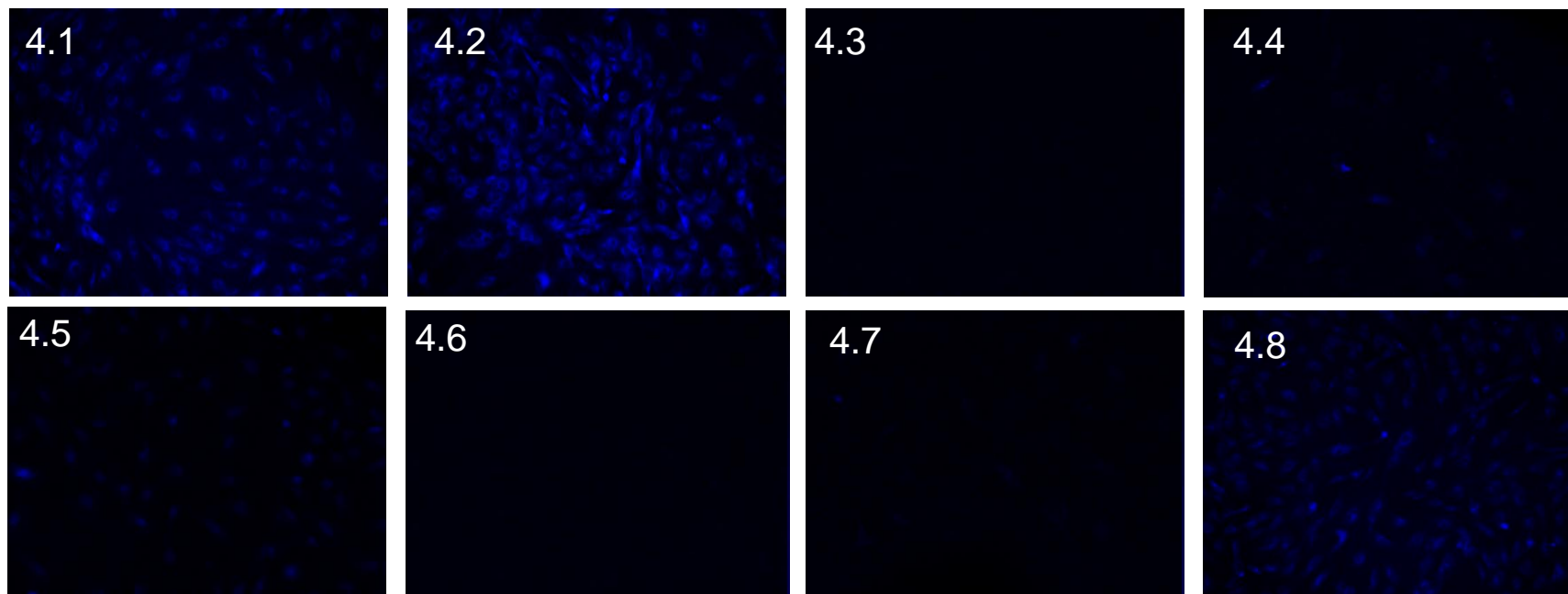


Figure 4.2 Fluorescence images of BMSCs labeled with different pyrene-derivatized boronic acids (**4.1-4.7**) and pyrene (**4.8**).

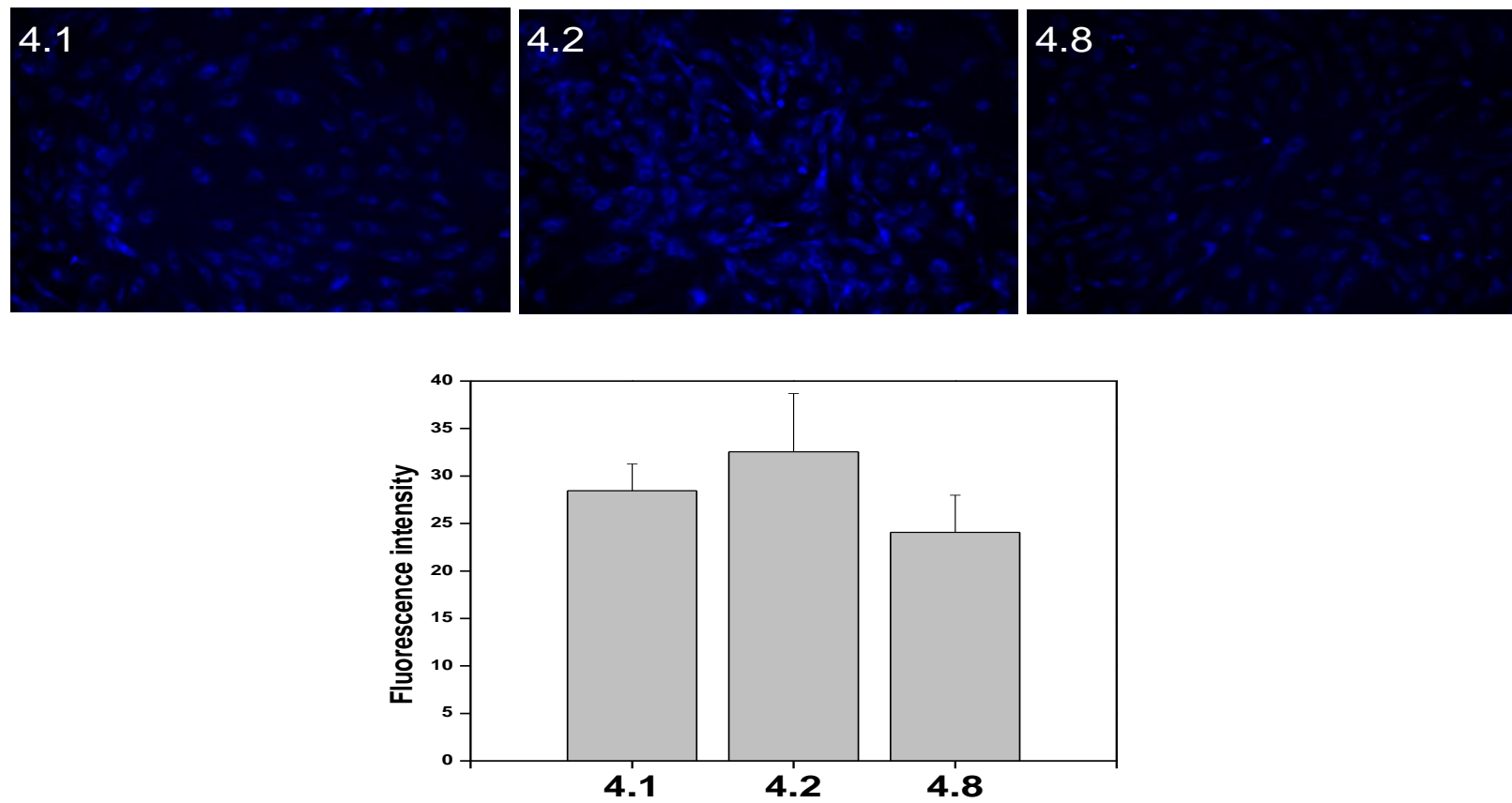


Figure 4.3. Fluorescence images of BMSCs labeled with dyes **4.1**, **4.2** and **4.8** and the corresponding fluorescent intensities.

separating the pyrene and the pyridinium boronic acid did not show any staining. However, pyrene (**8**), which was not functionalized with boronic acid showed staining comparable to **4.1** and **4.2** (Figure 4.3). We thus concluded that pyrene-boronic acids with short alkyl group separating them and linked by amide groups were more suitable for labeling the glycans than those with polyethylene linkers and the amphiphiles. Internalization of the dyes was also observed, which is consistent with the boronate ester-aided transport of molecules across the cell membrane. However, pyrene (**8**), which has no boronic acid attached was also internalized; thus the hydrophobicity pyrene moiety could also have contributed to the internalization of the dyes.

To further establish the mechanism of the labeling and the internalization of the dyes, two naphthalimide boronic acid dyes **4.9** and **4.10** were synthesized. After incubating the dyes with BMSCs and collecting the images of the stained samples, we observed that both dyes showed labeling and internalization, but the fluorescent intensity of **4.10** was higher than that of the amphiphilic dye **4.9**. (Figure 4.4).

4.3 CONCLUSION

Pyrene- and naphthalimide-derivatized boronic acid dyes were synthesized for labeling cell surface glycans. The pyrenes, separated by alkyl chains and linked to the boronic acids by amide bonds showed the highest fluorescent intensity. The amphiphilic dyes showed lower fluorescence intensity than the hydrophobic dyes. After the surface binding, via the reaction of the boronic motifs with the diols to form boronate esters, the dyes entered the cytoplasm. This is evident by the labeling of the cytoplasm by the dye. However, the incubation of the cells with a pyrene without boronic acid attached showed the hydrophobicity of the pyrene might have also contributed significantly to the

permeating of the dyes through the cell membrane to label the cytoplasm. We therefore concluded that the pyrenes-derivatized boronic acid were not suitable for selectively labeling glycans on cells. A suitable dye that is less hydrophobic, is therefore required to carry the boronic acid motif for the selective labeling of cellular glycans.

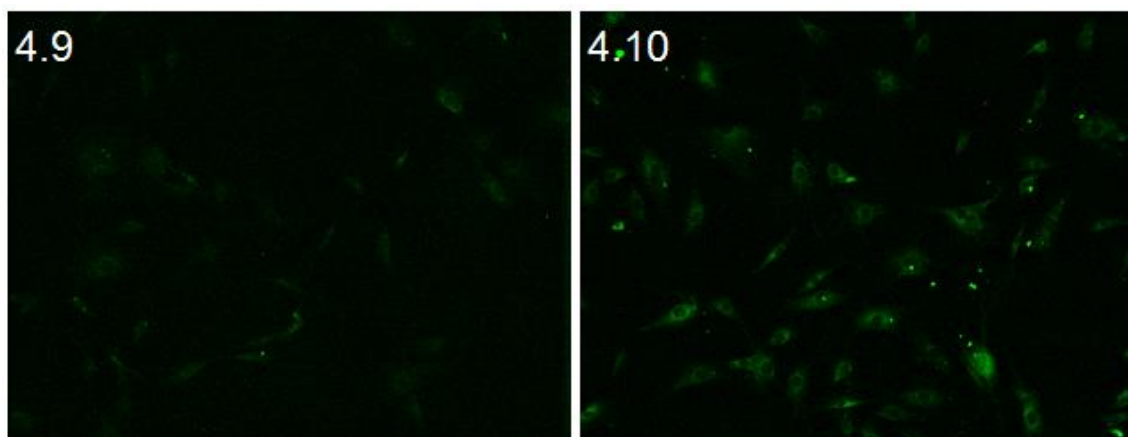
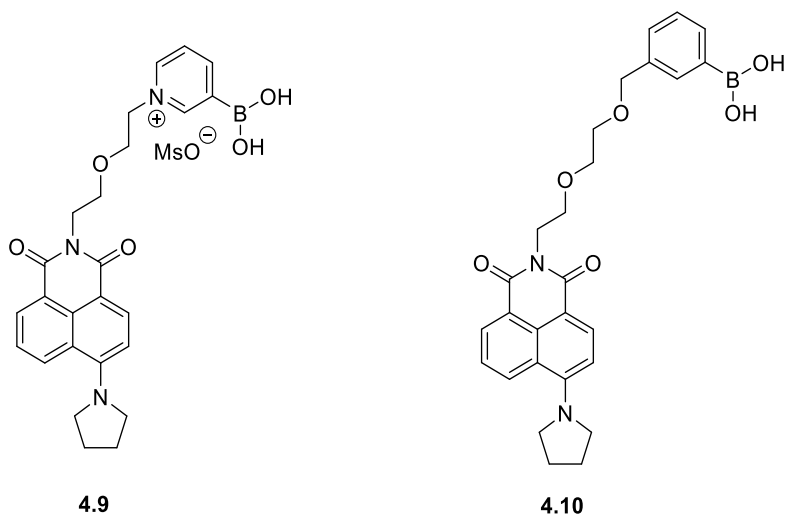
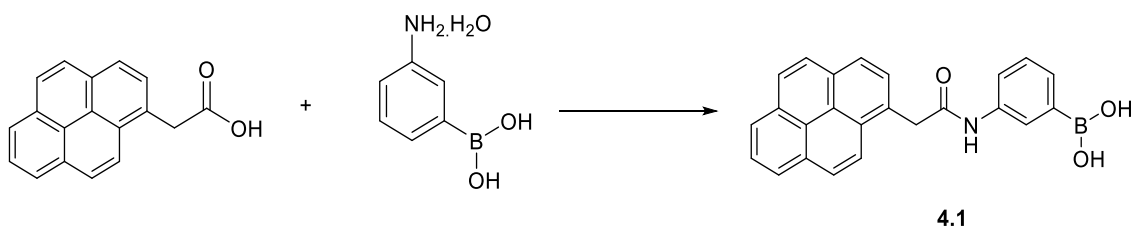


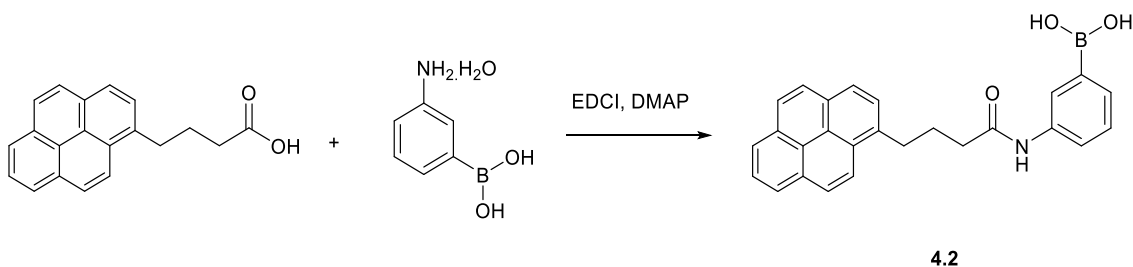
Figure 4.4 Fluorescence images of BMSCs labeled with naphthalimide-derivatized boronic acid dyes **4.9** and **4.10**.

4.4 EXPERIMENTAL SECTION

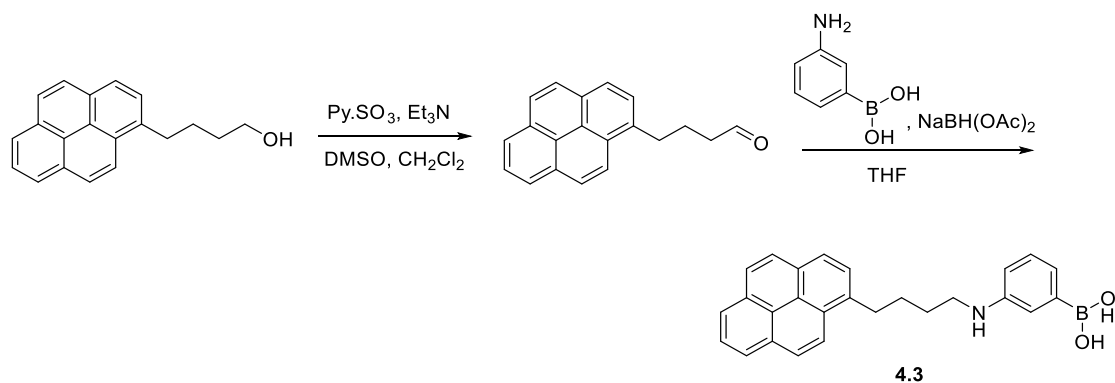
General. Unless otherwise specified all reagents and solvents were of commercial grade. NMR spectra were recorded on Bruker 300 or 400 instruments. Flash column chromatography was performed with silica gel (32-63 μm). High resolution mass spectrometry (HRMS) was obtained using a magnetic sector mass spectrometer.



(3-(2-Pyrene-1-yl)acetamido)phenylboronic acid (4.1). Pyrene-1-acetic acid (50.0 mg, 0.19 mmol) in DMF (5 mL) was added EDCI (53.0 mg, 0.34 mmol) and DMAP (2.0 mg, 0.0017 mmol) at room temperature and stirred for 10 minutes, followed by addition of 3-aminophenylboronic acid.monohydrate (31.0 mg, 0.20 mmol). The mixture was further stirred at room temperature for 18 h. After the reaction was completed, the mixture was diluted with ethyl acetate (20 mL) and washed with 1 N HCl and water. The organic layer was dried over anhydrous sodium sulfate and concentrated *in vacuo* to obtain a light yellow solid (60.0 mg, 81%). ^1H NMR (400 MHz, DMSO) δ 10.41–10.39 (br s, 1H), 8.39 (t, J = 23.1 Hz, 1H), 8.30 – 8.19 (m, 4H), 8.17 – 8.00 (m, 7H), 7.89 (d, J = 15.5 Hz, 1H), 7.70 (d, J = 8.1 Hz, 1H), 7.46 (d, J = 7.2 Hz, 1H), 7.26 (t, J = 7.7 Hz, 1H), 4.42 (s, 2H). ^{13}C NMR (101 MHz, DMSO) δ 169.67, 138.70, 131.24, 130.99, 130.76, 130.31, 129.69, 129.51, 129.22, 128.34, 127.89, 127.86, 127.43, 126.77, 125.75, 125.68, 125.50, 125.30, 124.55, 124.38, 124.32, 121.85, 41.30. HRMS (ESI): m/z (M-H) calcd for $\text{C}_{24}\text{H}_{18}\text{BNO}_3$: 377.1338; Found: 377.1347



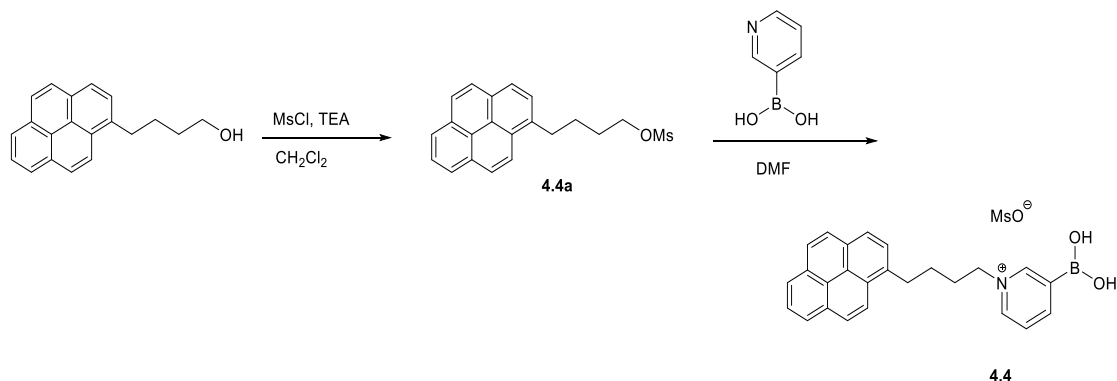
(3-(4-(Pyren-1-yl)butanamido)phenyl)boronic acid (4.2). Pyrene-1-butanoic acid (100.0 mg, 0.34 mmol) in DMF (5 mL) was added EDCI (105.0 mg, 0.68 mmol) and DMAP (4.0 mg, 0.0034 mmol) at room temperature and stirred for 10 minutes, followed by addition of 3-aminophenylboronic acid.monohydrate (47.4 mg, 0.34 mmol). The mixture was further stirred at room temperature for 18 h. The mixture was diluted with ethyl acetate and washed with 1 N HCl (20 mL) and water (2 x 20 mL). The organic layer was dried over anhydrous sodium sulfate and concentrated *in vacuo* to obtain a yellow solid (123.0 mg, 89%). ¹H NMR (400 MHz, DMSO) δ 9.93 (s, 1H), 8.35 (t, *J* = 10.0 Hz, 1H), 8.24 (dd, *J* = 7.6, 2.7 Hz, 2H), 8.19 (dd, *J* = 8.4, 6.8 Hz, 2H), 8.09 (d, *J* = 1.9 Hz, 1H), 8.03 (t, *J* = 7.6 Hz, 1H), 7.92 (t, *J* = 8.2 Hz, 1H), 7.87 (s, 1H), 7.71 (d, *J* = 8.0 Hz, 1H), 7.48 (d, *J* = 7.3 Hz, 1H), 3.43–3.29 (m, 2H), 2.47 (t, *J* = 7.2 Hz, 1H), 2.10 (dd, *J* = 14.7, 7.2 Hz, 2H). ¹³C NMR (101 MHz, DMSO) δ 171.77, 138.73, 136.88, 131.30, 130.83, 129.77, 129.50, 128.58, 128.28, 128.02, 127.90, 127.74, 126.99, 126.65, 125.77, 125.43, 125.28, 124.67, 124.56, 123.87, 121.97, 36.39, 32.63, 27.86. HRMS (ESI-H): *m/z* (M-H) calcd for C₂₆H₂₂BNO₃: 405.1649; found: 405.1651.



Pyrene-1-butanaldehyde. To a solution of pyrenbutanol (274.0 mg, 1.0 mmol) in CH_2Cl_2 (4 mL) and DMSO (830 μL) was added Et_3N (572 μL , 4.0 mmol) followed by addition of $\text{SO}_3\cdot\text{pyridine}$ (326.0 mg, 2.06 mmol) in 3 portions over 20 minutes. The mixture was stirred for another 2 hours, diluted with ethyl acetate (10 mL) and washed with 1 N HCl and water. The organic layer was concentrated *in vacuo* to afford a white solid, which was further washed with diethyl ether to obtain pyrenebutanaldehyde (220.0 mg, 80%). ^1H NMR (300 MHz, CDCl_3) δ 9.82 (t, $J = 1.4$ Hz, 1H), 8.30 (d, $J = 9.3$ Hz, 1H), 8.23–8.10 (m, 4H), 8.09 – 7.94 (m, 3H), 7.86 (d, $J = 7.8$ Hz, 1H), 3.45 – 3.34 (t, $J = 7.5$ Hz, 2H), 2.62–2.56 (m, 2H), 2.33–2.13 (m, 2H).

4.3. To a solution of pyrene-1-butanaldehyde (214.0 mg, 0.78 mmol) in THF (10 mL) was added a drop of acetic acid and 3-aminophenylboronic acid.monohydrate (120 mg, 0.78 mmol). After stirring for 5 minutes, $\text{NaBH}(\text{OAc})_3$ (330.0 mg, 1.57 mmol) was added. The mixture was left to stir at room temperature overnight (18 h). The mixture was diluted with ethyl acetate and washed with sodium bicarbonate. The organic layer was dried over anhydrous sodium sulfate, concentrated and dried *in vacuo* to obtain a white solid (280.0 mg, 91%). ^1H NMR (400 MHz, DMSO) δ 8.36 (d, $J = 9.3$ Hz, 1H), 8.30–8.18 (m, 5H), 8.17–8.00 (m, 5H), 7.96 (d, $J = 7.8$ Hz, 1H), 7.90–7.74 (m, 1H), 7.69 (s, 2H), 7.50–7.25

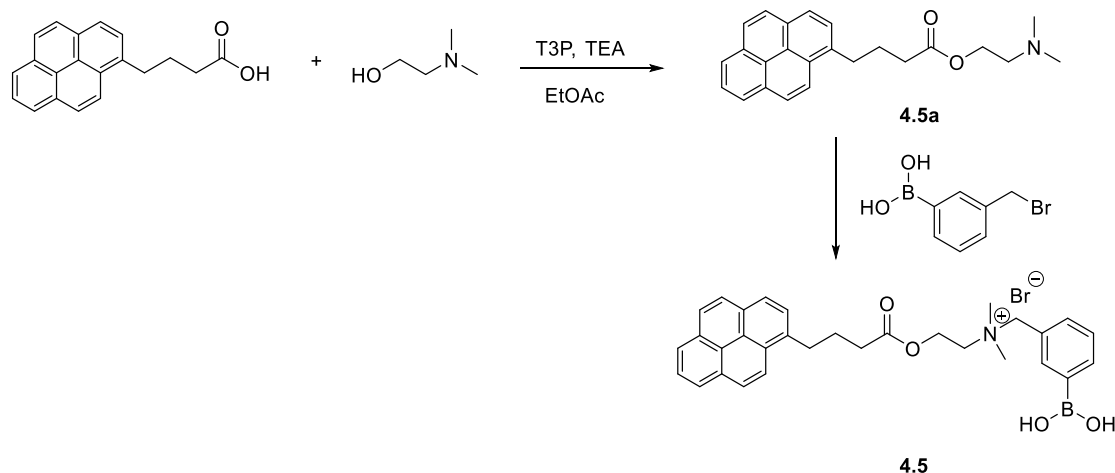
(m, 2H), 1.88 (d, $J = 29.5$ Hz, 4H). * 4 Protons under DMSO water peak. ^{13}C NMR (101 MHz, DMSO) δ 136.97, 131.36, 130.89, 129.76, 129.15, 128.56, 127.96, 127.91, 127.71, 127.00, 126.62, 125.39, 125.26, 124.70, 124.61, 123.98, 32.59, 28.93. HRMS (ESI): m/z (M+H) calcd for $\text{C}_{24}\text{H}_{25}\text{NO}_2$: 394.2007; found: 394.2009.



4-(pyrene-1-yl)-butyl methanesulfonate (4.4a). To pyrene-1-butanol (300.0 mg, 1.05 mL) in CH_2Cl_2 (10 mL) was added MsCl (89 μL , 1.15 mmol) and TEA (417 μL , 3.0 mmol). The mixture was stirred at room temperature overnight (18 h) and partitioned between 1 N HCl and CH_2Cl_2 . The organic layer was washed with water, dried over anhydrous sodium sulfate, concentrated and dried *in vacuo* to obtain a light yellow liquid (360 mg, quant) as the intermediate. ^1H NMR (300 MHz, CDCl_3) δ 8.27 (d, $J = 9.3$ Hz, 1H), 8.22–8.09 (m, 4H), 8.07–7.97 (m, 3H), 7.87 (d, $J = 7.8$ Hz, 1H), 4.26 (t, $J = 6.3$ Hz, 2H), 3.41 (t, $J = 7.3$ Hz, 2H), 2.96 (s, 3H), 2.51 (s, 3H), 2.14–1.81 (m, 4H).

4.4. The intermediate, 4-(pyrene-1-yl)-butyl methanesulfonate (180.0 mg, 0.48 mmol) was dissolved in DMF (1 mL) and 3-pyridyl boronic acid was added. The mixture was heated to 100 $^\circ\text{C}$ for 36 h. Diethyl ether (10 mL x 2) was added to the reaction mixture and the solvent decanted. An oily residue formed was dried *in vacuo* to obtain a brown solid (120 mg, 52%). ^1H NMR (300 MHz, MeOD) δ 8.86 (d, $J = 6.6$ Hz, 2H), 8.12–7.84 (m, 5H),

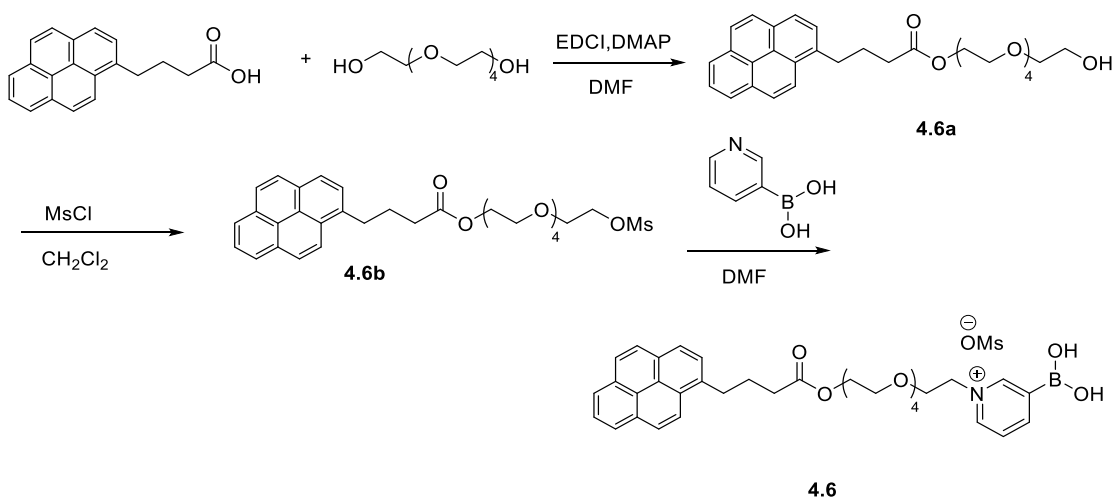
7.82–7.43(m, 6H), 4.72–4.40 (m, 1H), 3.45–3.28 (m, 2H), 2.25–2.00 (m, 1H), 2.02–1.98 (m, 1H). ^{13}C NMR (75 MHz, MeOD) δ 145.25, 135.51, 131.37, 130.82, 130.01, 128.38, 127.94, 127.15, 127.12, 127.09, 126.42, 125.72, 124.69, 124.57, 124.51, 122.85, 61.48, 32.08, 30.77, 27.75. HRMS (ESI): m/z calcd for: 379.1853; found: 379.1852.



4.5a. Pyrene-1-butanoic acid (500.0 mg, 1.7 mmol) in ethyl acetate (20 mL) was added 50% propylphosphonic anhydride in ethyl acetate (1.07 mL, 3.6 mmol), dimethylaminoethanol (465 μL , 4.5 mmol) and trimethylamine (614 μL , 4.5 mmol) and stirred at room temperature for 1 h. The mixture was diluted with ethyl acetate and washed with saturated sodium bicarbonate and water. The organic layer was dried over anhydrous sodium sulfate and concentrated *in vacuo* to obtain compound **4.5a**, as a dark oil (550.0 mg, 90%). ^1H NMR (400 MHz, CDCl_3) δ 8.29 (d, $J = 9.2$ Hz, 1H), 8.17 (dd, $J = 7.2, 4.1$ Hz, 2H), 8.12 (dd, $J = 8.5, 3.3$ Hz, 2H), 8.06–7.95 (m, 3H), 7.85 (d, $J = 13.6$, 1H), 4.30 (t, $J = 5.3$ Hz, 2H), 4.28–4.09 (m, 1H), 3.41 (t, $J = 7.6$ Hz, 2H), 2.76 (t, $J = 5.3$ Hz, 2H), 2.52 (t, $J = 7.2$ Hz, 2H), 2.44 (s, 6H), 2.27–2.12 (m, 2H). ^{13}C NMR (101 MHz, CDCl_3) δ 211.35, 172.98, 135.65, 131.41, 130.89, 130.01, 128.77, 127.50, 126.79, 125.94, 125.01, 123.31, 67.91,

59.54, 44.16, 38.75, 33.52, 32.52, 26.36. HRMS (ESI): m/z ($M+H$) calcd for $C_{24}H_{25}NO_2$: 360.1964; found: 360.1965.

4.5. To **4.5a** (440 mg, 1.2 mmol) in a mixture of THF (10 mL) and DMF (1 mL) was added (3-bromomethyl)phenylboronic acid (262.0 mg, 1.2 mmol) and stirred at room temperature for 5 h. The THF was removed and diethyl ether (20 mL) was added to precipitate the product. The precipitate was filtered and dried *in vacuo* to obtain a light yellow solid as the desired product (415.1 mg, 70%). 1H NMR (300 MHz, MeOD) δ 8.34 (d, $J = 9.3$ Hz, 1H), 8.18 (d, $J = 7.8$ Hz, 2H), 8.12 (s, 1H), 8.09 (d, $J = 2.4$ Hz, 1H), 8.05–8.01 (m, 2H), 7.98 (d, $J = 7.8$ Hz, 1H), 7.86 (t, $J = 9.9$ Hz, 2H), 4.54–4.41 (m, 4H), 3.57 (dd, $J = 5.8, 3.8$ Hz, 2H), 3.45–3.35 (m, 2H), 2.98 (s, 6H), 2.54 (t, $J = 7.2$ Hz, 2H), 2.31–2.07 (m, 2H). ^{13}C NMR (101 MHz, MeOD) δ 172.70, 135.59, 131.40, 130.00, 128.58, 127.14, 126.40, 125.67, 124.67, 124.54, 123.02, 68.98, 62.36, 57.08, 49.43, 32.84, 32.03, 25.99. HRMS (ESI): m/z (M^+) calcd for $C_{31}H_{33}BNO_4^+$: 493.2539; found: 493.2547.

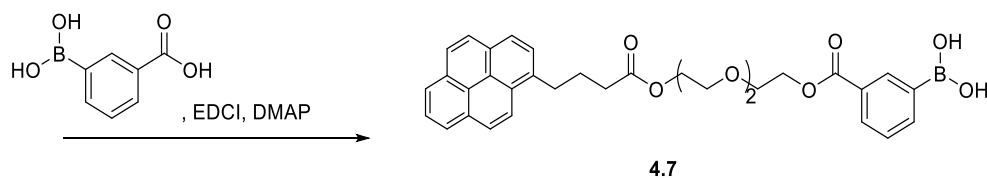


4.6a. To pyrene-1-butanoic acid (1.4 g, 5.0 mmol) in DMF (20 mL) was added EDCI (1.05 g, 5.5 mmol) and DMAP (0.1 g, 0.5 mmol) at 0 °C. The mixture was stirred at room temperature for 10 minutes followed by addition of pentaerythritol (2.1 mL, 10.5 mmol). The mixture was further stirred at room temperature for 18 h. The crude was diluted with ethyl acetate and washed with 1N HCl and water. The organic layer was concentrated, dried *in vacuo* and purified on silica gel column using CH₂Cl₂:CH₃OH (10:0.1–10:1) gradient to obtain a yellow oil. (1.3 g, 51%). ¹H NMR (400 MHz, CDCl₃) δ 8.26–8.20 (m, 1H), 8.12–8.01 (m, 4H), 7.96–7.87 (m, 3H), 7.83–7.76 (m, 1H), 4.21–4.11 (m, 2H), 3.65–3.60 (m, 4H), 3.59–3.43 (m, 14H), 3.31 (t, *J* = 7.6 Hz, 2H), 2.51 (s, 3H), 2.41 (t, *J* = 7.6 Hz, 2H), 2.22–2.02 (m, 2H). ¹³C NMR (101 MHz, CDCl₃) δ 173.49, 135.77, 131.42, 130.91, 129.98, 128.76, 127.50, 127.41, 126.72, 125.86, 125.10, 125.00, 124.92, 124.83, 124.78, 123.37, 72.51, 70.56, 70.51, 70.28, 69.17, 63.51, 61.74, 33.81, 32.76, 26.80.

4.6b. To compound **4.6a** (800.0 mg, 1.6 mmol) in CH₂Cl₂ (20 mL) was added MsCl (198.4 mg, 1.72 mmol) and TEA (445 μL, 3.2 mmol). The mixture was stirred at room temperature for 2 h. The crude was washed with 1 N HCl and water. The organic layer was dried over anhydrous sodium sulfate, concentrated and purified on silica gel using CH₂Cl₂ to obtain

compound **4.6b** as a dark oil (795 mg, 86%). ^1H NMR (300 MHz, CDCl_3) δ 8.24 (d, J = 9.3 Hz, 1H), 8.13–8.01 (m, 4H), 7.97–7.95 (m, 2H), 7.92 (t, J = 7.6 Hz, 1H), 7.80 (d, J = 7.8 Hz, 1H), 4.23–4.14 (m, 2H), 3.68–3.59 (m, 4H), 3.58–3.45 (m, 12H), 3.33 (t, J = 7.8 Hz, 2H), 2.97 (s, 3H), 2.43 (t, J = 7.3 Hz, 2H), 2.22–2.02 (m, 2H), 1.57–1.50 (m, 2H). ^{13}C NMR (101 MHz, CDCl_3) δ 127.50, 127.41, 126.73, 125.87, 124.93, 124.79, 123.37, 70.59, 70.56, 70.47, 69.25, 69.18, 68.98, 63.50, 37.72, 33.82, 32.75, 26.80. HRMS (ESI): m/z (M^+) calcd for $\text{C}_{31}\text{H}_{38}\text{O}_9\text{S}$: 587.2315; found: 587.2333

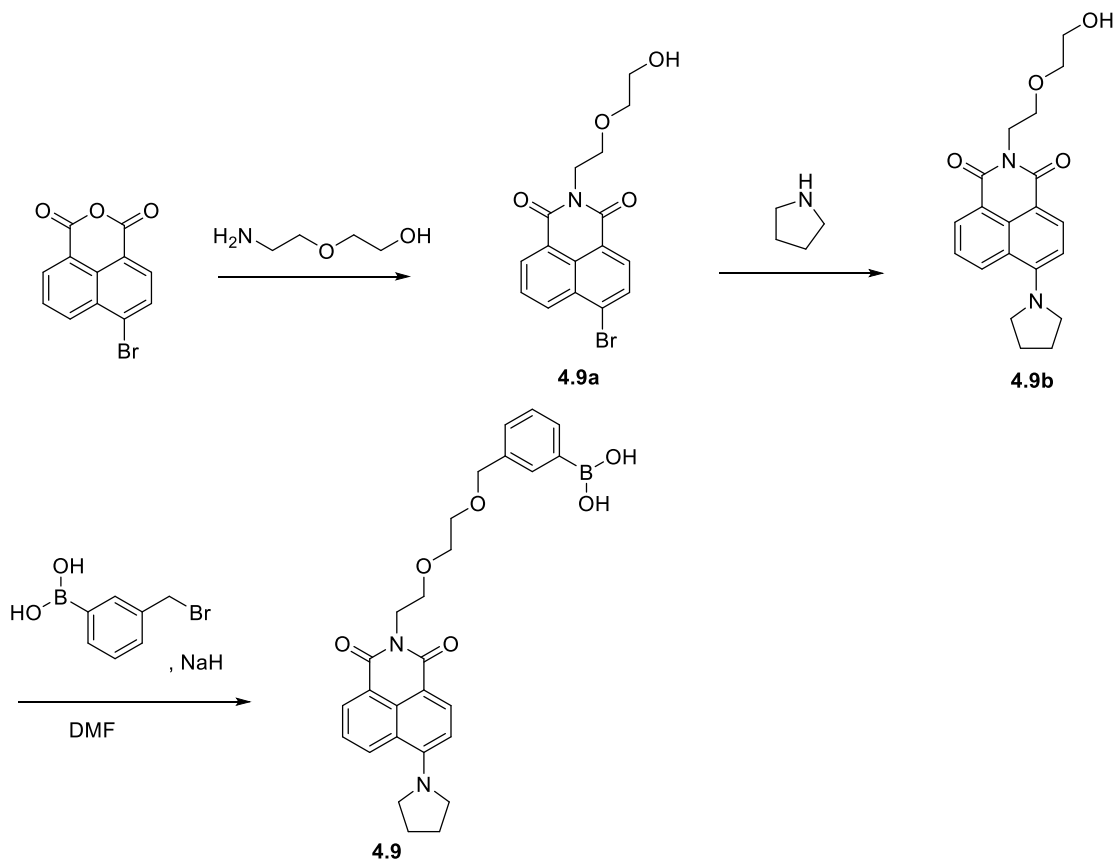
4.6. A mixture of compound **4.6b** (680.0 mg, 1.16 mmol) and 3-pyridyl boronic acid (141 mg, 1.16 mmol) in DMF (5 mL) was heated to 60 °C and stirred for 18 h. The mixture was cooled to room temperature and diethyl ether was added. A precipitate formed was filtered and dried *in vacuo* to obtain **4.6** as a yellow solid (310 mg, 43%) ^1H NMR (300 MHz, MeOD) δ 8.86 (d, J = 6.6 Hz, 1H), 8.12–7.84 (m, 5H), 7.82–7.43 (m, 6H) δ 4.67–4.48 (m, 2H), 4.27–4.08 (m, 2H), 3.87–3.72 (m, 2H), 3.72–3.64 (m, 2H), 3.62–3.48 (m, 4H), 3.49–3.34 (m, 10H) 2.50 (t, J = 7.1 Hz, 2H), 2.27–1.96 (m, 2H). ^{13}C NMR (75 MHz, MeOD) δ 175.89, 136.31, 132.03, 131.17, 130.52, 129.22, 127.26, 127.04, 126.37, 125.70, 125.15, 124.64, 124.50, 123.12, 70.02, 69.90, 68.72, 63.17, 33.25, 32.16, 26.76. HRMS (ESI): m/z (M^+) calcd for $\text{C}_{25}\text{H}_{23}\text{BNO}_2$: 613.2916; found: 613.2972.



4.7a. To pyrene-1-butyric acid (576.0 mg, 2.0 mmol) in DMF (10 mL) was added EDCI (930 mg, 6.0 mmol) and DMAP (24.0 mg, 0.2 mmol) at 0 °C. The mixture was stirred at room temperature for 5 minutes followed by addition of triethylene glycol (818.0 mg, 6.0 mmol). The reaction was further stirred at room temperature overnight. The mixture was diluted with ethyl acetate and washed with 1 N HCL and water. The organic layer was dried over anhydrous sodium sulfate, concentrated *in vacuo*, and purified on silica gel column using CH₂Cl₂: MeOH (1.0:0 to 1.0-0.05) gradient as eluent to obtain **4.7a** as a light yellow liquid (450.0 mg, 53%). ¹H NMR (400 MHz, CDCl₃) δ 8.26-8.20 (m, 1H), 8.12–8.01 (m, 4H), 7.96–7.87 (m, 3H), 7.78 (d, *J* = 7.8 1H), 3.64–3.59 (m, 2H), 3.57–3.44 (m, 12H), 3.35–3.25 (m, 2H), 2.88–2.72 (m, 2H), 2.40 (dt, *J* = 19.7, 8.6 Hz, 2H), 2.20–1.97 (m, 2H). ¹³C NMR (75 MHz, MeOD) δ 173.77, 166.87, 135.75, 131.37, 130.86, 129.91, 129.03, 128.49, 127.32, 127.12, 126.96, 126.28, 125.56, 124.76, 124.67, 124.53, 124.41, 123.02, 70.16, 70.08, 68.72, 68.69, 63.74, 63.21, 33.17, 32.11, 26.61.

4.7. To 3-boronobenzoic acid (100.0 mg, 0.60 mmol) in DMF (1 mL) was added EDCI (186 mg, 1.2 mmol) and DMAP (12.2 mg, 0.1 mmol). The mixture was stirred at room temperature for 30 minutes followed by addition of pyrenebutyltriethyleneglycol ester **4.7a**. (126. 0mg, 0.3 mmol) the reaction was further stirred at room temperature for 48 h. The mixture was diluted with ethyl acetate and washed with 1 N HCl and water. The organic layer was dried over anhydrous sodium sulfate and concentrated *in vacuo*. The crude was purified on silica gel column using hexane:ethyl acetate (1:3) to obtain a thick brown liquid (45 mg,) ¹H NMR (300 MHz, MeOD) δ 8.45-8.32 (m, 1H), 8.26-8.19 (m, 1H), 8.14-8.00 (m, 4H), 7.99–7.85 (m, 4H), 7.80 (d, *J* = 7.8 1H), 7.50 – 7.24 (m, 2H), 4.63-4.50 (m, 2H), 4.39–4.25 (m, 2H), 4.21–4.07 (m, 2H), 3.71–3.56 (m, 4H), 3.54-3.51 (m,

4H), 3.48-3.21 (m, 1H), 2.39 (t, $J = 7.2$ Hz, 2H), 2.22–1.86 (m, 2H). ^{13}C NMR (75 MHz, MeOD) δ 173.77, 166.87, 135.75, 131.37, 130.86, 129.91, 129.03, 128.49, 127.32, 127.12, 126.96, 126.28, 125.56, 124.76, 124.67, 124.53, 124.41, 123.02, 70.16, 70.08, 68.72, 68.69, 63.74, 63.21, 33.17, 32.11, 26.61. HRMS (ESI): m/z ($M+\text{Na}$) calcd for $\text{C}_{33}\text{H}_{33}\text{BO}_8$: 590.2202; found: 590.2197.



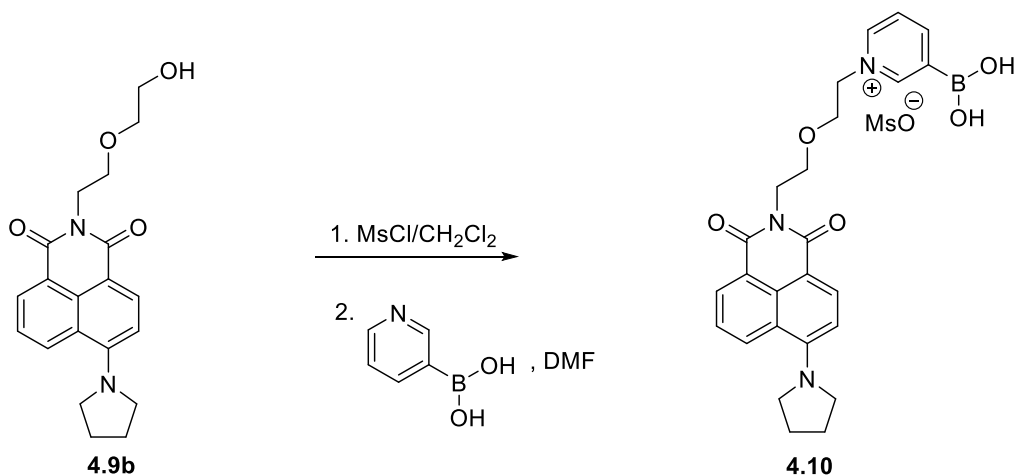
4.9a. To 8-bromonaphthalimide anhydride (600.0 mg, 2.2 mmol) in EtOH (5 mL) was added 2-(2-aminoethoxy) ethan-1-ol (1.0g, 9.5 mmol). The mixture was stirred at room temperature for 5 h. A precipitate formed was filtered and dried to obtain a white solid (660.5 mg, 83.0 mmol) ^1H NMR (300 MHz, CDCl_3) δ 8.68 (d, $J = 7.1$ Hz, 1H), 8.60 (d, $J = 8.4$ Hz, 1H), 8.44 (d, $J = 7.8$ Hz, 1H), 8.06 (d, $J = 7.8$ Hz, 1H), 7.87 (t, $J = 7.9$ Hz, 1H), 4.45 (t, $J = 5.3$ Hz, 2H), 3.87 (t, $J = 5.3$ Hz, 2H), 3.76-3.21 (m, 4H). ^{13}C NMR (101 MHz,

CDCl₃) δ 163.97, 133.52, 132.31, 131.48, 131.18, 129.57, 128.15, 124.30, 122.38, 72.25, 68.37, 61.86, 39.67. HRMS (ESI): m/z (M+H) calcd for C₁₆H₁₄BrNO₄: 364.0180; found: 364.0179.

4.9b. To **4.9a** (330.2 mg, 0.9 mmol) was added pyrrolidine (1 mL) and the mixture refluxed for 4 h. The mixture was cooled to room temperature, diluted with ethyl acetate and washed with 1 N HCL, concentrated sodium bicarbonate and brine. The organic layer was concentrated and dried *in vacuo* to obtain an orange solid (290 mg, 90%). ¹H NMR (300 MHz, CDCl₃) δ 8.64–8.54 (m, 1H), 8.42 (d, J = 8.6 Hz, 1H), 7.59–7.49 (m, 1H), 6.83 (d, J = 8.7 Hz, 1H), 4.44 (t, J = 5.4 Hz, 2H), 3.85 (t, J = 5.4 Hz, 2H), 3.80 (t, J = 6.3 Hz, 4H), 3.73–3.64 (m, 4H), 2.16–2.06 (m, 4H). ¹³C NMR (101 Mhz, CDCl₃) δ 164.32, 133.58, 132.02, 131.40, 123.37, 122.69, 122.41, 109.12, 72.23, 68.67, 61.89, 53.49, 39.29, 26.03. HRMS (ESI): m/z (M+H) calcd for: C₂₀H₂₂N₂O₄ 355.1649; found: 355.1652.

4.9. To **3.27** (88.0 mg, 0.25 mmol) in DMF (2 ML) was added 90% NaH (26.0 mg, 1.0 mmol) and stirred at room temperature for 10 minutes. 3-benzylbromide-boronic acid (44.0 mg, 0.25 mmol) was added and the mixture left to stir at room temperature of 8 h. The mixture was diluted with ethyl acetate and washed with brine and water. The organic layer was dried over anhydrous sodium sulfate and purified on silica gel column using hexane:ethyl acetate (1:0 – 1:1) to obtain an orange liquid (40 mg 32%) ¹H NMR (400 MHz, MeOD) δ 8.61 (d, J = 8.5 Hz, 1H), 8.43–8.33 (m, 1H), 8.19 (d, 8.8 Hz, 1H), 7.59 (s, 1H), 7.54–7.42 (m, 2H), 7.25–7.12 (m, 2H), 6.88–6.59 (m, 2H), 4.66–4.54 (m, 4H), 4.44–4.34 (m, 2H), 3.87–3.67 (m, 4H), 3.67–3.43 (m, 4H), 2.08 (t, J = 13.8 Hz, 4H). ¹³C NMR (101 MHz, MeOD) δ 165.28, 164.45, 164.19, 152.91, 133.21, 132.74, 130.75, 130.69,

122.58, 122.06, 121.43, 108.20, 72.05, 70.18, 69.18, 67.79, 67.64, 60.87, 52.89, 52.85, 38.78, 38.66, 25.60. HRMS (ESI): m/z (M^+) calcd for $C_{27}H_{29}BN_2O_6$: 488.2232; Found: 488.228.



4.10. Compound **4.9b** (162.0 mg, 0.45 mmol) in CH_2Cl_2 was added MsCl (84 μL , 1.0 mmol) and TEA (100 μL). The mixture was stirred at room temperature overnight (22 h). The mixture was afterwards diluted with ethyl acetate and washed with 1 N HCl, concentrated sodium bicarbonate and brine. The organic layer was dried over sodium sulfate anhydrous and concentrate *in vacuo*. The crude was redissolved in DMF (1 mL) and 3-pyridine boronic acid (55.0 mg, 0.45 mmol) was added and stirred at 90 $^\circ\text{C}$ for 36 h. The reaction mixture was cooled to room temperature and diethyl ether was added to the reaction mixture. A black oily residue was formed at the bottom. The diethyl ether was decanted and the oily residue further washed twice with diethyl ether and dried *in vacuo* to obtain a yellow solid (145 mg, 58%) as **4.10**. ^1H NMR (400 MHz, MeOD) δ 8.92–8.78 (m, 2H), 8.70 – 8.57 (m, 1H), 8.54 (d, J = 8.0 Hz, 1H), 8.40–8.24 (m, 2H), 8.15–8.01 (m, 1H), 7.87 (t, J = 6.8 Hz, 1H), 7.48 (dd, J = 15.7, 7.8 Hz, 1H), 4.34 –4.14 (m, 2H), 4.07 –3.92

(m, 2H), 3.87–3.70 (m, 6H), 3.68–3.55 (m, 2H) 2.52 (s, 3H), 2.19–2.08 (m, 4H). ^{13}C NMR (101 MHz, MeOD) δ 164.69, 152.78, 145.31, 145.09, 133.28, 132.79, 130.78, 127.41, 122.57, 121.93, 121.18, 108.17, 72.07, 68.12, 67.96, 67.78, 61.35, 60.88, 52.94, 52.88, 38.36, 38.12, 34.04, 25.63. HRMS(ESI): m/z Calcd For $\text{C}_{25}\text{H}_{27}\text{BN}_3\text{O}_5$: 459.2075; Found: 459.2075

4.5 REFERENCES

- (1) Tian, Y.; Zhou, Y.; Elliott, S.; Aebersold, R.; Zhang, H.: Solid-phase extraction of N-linked glycopeptides. *Nat. Protocols* **2007**, 2, 334-339.
- (2) Marth, J. D.; Grewal, P. K.: Mammalian glycosylation in immunity. *Nat. Rev. Immunol.* **2008**, 8, 874-887.
- (3) Donin, N.; Jurianz, K.; Ziporen, L.; Schultz, S.; Kirschfink, M.; Fishelson, Z.: Complement resistance of human carcinoma cells depends on membrane regulatory proteins, protein kinases and sialic acid. *Clin. Exp. Immunol.* **2003**, 131, 254-263.
- (4) Hakomori, S.: Aberrant glycosylation in cancer cell-membranes as focused on glycolipids - overview and perspectives. *Cancer Res.* **1985**, 45, 2405-2414.
- (5) Kim, Y. J.; Varki, A.: Perspectives on the significance of altered glycosylation of glycoproteins in cancer. *Glycoconj. J.* **1997**, 14, 569-576.
- (6) Dube, D. H.; Bertozzi, C. R.: Glycans in cancer and inflammation. Potential for therapeutics and diagnostics. *Nat. Rev. Drug Discov.* **2005**, 4, 477-488.
- (7) Lindberg, G.; Eklund, G. A.; Gullberg, B.; Råstam, L.: Serum sialic acid concentration and cardiovascular mortality. *Br. Med. J.* **1991**, 302, 143-146.
- (8) Varki, A.: Sialic acids in human health and disease. *Trends Mol. Med.* **2008**, 14, 351-360.
- (9) de Leoz, M. L. A.; Young, L. J. T.; An, H. J.; Kronewitter, S. R.; Kim, J. H.; Miyamoto, S.; Borowsky, A. D.; Chew, H. K.; Lebrilla, C. B.: High-Mannose Glycans are Elevated during Breast Cancer Progression. *Mol. Cell. Proteomics* **2011**, 10.
- (10) Ang, I. L.; Poon, T. C. W.; Lai, P. B. S.; Chan, A. T. C.; Ngai, S.-M.; Hui, A. Y.; Johnson, P. J.; Sung, J. J. Y.: Study of Serum Haptoglobin and Its Glycoforms in the

Diagnosis of Hepatocellular Carcinoma: A Glycoproteomic Approach. *J. Proteome Res.* **2006**, *5*, 2691-2700.

(11) Rudd, P. M.; Dwek, R. A.: Rapid, sensitive sequencing of oligosaccharides from glycoproteins. *Curr. Opin. Biotechnol.* **1997**, *8*, 488-497.

(12) Shriver, Z.; Raguram, S.; Sasisekharan, R.: Glycomics: a pathway to a class of new and improved therapeutics. *Nat. Rev. Drug Discov.* **2004**, *3*, 863-873.

(13) Harvey, D. J.: Proteomic analysis of glycosylation: structural determination of N- and O-linked glycans by mass spectrometry. *Expert Rev. Proteomics* **2005**, *2*, 87-101.

(14) Frullano, L.; Rohovec, J.; Aime, S.; Maschmeyer, T.; Prata, M. I.; de Lima, J. J. P.; Geraldes, C. F. G. C.; Peters, J. A.: Towards Targeted MRI: New MRI Contrast Agents for Sialic Acid Detection. *Chem. Euro. J.* **2004**, *10*, 5205-5217.

(15) Neves, A. A.; Wainman, Y. A.; Wright, A.; Kettunen, M. I.; Rodrigues, T. B.; McGuire, S.; Hu, D.-E.; Bulat, F.; Geninatti Crich, S.; Stöckmann, H.; Leeper, F. J.; Brindle, K. M.: Imaging Glycosylation In Vivo by Metabolic Labeling and Magnetic Resonance Imaging. *Angew. Chem. Int. Ed.* **2016**, *55*, 1286-1290.

(16) Mun, J.-Y.; Lee, K. J.; Seo, H.; Sung, M.-S.; Cho, Y. S.; Lee, S.-G.; Kwon, O.; Oh, D.-B.: Efficient Adhesion-Based Plasma Membrane Isolation for Cell Surface N-Glycan Analysis. *Anal. Chem.* **2013**, *85*, 7462-7470.

(17) Xie, R.; Hong, S.; Chen, X.: Cell-selective metabolic labeling of biomolecules with bioorthogonal functionalities. *Curr. Opin. Chem. Biol.* **2013**, *17*, 747-752.

(18) Laughlin, S. T.; Baskin, J. M.; Amacher, S. L.; Bertozzi, C. R.: In vivo imaging of membrane-associated glycans in developing zebrafish. *Science* **2008**, *320*, 664-667.

- (19) Breidenbach, M. A.; Gallagher, J. E. G.; King, D. S.; Smart, B. P.; Wu, P.; Bertozzi, C. R.: Targeted metabolic labeling of yeast N-glycans with unnatural sugars. *Proc. Natl. Acad. Sci.* **2010**, *107*, 3988-3993.
- (20) Sletten, E. M.; Bertozzi, C. R.: Bioorthogonal Chemistry: Fishing for Selectivity in a Sea of Functionality. *Angew. Chem. Int. Ed.* **2009**, *48*, 6974-6998.
- (21) Matsumoto, A.; Cabral, H.; Sato, N.; Kataoka, K.; Miyahara, Y.: Assessment of Tumor Metastasis by the Direct Determination of Cell-Membrane Sialic Acid Expression. *Angew. Chem. Int. Ed.* **2010**, *49*, 5494-5497.
- (22) Prescher, J. A.; Bertozzi, C. R.: Chemistry in living systems. *Nat. Chem. Biol.* **2005**, *1*, 13-21.
- (23) Dam, T. K.; Brewer, C. F.: Lectins as pattern recognition molecules: The effects of epitope density in innate immunity. *Glycobiology* **2010**, *20*, 270-279.
- (24) Sun, X.; Zhai, W.; Fossey, J. S.; James, T. D.: Boronic acids for fluorescence imaging of carbohydrates. *Chem. Commun.* **2016**, *52*, 3456-3469.
- (25) Ghazarian, H.; Idoni, B.; Oppenheimer, S. B.: A glycobiology review: Carbohydrates, lectins and implications in cancer therapeutics. *Acta Histochem.* **2011**, *113*, 236-247.
- (26) James, T. D.; Phillips, M. D.; Shinkai, S.: The Molecular Recognition of Saccharides. Complexation of Boronic Acids with Saccharides. Fluorescent Sensors. Modular Fluorescent Sensors. Other Types of Sensor. Other Systems for Saccharide Recognition. In *Boronic Acids in Saccharide Recognition*; The Royal Society of Chemistry, 2006; pp 3-176.

- (27) Vandenburg, Y. R.; Zhang, Z.-Y.; Fishkind, D. J.; Smith, B. D.: Enhanced cell binding using liposomes containing an artificial carbohydrate-binding receptor. *Chem. Commun.* **2000**, 149-150.
- (28) Yang, W.; Fan, H.; Gao, X.; Gao, S.; Karnati, V. V. R.; Ni, W.; Hooks, W. B.; Carson, J.; Weston, B.; Wang, B.: The First Fluorescent Diboronic Acid Sensor Specific for Hepatocellular Carcinoma Cells Expressing Sialyl Lewis X. *Chem. Biol.* **11**, 439-448.
- (29) Aotake, T.; Tanimoto, H.; Hotta, H.; Kuzuhara, D.; Okujima, T.; Uno, H.; Yamada, H.: In situ preparation of highly fluorescent pyrene-dyes from non-luminous precursors upon photoirradiation. *Chem. Commun.* **2013**, *49*, 3661-3663.
- (30) Weigel, W.; Rettig, W.; Dekhtyar, M.; Modrakowski, C.; Beinhoff, M.; Schlüter, A. D.: Dual Fluorescence of Phenyl and Biphenyl Substituted Pyrene Derivatives. *J. Phys. Chem. A* **2003**, *107*, 5941-5947.
- (31) Yang, S.-W.; Elangovan, A.; Hwang, K.-C.; Ho, T.-I.: Electronic Polarization Reversal and Excited State Intramolecular Charge Transfer in Donor/Acceptor Ethynylpyrenes. *J. Phys. Chem. B* **2005**, *109*, 16628-16635.
- (32) Qian, X.; Xiao, Y.; Xu, Y.; Guo, X.; Qian, J.; Zhu, W.: "Alive" dyes as fluorescent sensors: fluorophore, mechanism, receptor and images in living cells. *Chem. Commun.* **2010**, *46*, 6418-6436.